# μ(I) rheology for granular flows with applications for avalanches and column collapse


Pierre-Yves Lagrée[*],

Lydie Staron[*], Stéphane Popinet [*o], (Daniel Lhuillier [*], Christophe Josserand [*])

[*]Institut Jean le Rond d'Alembert, CNRS, Université Pierre & Marie Curie, 4 place Jussieu, Paris, France

[o] National Institute of Water and Atmospheric Research, PO Box 14-901 Kilbirnie, Wellington, New Zealand

## Saint Gobain 05/04/12

# Institut Jean Le Rond d'Alembert

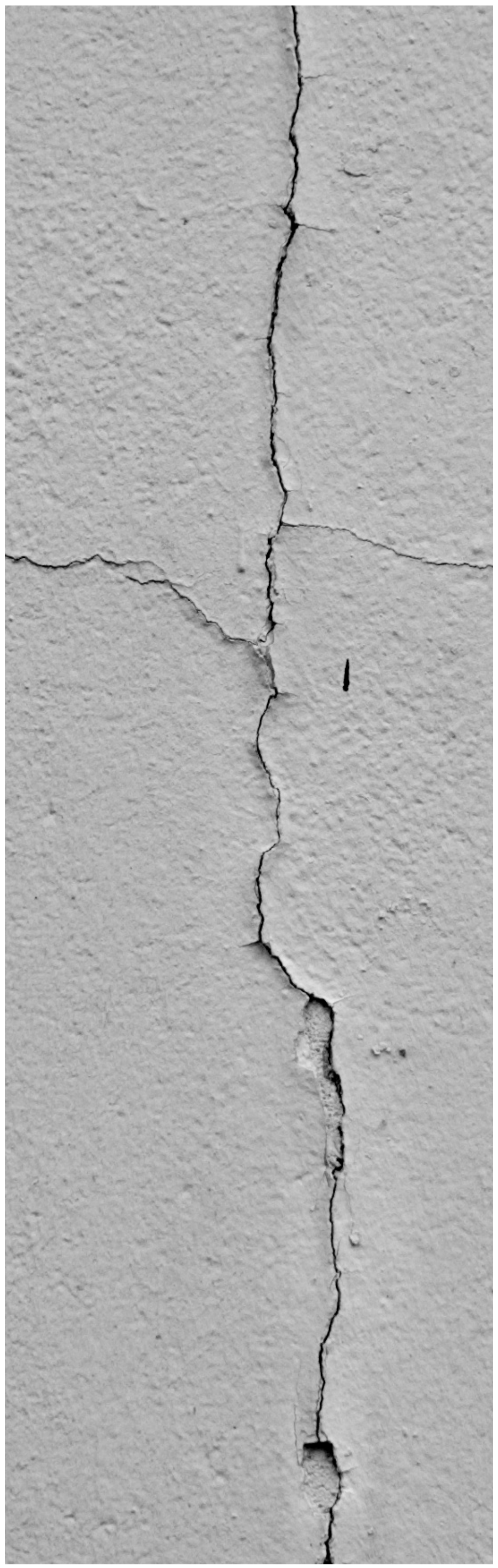

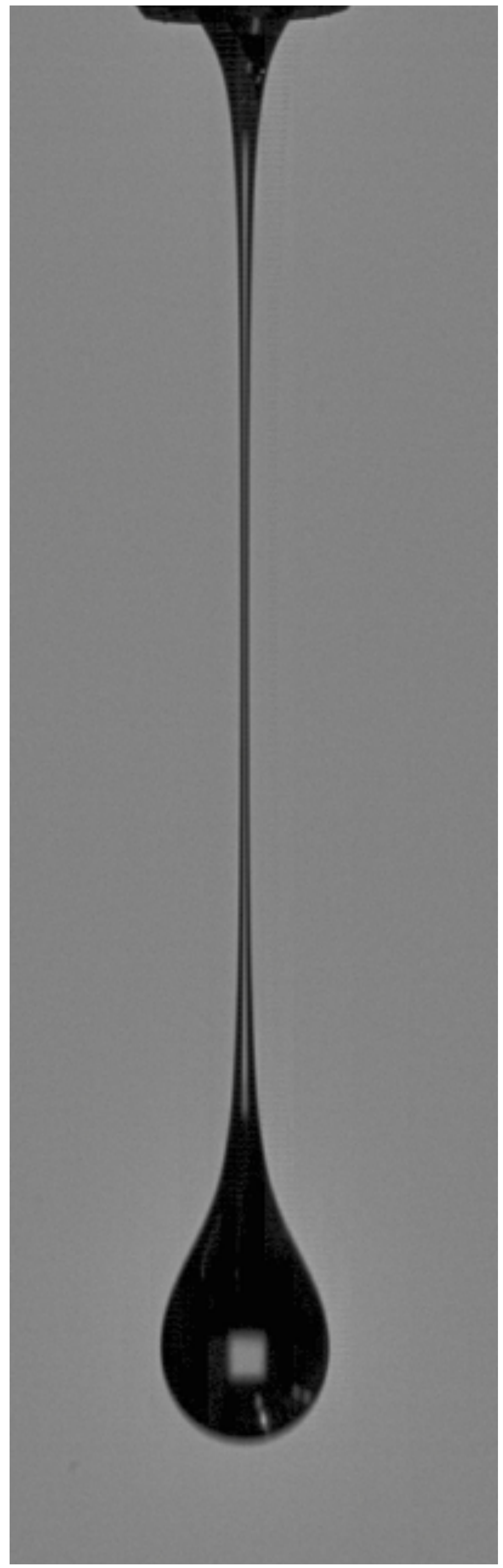

# outline

- what is a granular fluid? some images
- the μ(I) friction law obtained from experiments and discrete simulation
- the viscosity associated to the μ(I) friction law
- the Saint Venant Savage Hutter Hyperbolic model
- implementing the μ(I) friction law in Navier Stokes
- Examples of flows: focusing on the granular column collapse and the Hour Glass

- What is a granular media?
- size > 100μm
- grains of sand, small rocks, glass beads, animal feed pellet, medicines, cereals, wheat, sugar, rice...
- 50 % of the traded products

1. Introduction 3

FIG. 1.2 – Les milieux granulaires forment une famille extrêmement vaste.

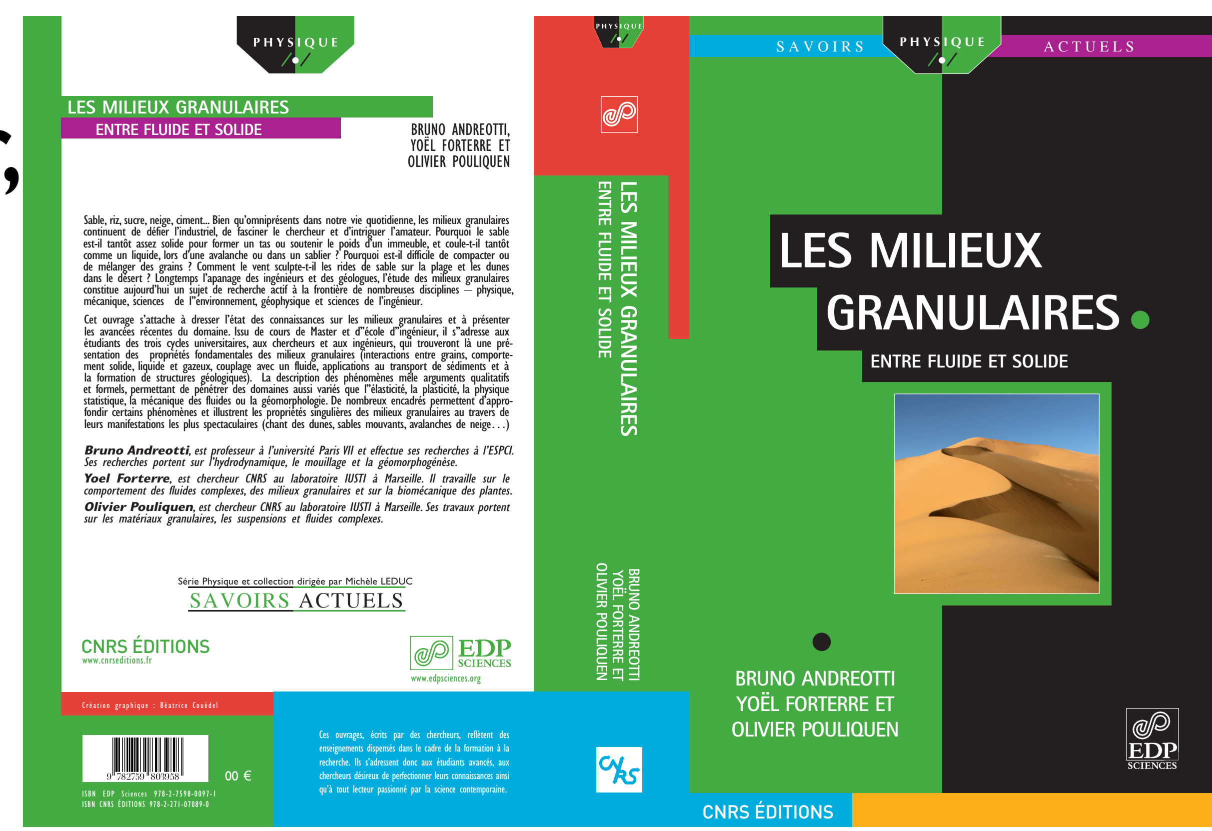


spoil tip (boney pile, gob pile, bing or pit heap), «terril» in french


pyl


pyl


pyl

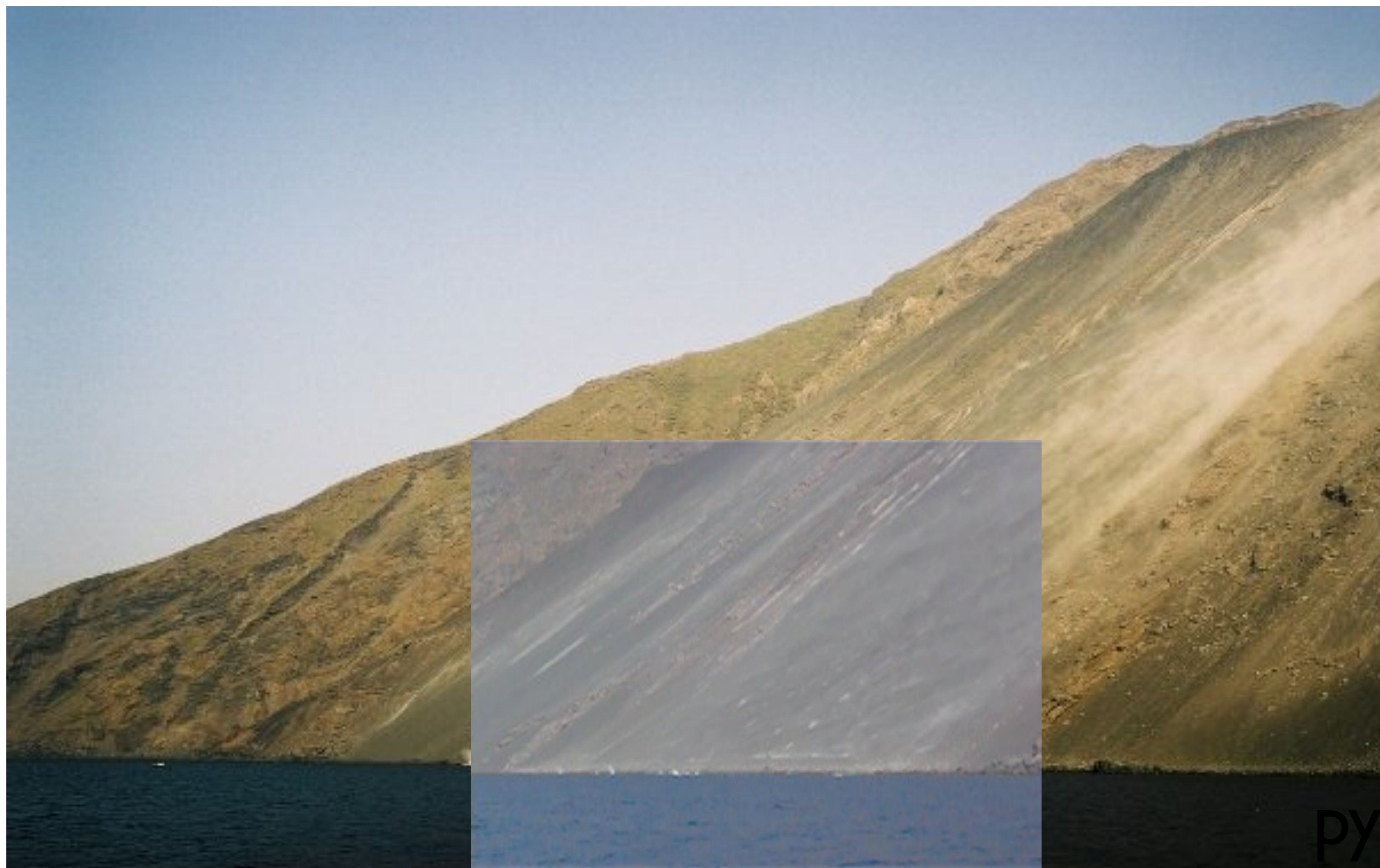

- the Saint Venant Savage Hutter Hyperbolic model

Fig. 20. Frank slide.

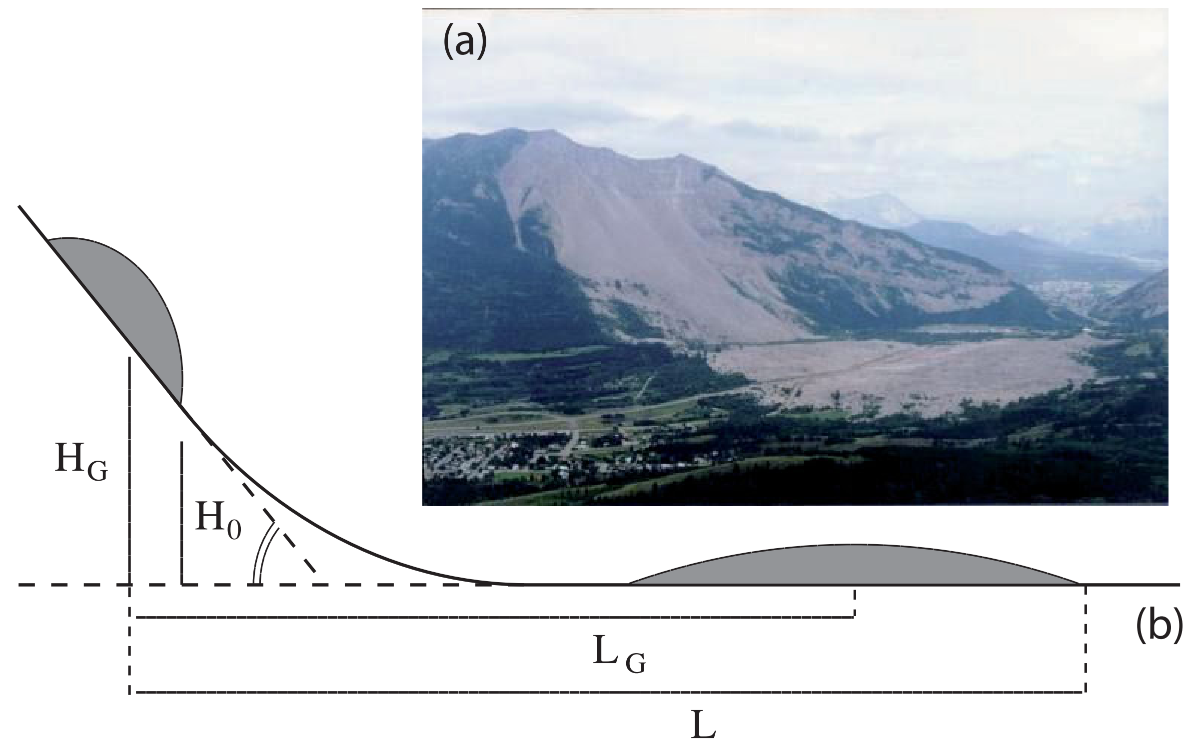


H x L = 1000m x 2500m

Staron

Environmental Modelling & Software xx (2006) 1e18
www.elsevier.com/locate/envsoft
The effect of the earth pressure coefficients on the runout of granular material
Marina Pirulli [a,*], Marie-Odile Bristeau [b], Anne Mangeney [c], Claudio Scavia

1903, Alberta Canada
90 morts


http://www.pbase.com/image/63044602 2006 Gary Hebert

# Lofoten Norway



photo PYL

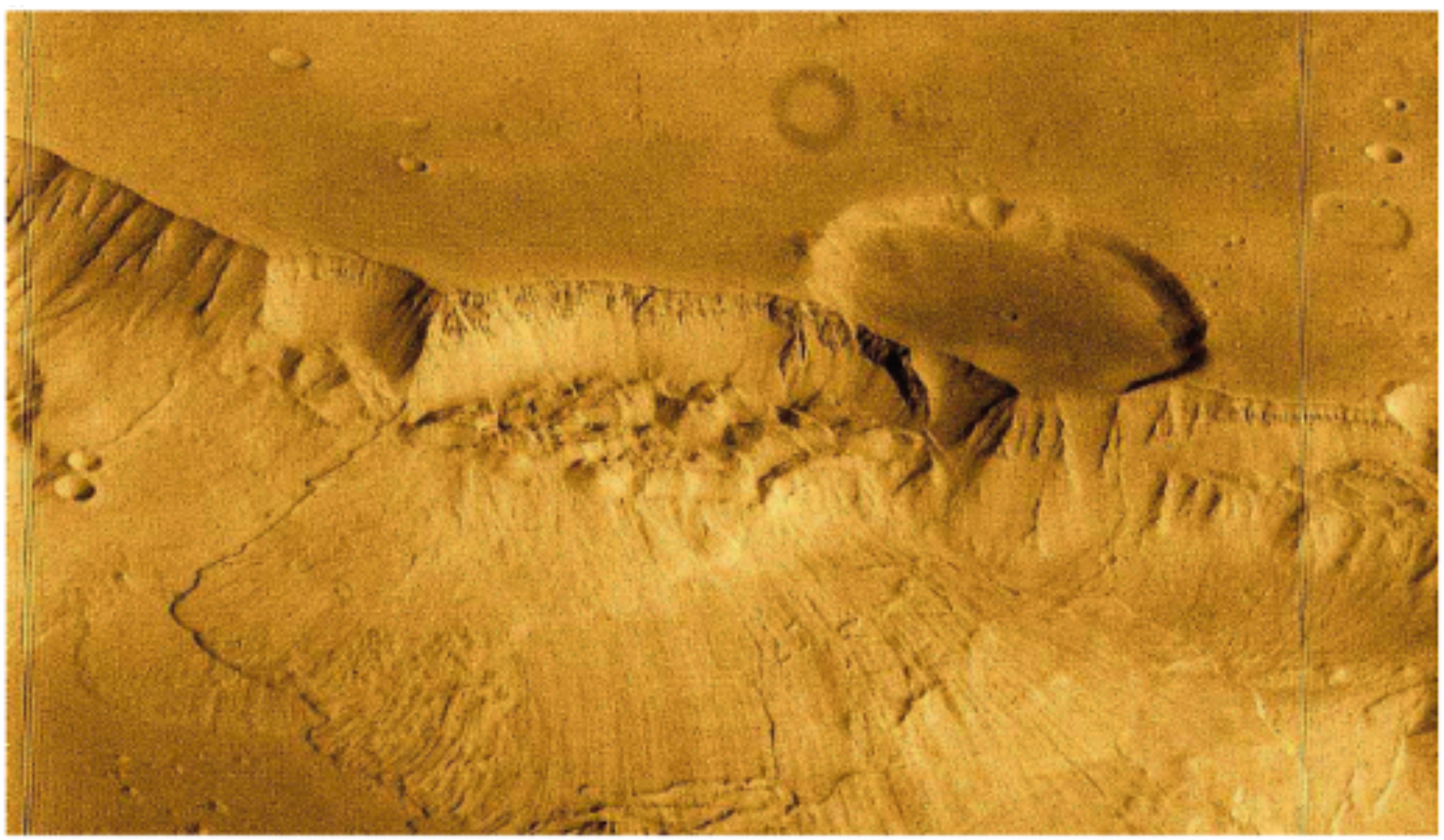

b

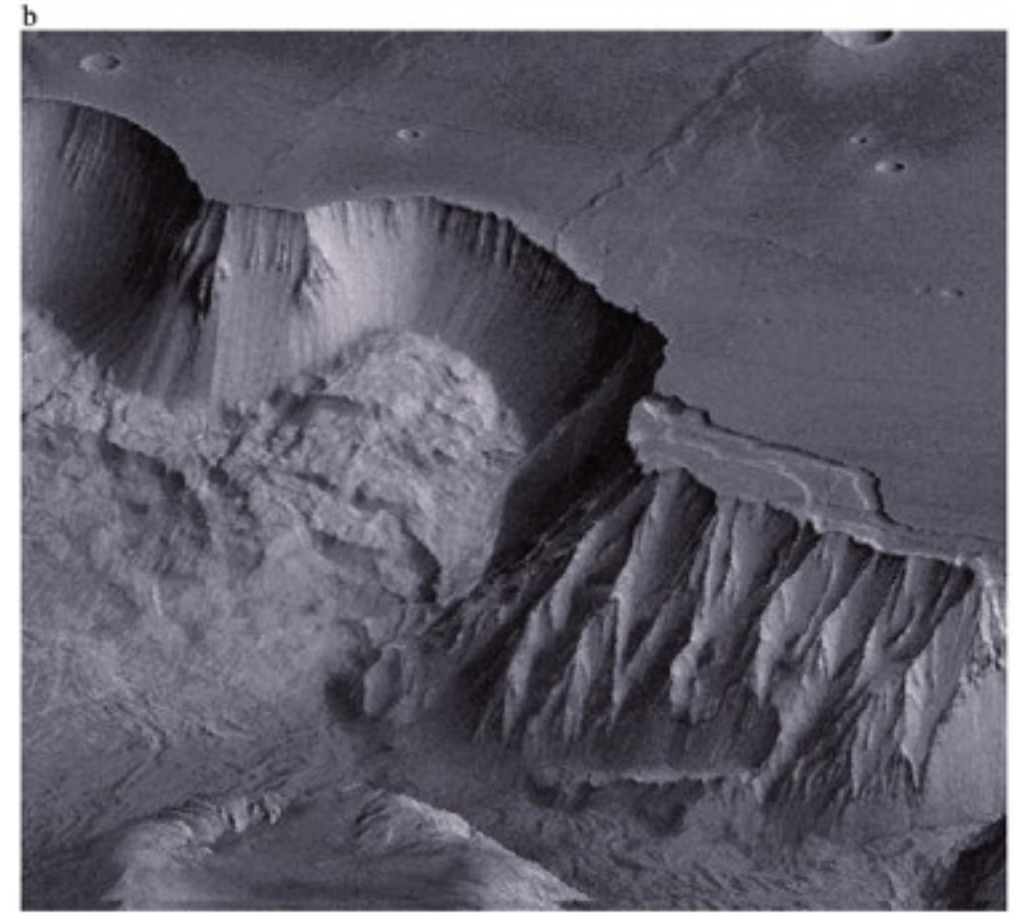

http://books.google.fr/books?id=HY6Z5od4-E4C&pg=PA49&dq=granular+flow&hl=fr&ei=lamtTaa_NYyVOoToldcL&sa=X&oi=book_result&ct=result&resnum=10&ved=0CFkQ6AEwCTgK#v=onepage&q&f=true


http://www.cieletespace.fr/image-du-jour/5126_la-saison-des-avalanches-sur-mars

# Granular Column Collapse

## A model for avalanches

The sand pit problem: quickly remove the bucket of sand

http://www.mylot.com/w/photokeywords/pail.asp

# Granular Column Collapse

E. Lajeunesse A. Mangeney-Castelnau and J. P. Vilotte PoF 2004

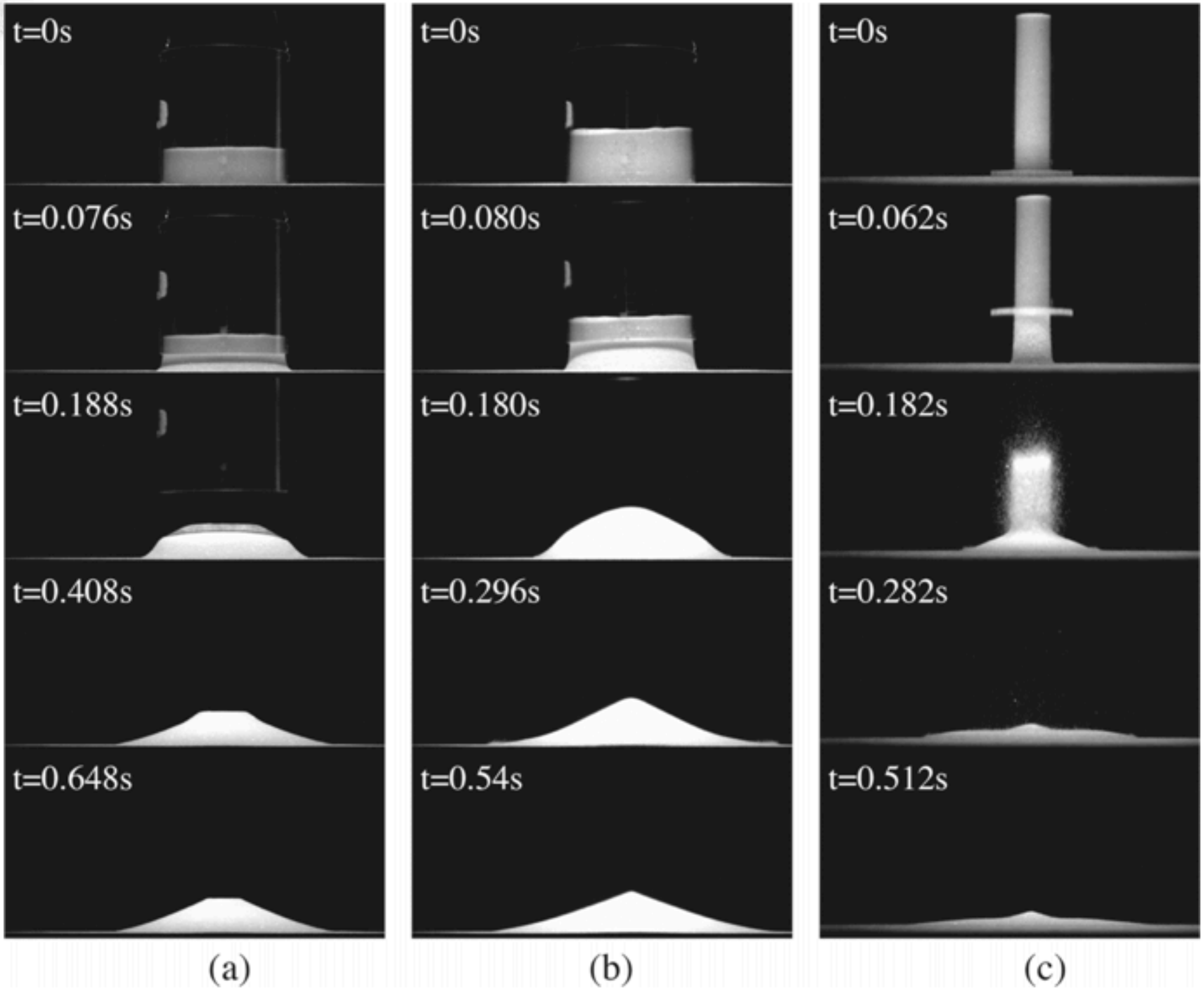


The sand pit problem: quickly remove the bucket of sand

http://www.mylot.com/w/photokeywords/pail.asp

# Granular Column Collapse

aspect ratio $a = H_0/R_0 = H_0/L_0$

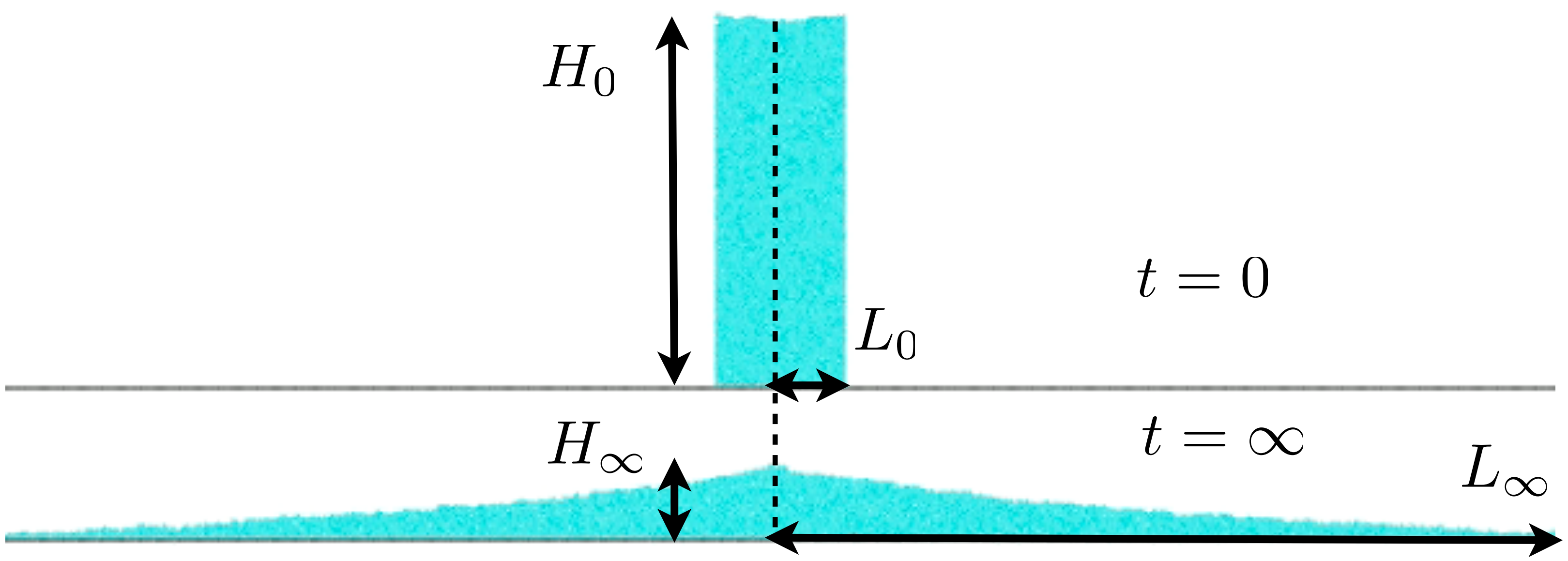


The sand pit problem: quickly remove the bucket of sand

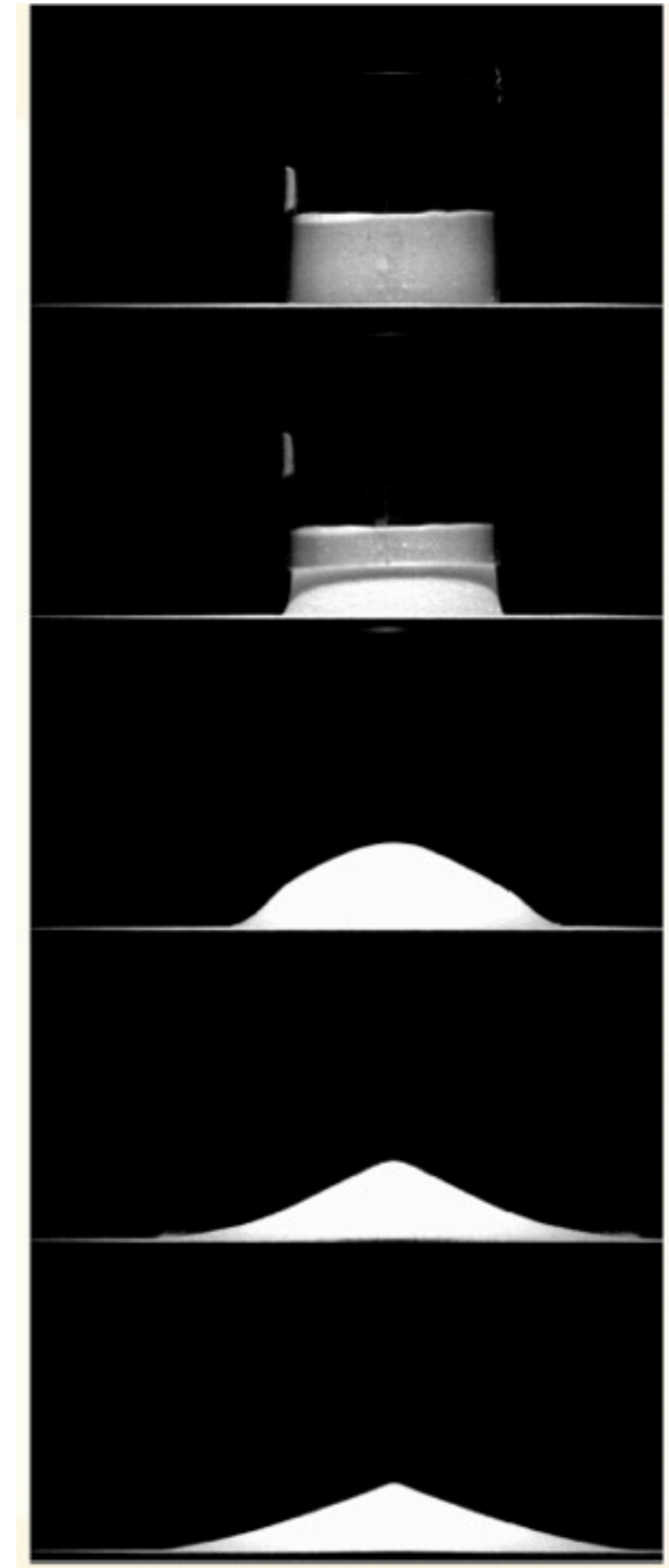

Lajeunesse et al., 2004

# Granular Column Collapse

A possible experimental set up is a container filled by sand (left), the aspect ratio (height/length) is *a*. At initial time, the gate is opened quickly. After the avalanche, the grains stop, the final configuration is at rest (right). We compare results from Discrete Contact Method Simulations (simulation of the displacement of each grain) to a continuum Navier Stokes simulation with the μ(I) rheology *Gerris*.

The sand pit problem: quickly remove the bucket of sand

E Lajeunesse J. B. Monnier and G. M. Homsy PoF 05

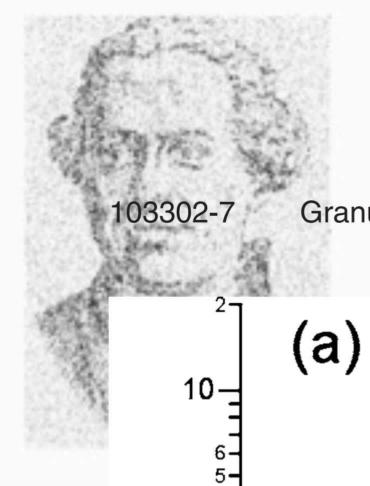



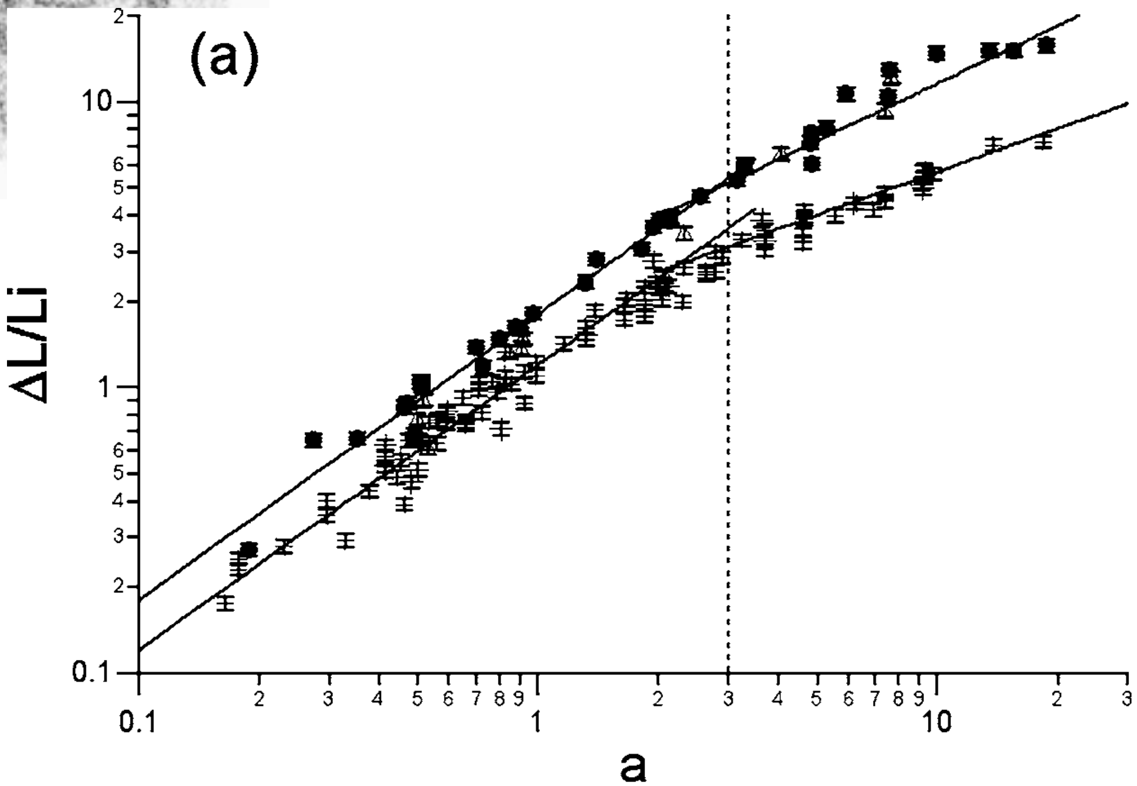


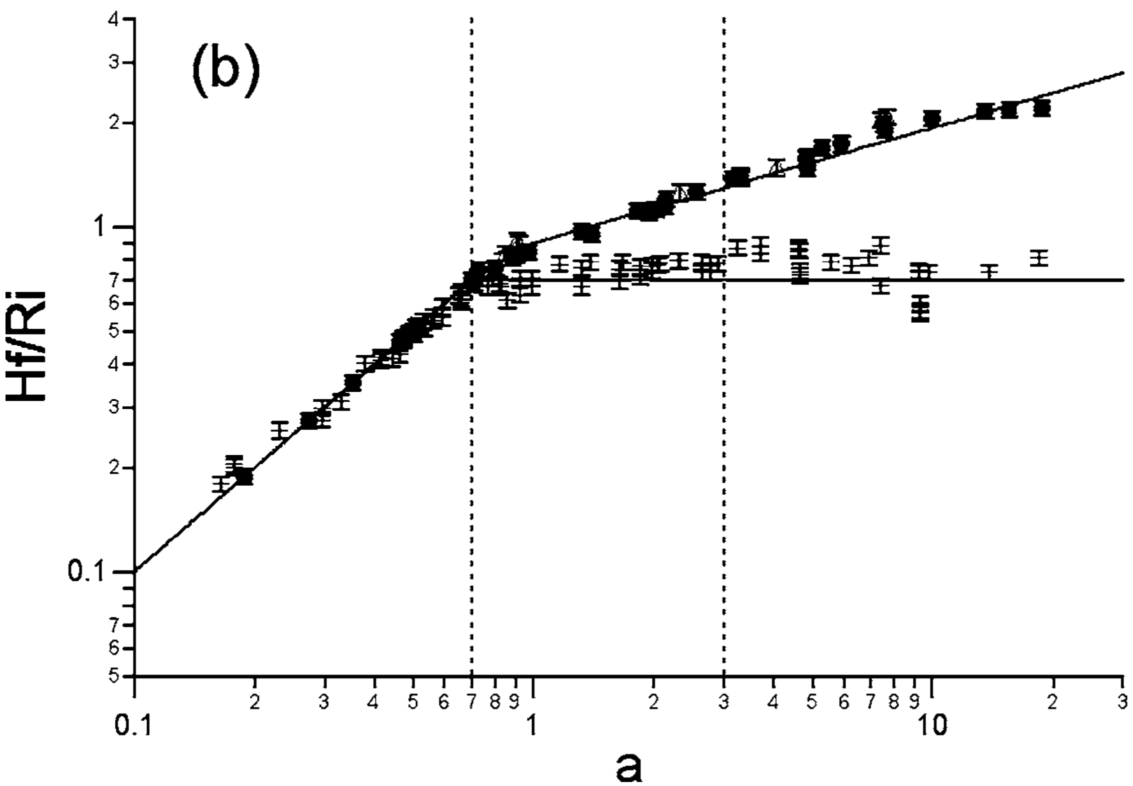


- In the axisymmetric geometry

$$\frac{H_f}{L_i} = \begin{cases} a & a \lesssim 0.74, \\ 0.74 & a \gtrsim 0.74, \end{cases}$$

$$\frac{\Delta L}{L_i} \propto \begin{cases} a & a \lesssim 3, \\ a^{1/2} & a \gtrsim 3. \end{cases}$$

- In the rectangular channel:

$$\frac{H_f}{L_i} \propto \begin{cases} a & a \lesssim 0.7, \\ a^{1/3} & a \gtrsim 0.7, \end{cases}$$

$$\frac{\Delta L}{L_i} \propto \begin{cases} a & a \lesssim 3, \\ a^{2/3} & a \gtrsim 3. \end{cases}$$

FIG. 6. Scaled runout $\Delta L/L_i$ (a) and scaled deposit height $H_f/L_i$ (b) as functions of $a$. Circles and triangles correspond to experiments performed in the 2D channel working respectively with glass beads of diameter $d$ =1.15 mm or $d$=3 mm. Crosses correspond to the data set of axisymmetric collapses from Lajeunesse *et al.* (Ref. 10).

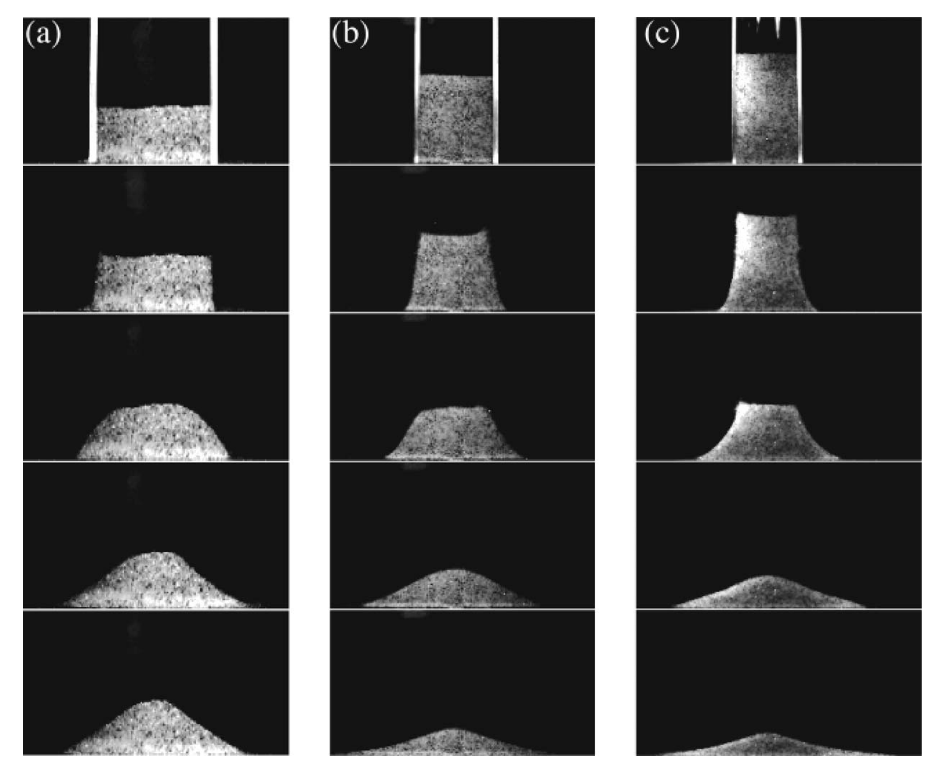

- Silo, hopper, hourglass

# outline

- what is a granular fluid? some images
- the μ(I) friction law obtained from experiments and discrete simulation
- the viscosity associated to the μ(I) friction law
- the Saint Venant Savage Hutter Hyperbolic model
- implementing the μ(I) friction law in Navier Stokes
- Examples of flows: focusing on the granular column collapse and the Hour Glass

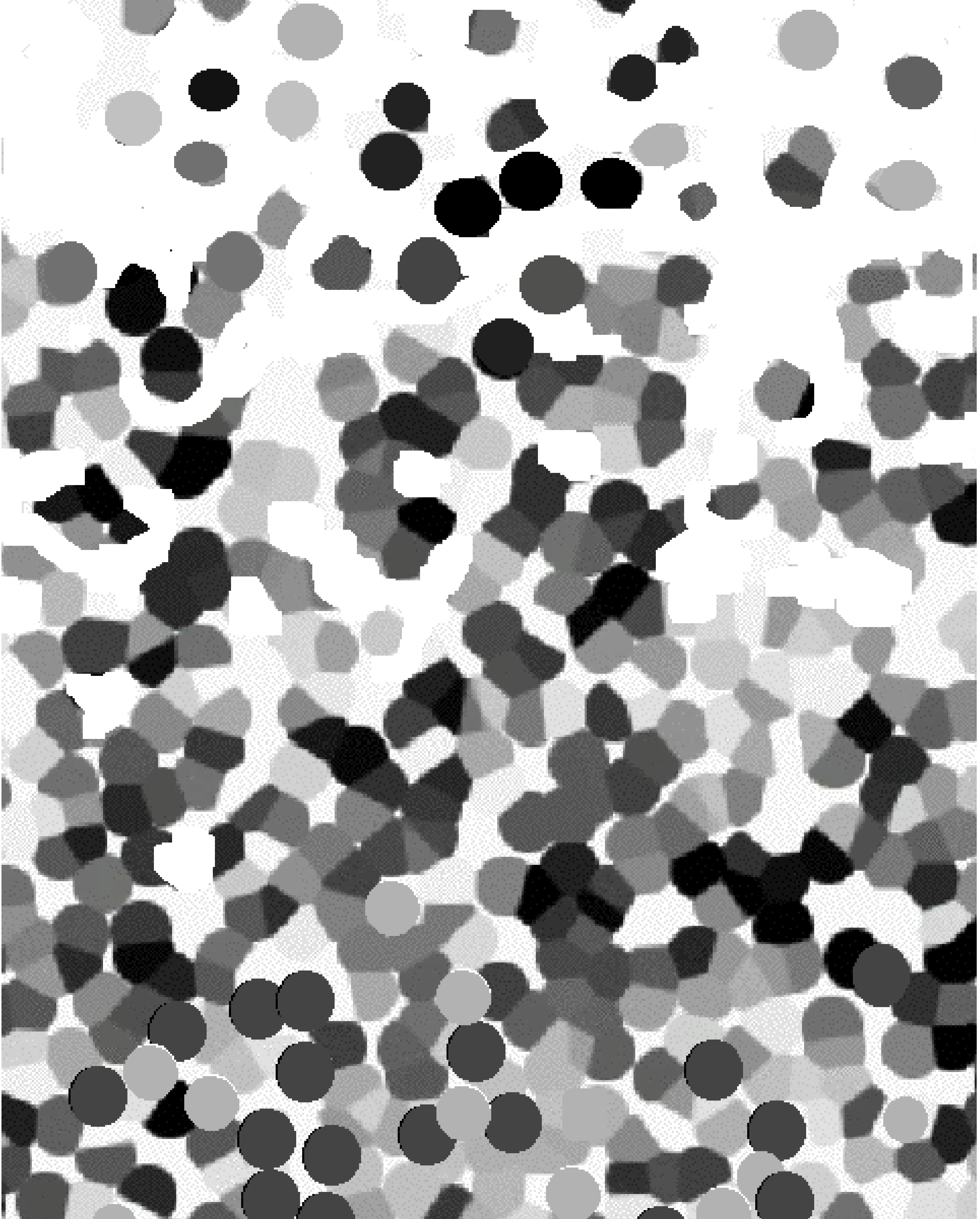

grains gaz

impacts:
suspension

granular media
contacts

liquid

like a solid:

from the grains to the fluid

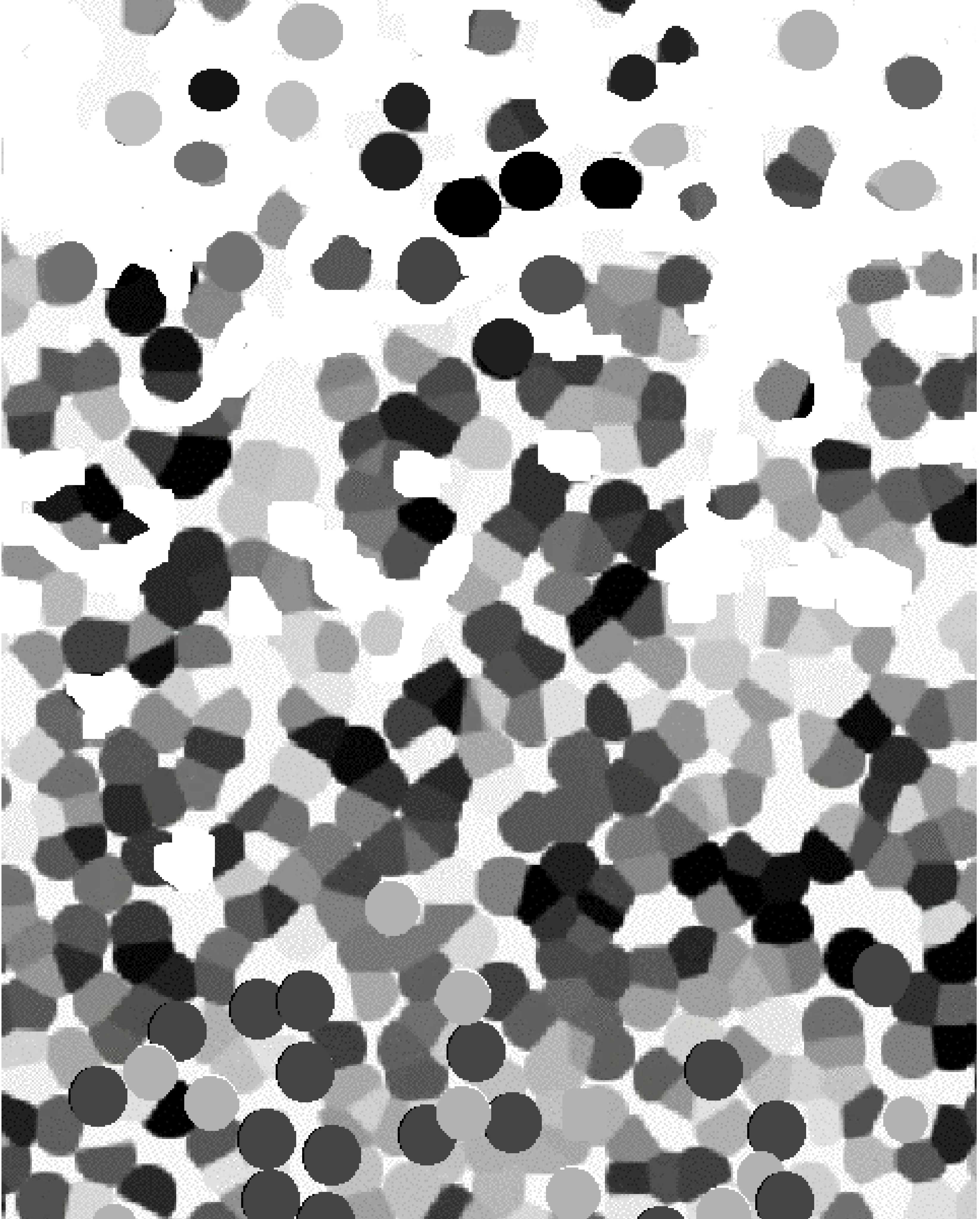

grains

$\phi_{min}$ 0.5 (2D) 0.55 (3D)

$\phi_{min} < \phi < \phi_{Max}$

$\phi_{max}$ 0.8 (2D) 0.65 (3D)

from the grains to the fluid

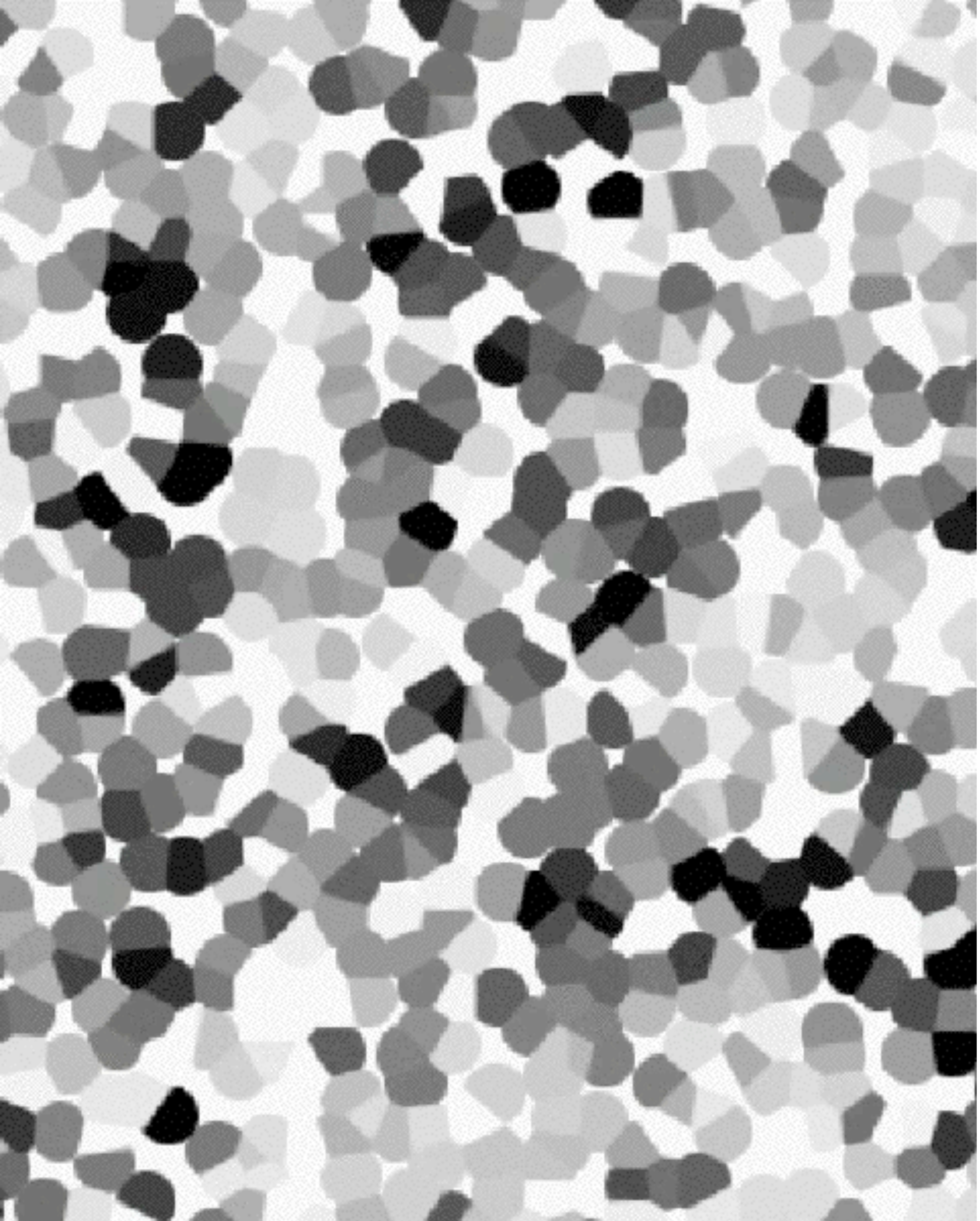

~~grains~~

continuum media hypothesis

from the grains to the fluid

- Looking for a continuum description
- Lot of recent experiments in simple configurations: shear/ inclined plane,

  with model material (glass beads, sand…)
- Simulations with Contact Dynamics

  (disks, polygona, spheres)

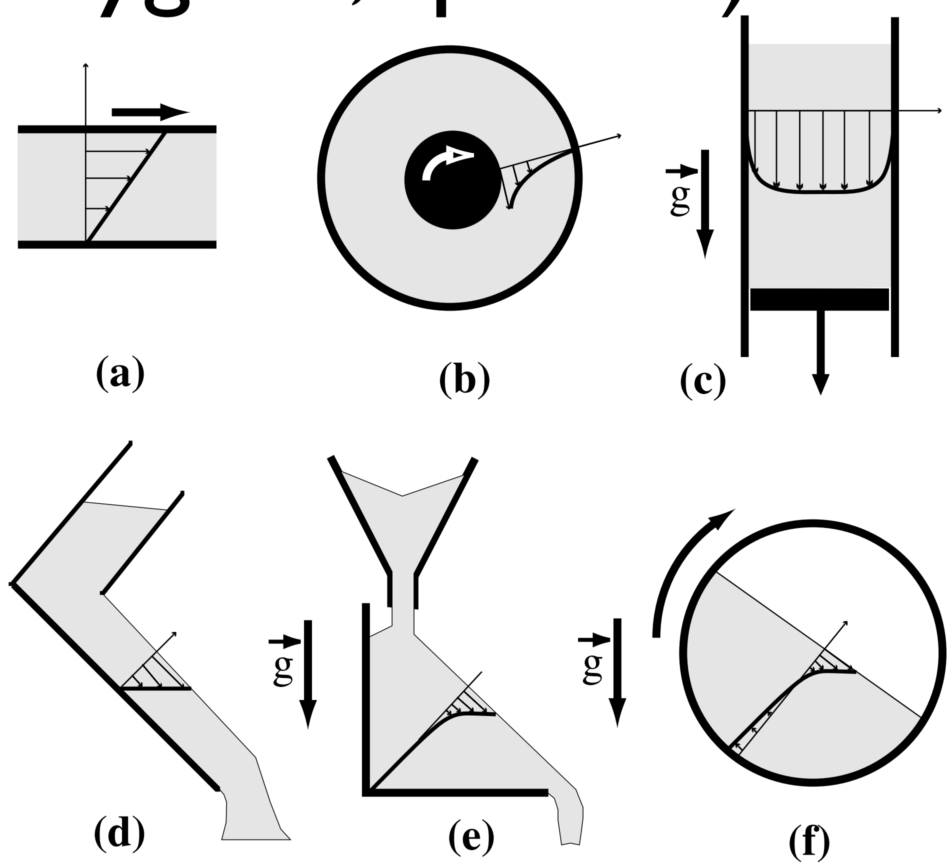


**Fig. 1.** The six configurations of granular flows: (a) plane shear, (b) annular shear, (c) vertical-chute flows, (d) inclined plane, (e) heap flow, (f) rotating drum.

GDR MiDi EPJ E 04

- Looking for a continuum description
- Lot of recent experiments in simple configurations: shear/ inclined plane,

  with model material (glass beads, sand…)
- Simulations with Contact Dynamics

  (disks, polygona, spheres)

- Defining a «viscosity»
- Implement it in the Navier Stokes solver *Gerris*
- Test on exact «Bagnold» avalanche solution
- Test on granular collapse and hourglass

# Molecular Dynamics:

$$m\frac{d}{dt}\overrightarrow{U} = \overrightarrow{F} + \overrightarrow{F}_n + \overrightarrow{F}_t$$ Newton’s equations

branch a spring -dashpot

$$F_n = -k\delta - \gamma\frac{d\delta}{dt}$$

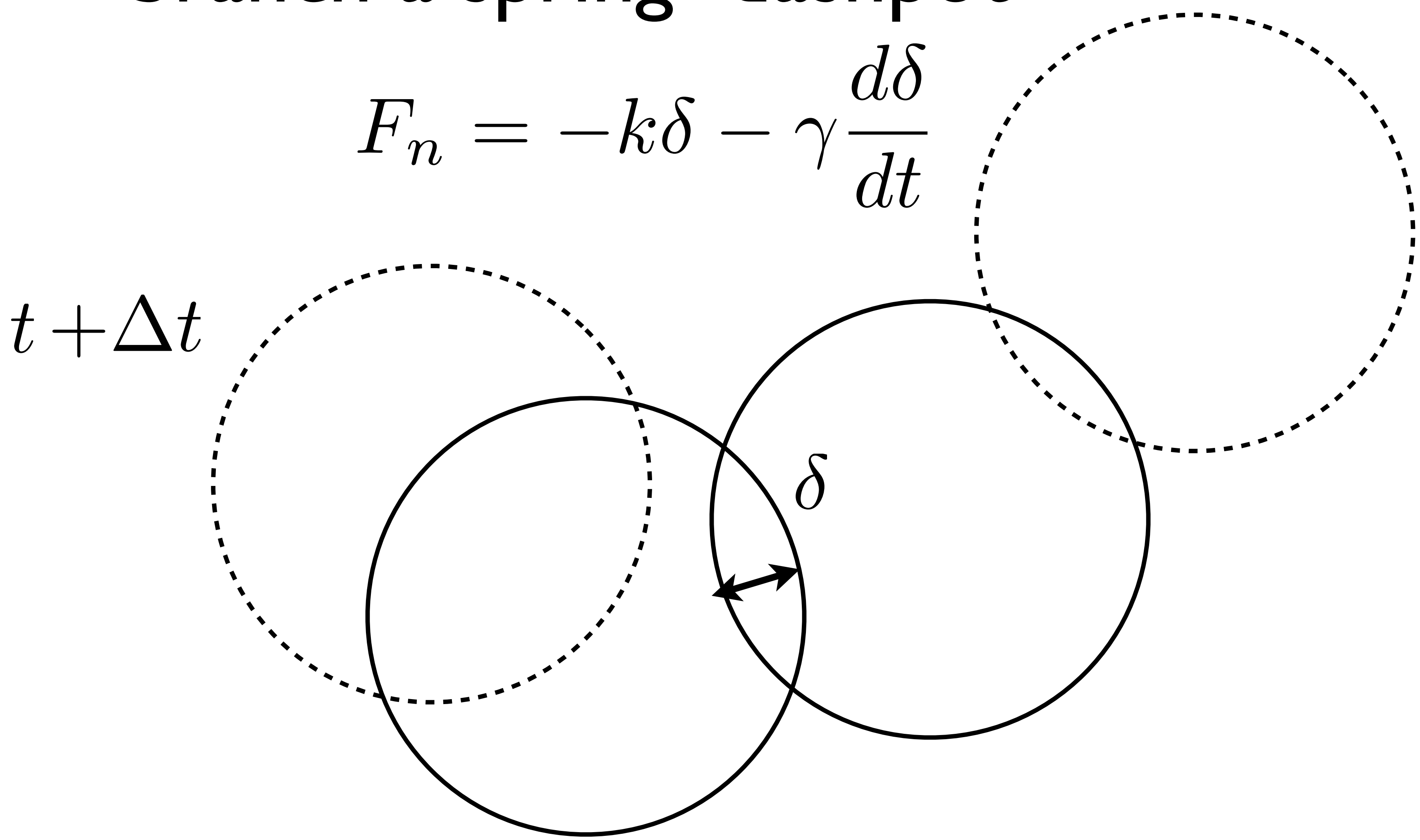


tangential Coulombic Friction $F_t < \mu F_n$

# Contact Dynamics de (Moreau 1988)

rigid grains
coefficient of friction μ

$$m(\overrightarrow{U}^{+} - \overrightarrow{U}^{-}) = \overrightarrow{F}\delta t$$ Newton's equations

take the form of an equality between the change of momenta and the average impulse during δt.

written for each grain at the contact

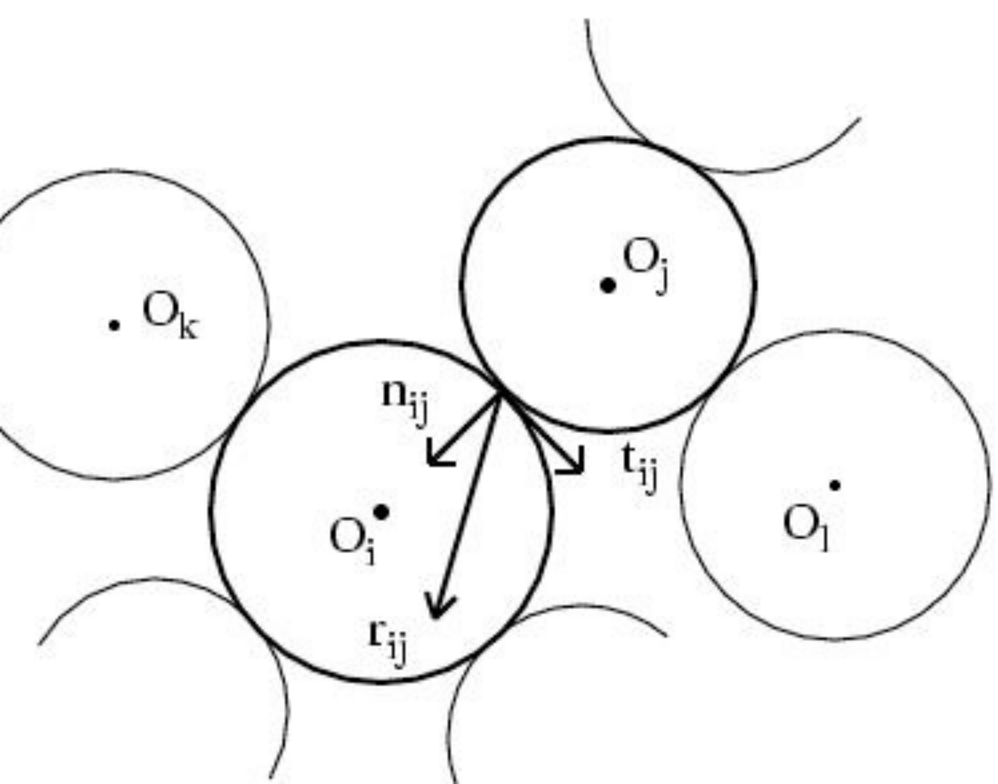


$u_n, u_t$

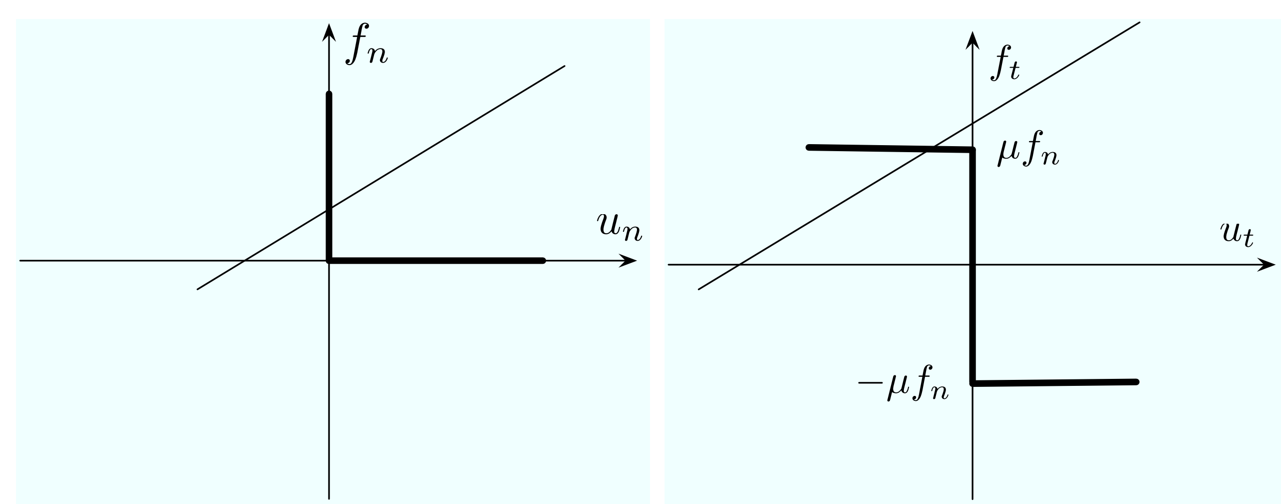

# The μ(I)-rheology

$$V(z)$$

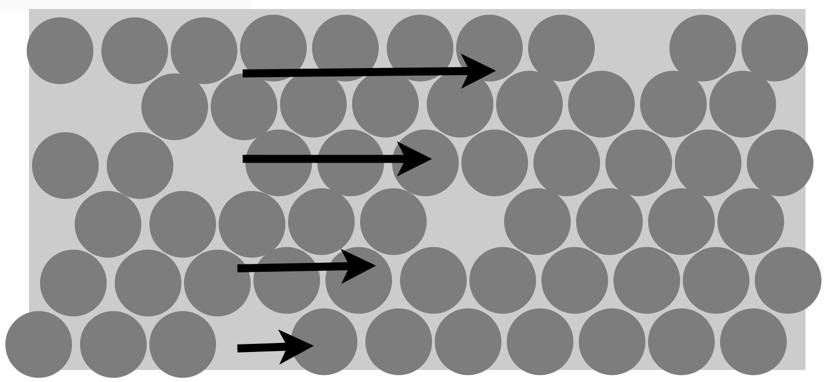

constitutive law?

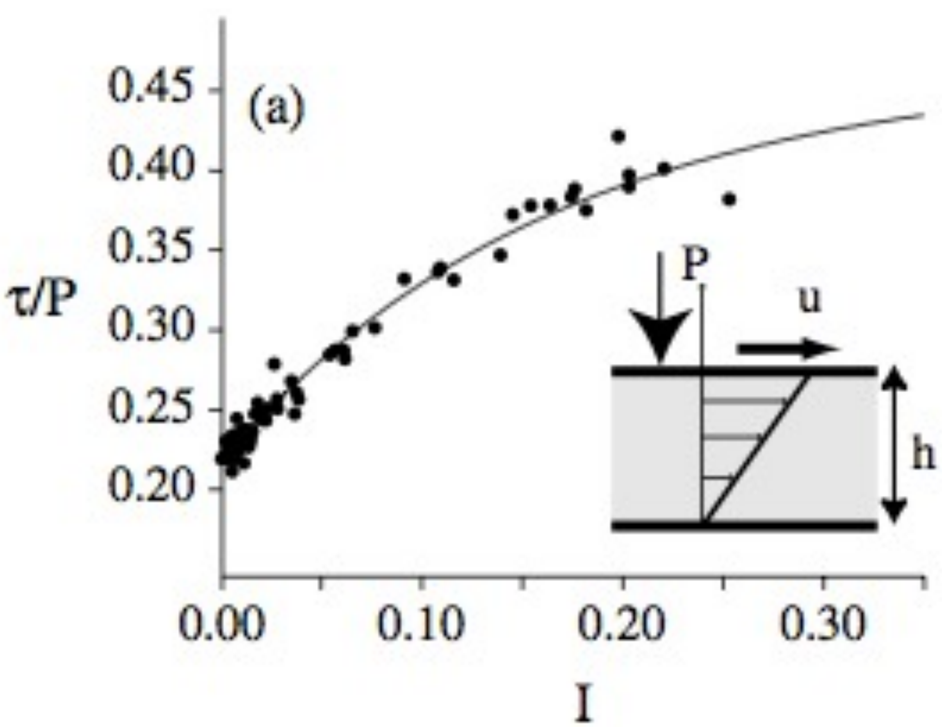


$$V(z)$$

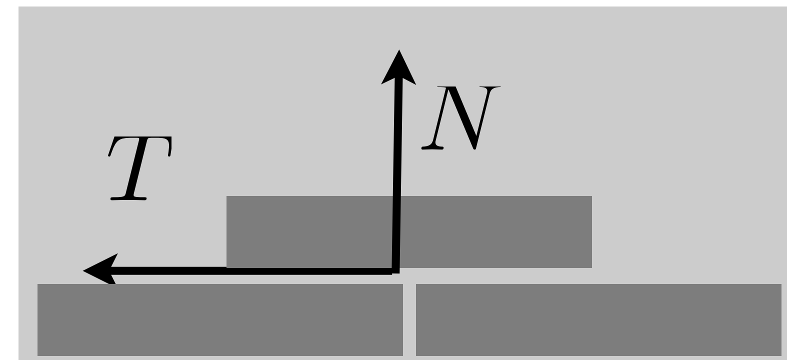


$$T = \mu N$$

Coulomb dry friction

Coulomb friction law

$$\tau = \mu P$$

# The μ(I)-rheology

$V(z)$

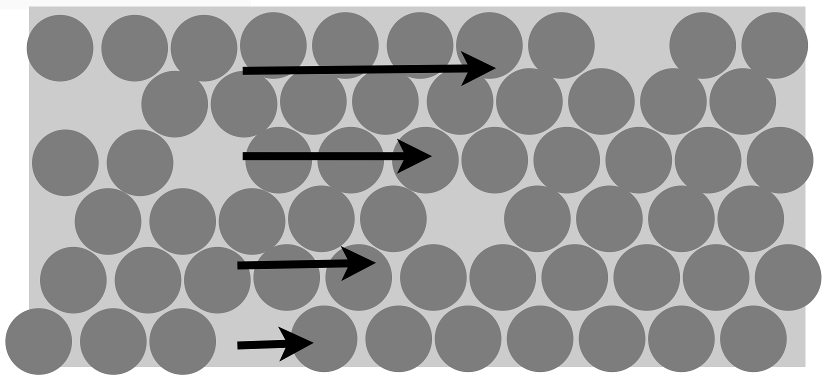

$V(z)$

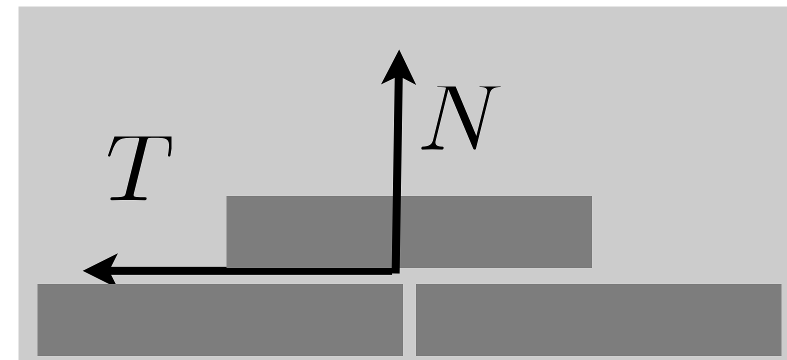


$$T = \mu N$$

Coulomb friction law

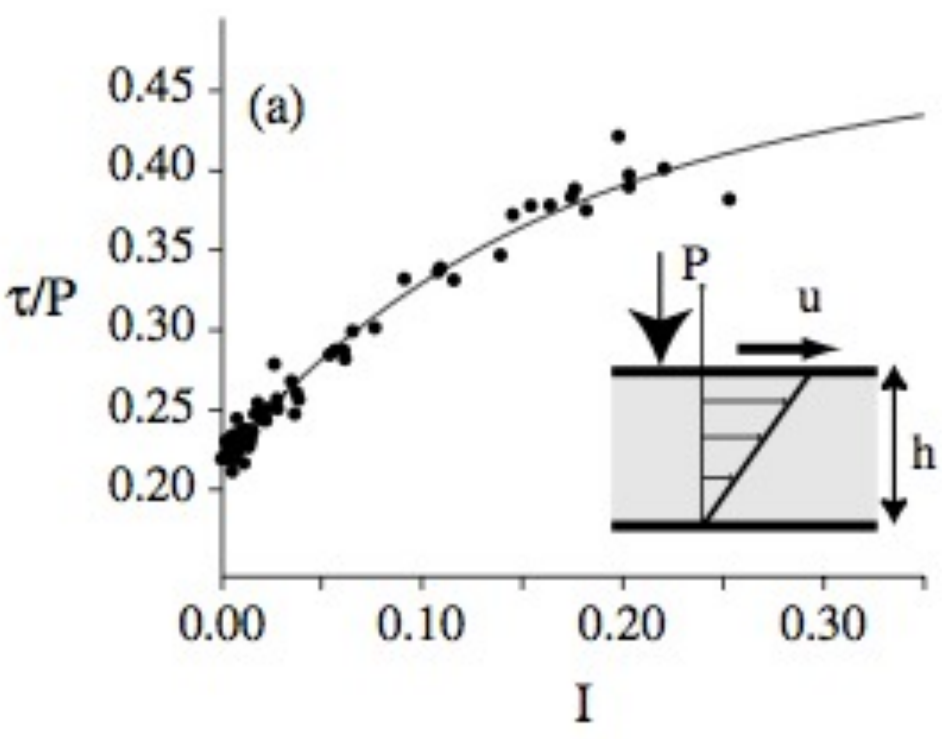


$$I = \frac{d \frac{\partial u}{\partial y}}{\sqrt{P/\rho}}$$

$$\tau = \mu(I) P$$

non dimensional number: «Froude»

local «Inertial Number» (Da Cruz 04-05)

# The μ(I)-rheology

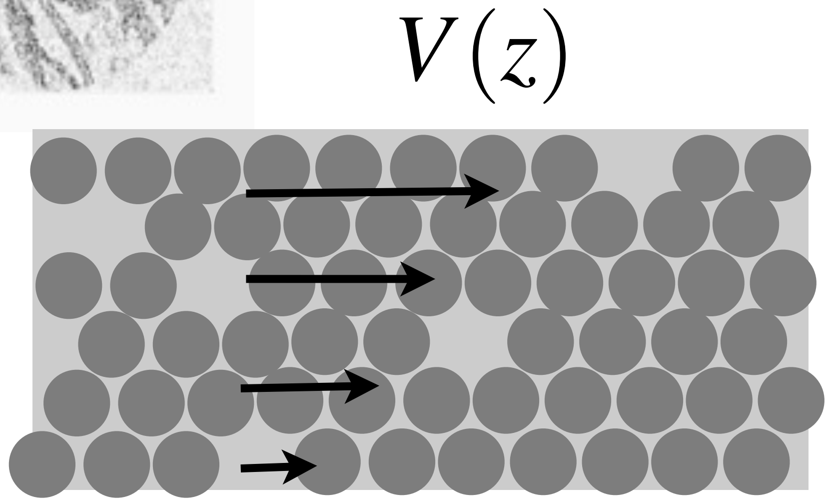



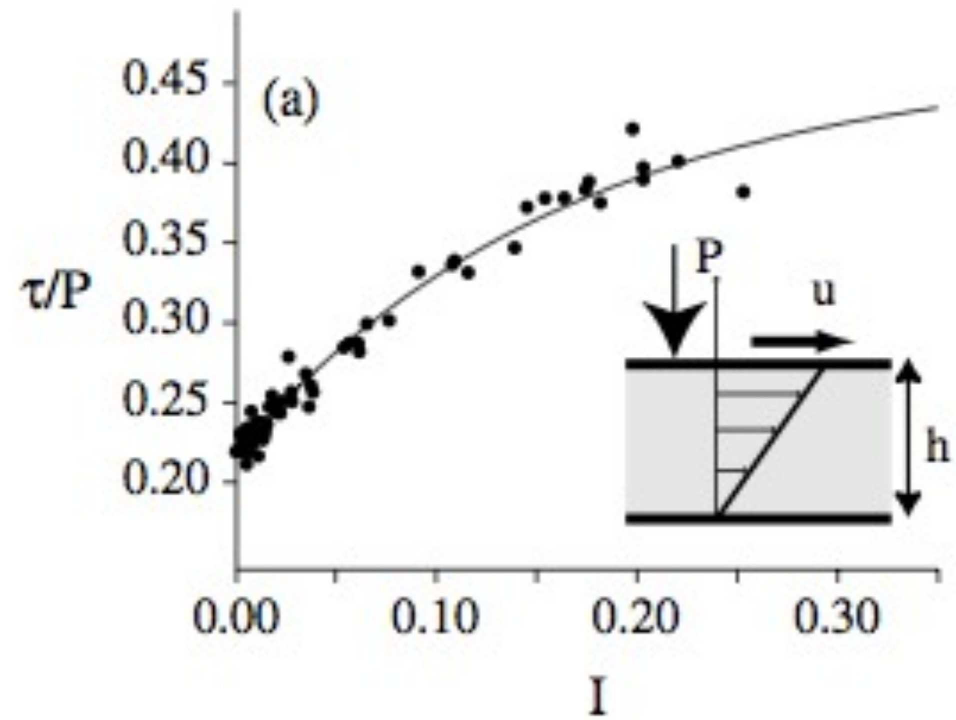



$$\frac{\text{falling time}}{\text{displacement time}} \qquad I = \frac{d\frac{\partial u}{\partial y}}{\sqrt{P/\rho}}$$

non dimensional number: «Froude»

local «Inertial Number» (Da Cruz 04-05)

# The μ(I)-rheology

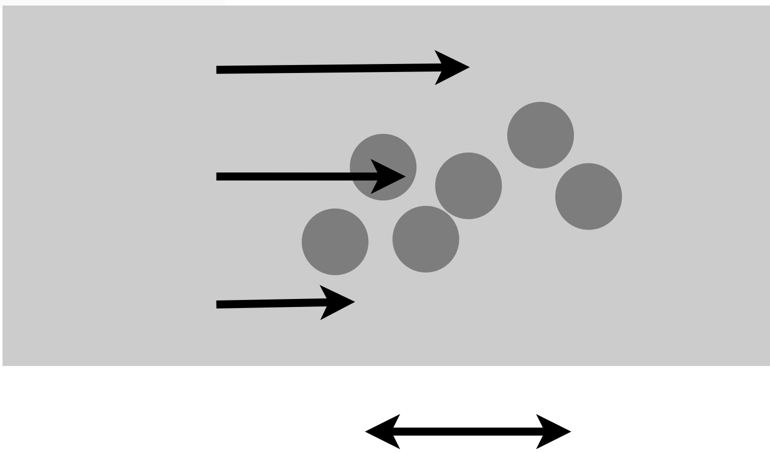

$$\frac{dx}{dt} = d\frac{\partial u}{\partial y} \qquad t = 1/\frac{\partial u}{\partial y}$$

$$\frac{\text{falling time}}{\text{displacement time}} \qquad I = \frac{d\frac{\partial u}{\partial y}}{\sqrt{P/\rho}}$$

# The μ(I)-rheology

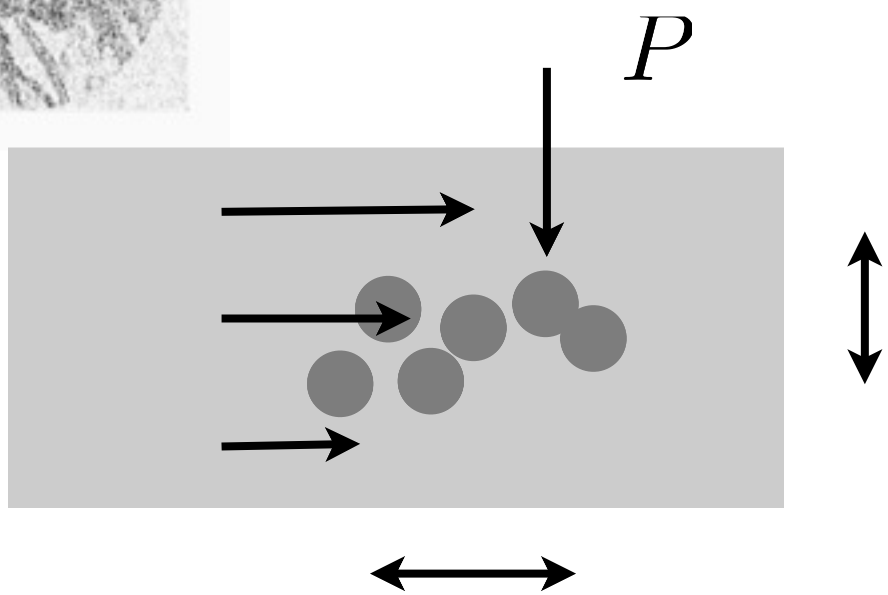


$$md^2y/dt^2 = Pd^2$$

$$t^2 = \rho d^2/(P)$$

$$t = 1/\frac{\partial u}{\partial y}$$

$$\frac{\text{falling time}}{\text{displacement time}}$$

$$I = \frac{d\frac{\partial u}{\partial y}}{\sqrt{P/\rho}}$$

# The μ(I)-rheology

$u(y)$

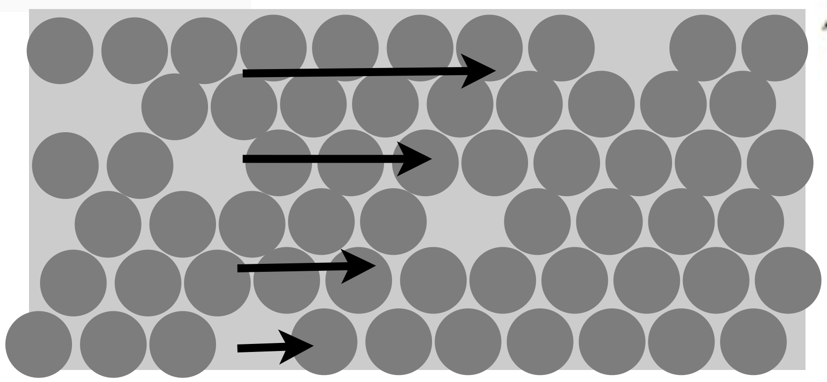

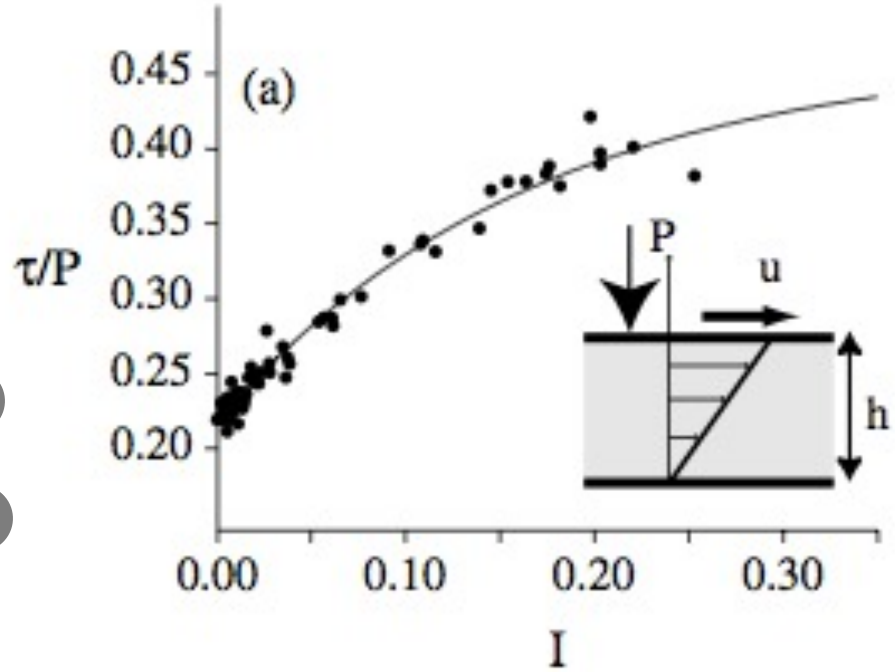


by grain dynamics

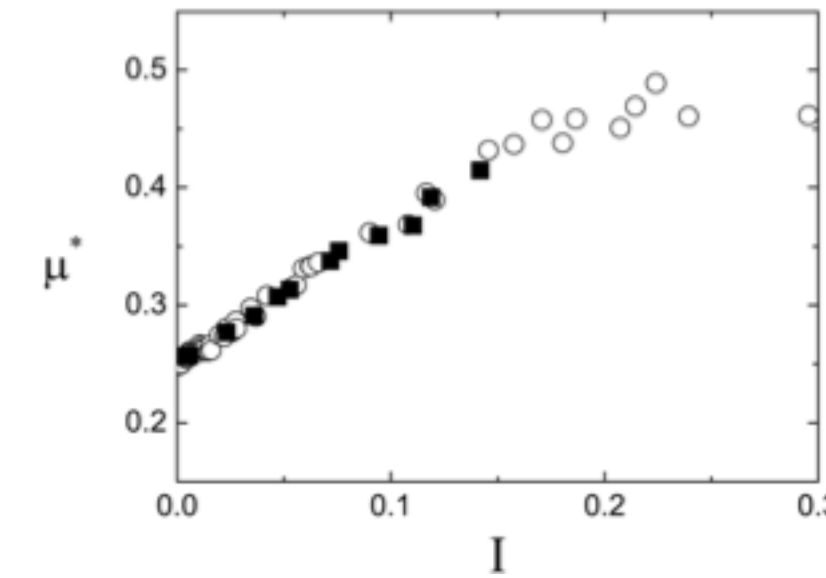


Da Cruz PRE 05

Coulomb friction law

$$\tau = \mu(I)P$$

$$\frac{\text{falling time}}{\text{displacement time}} \qquad I = \frac{d\frac{\partial u}{\partial y}}{\sqrt{P/\rho}}$$

Pouliquen 99
Pouliquen Forterre JSM 06
Da Cruz 04-05
GDR Midi 04
Josserand Lagrée Lhuillier 04

# The μ(I)-rheology

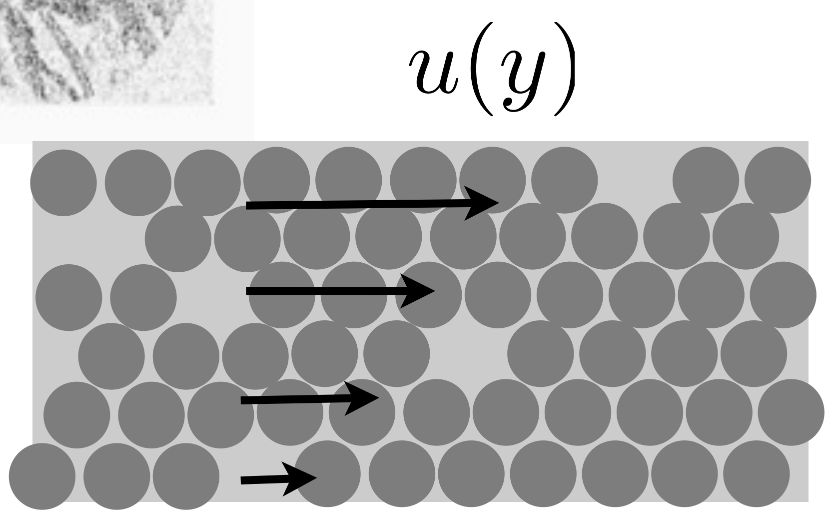


by grain dynamics

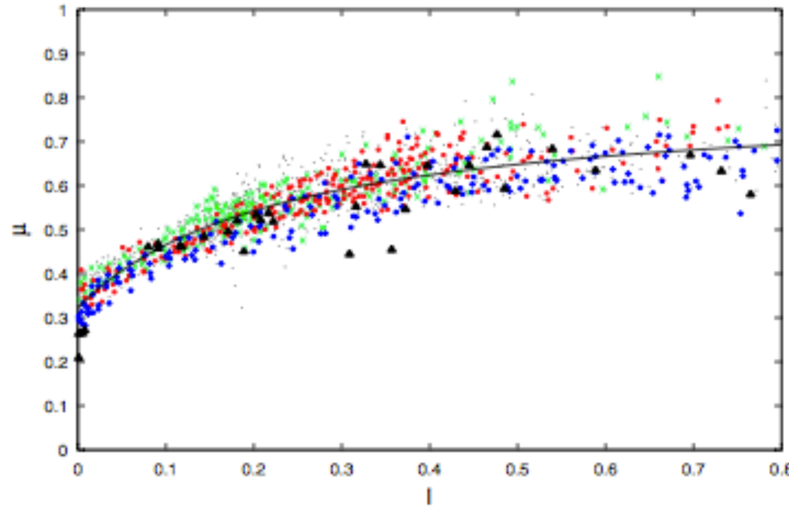


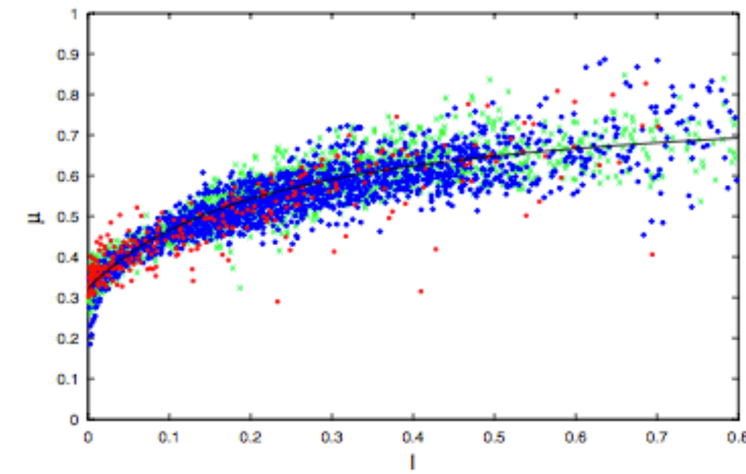


Lacaze Kerswell 09

## Coulomb friction law

$$\tau = \mu(I)P$$

$$I = \frac{d\frac{\partial u}{\partial y}}{\sqrt{P/\rho}}$$

$$\mu(I) = \mu_1 + \frac{\mu_2 - \mu_1}{I_0/I + 1}$$

$$\mu_1 \simeq 0.32 \quad (\mu_2 - \mu_1) \simeq 0.23 \quad I_0 \simeq 0.3$$

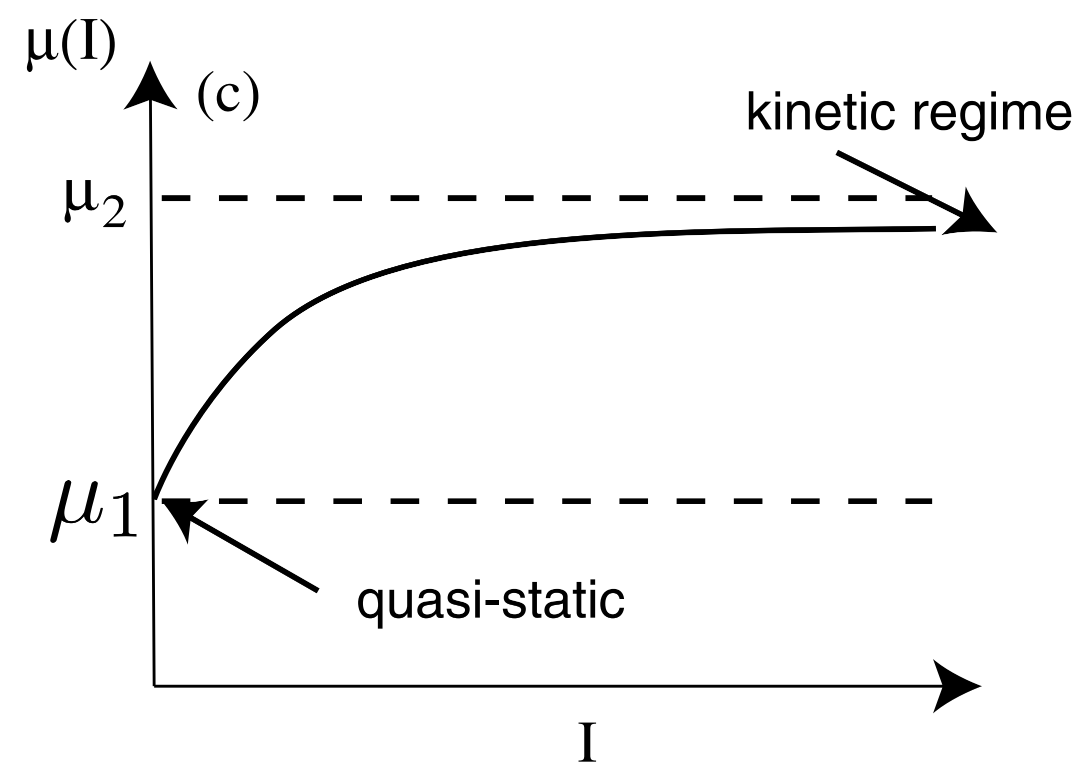

# The μ(I)-rheology

Jop Forterre Pouliquen 2005

$u(y)$

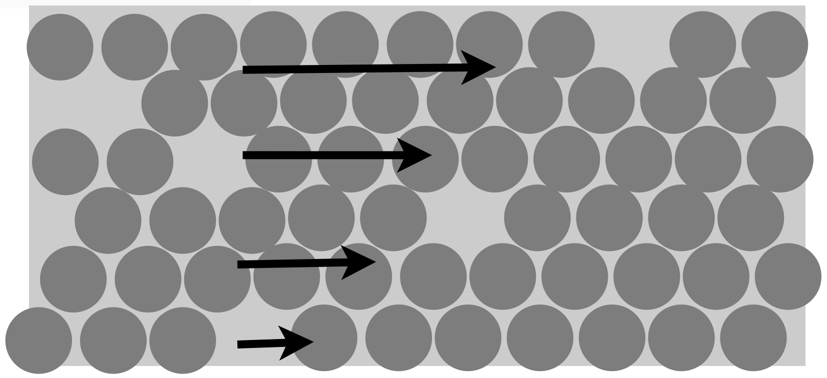

Coulomb friction law

$$\tau = \mu(I) P \qquad I = \frac{d\frac{\partial u}{\partial y}}{\sqrt{P/\rho}}$$

«Drucker-Prager» plastic flow

«equivalent» viscosity

$$\eta \frac{\partial u}{\partial y} = \mu(I) p \;\; \rightarrow \;\; \eta = \frac{\mu(I) p}{\frac{\partial u}{\partial y}}$$

# The μ(I)-rheology implementation in Navier Stokes?

Jop Forterre Pouliquen 2005

$$\mu(I) = \mu_1 + \frac{\mu_2 - \mu_1}{I_0/I + 1}$$

$$D_2 = \sqrt{D_{ij} D_{ij}} \qquad D_{ij} = \frac{u_{i,j} + u_{j,i}}{2}$$

construction of a viscosity based on the *D*2 invariant and redefinition of *I*

$$I = d\sqrt{2} D_2 / \sqrt{(|p|/\rho)}.$$

$$\eta = \left( \frac{\mu(I)}{\sqrt{2} D_2} p \right)$$

«Drucker-Prager»

$$\nabla \cdot \mathbf{u} = 0, \quad \rho \left( \frac{\partial \mathbf{u}}{\partial t} + \mathbf{u} \cdot \nabla \mathbf{u} \right) = -\nabla p + \nabla \cdot (2\eta \mathbf{D}) + \rho g,$$

Boundary Conditions: no slip and *P=0* at the interface

# outline

- what is a granular fluid? some images
- the μ(I) friction law obtained from experiments and discrete simulation
- the viscosity associated to the μ(I) friction law
- the Saint Venant Savage Hutter Hyperbolic model
- implementing the μ(I) friction law in Navier Stokes
- Examples of flows: focusing on the granular column collapse (limits of Saint Venant Savage Hutter Hyperbolic model)


ST VENANT
pyl

- # Couche Mince Saint Venant Shallow Water Savage Hutter

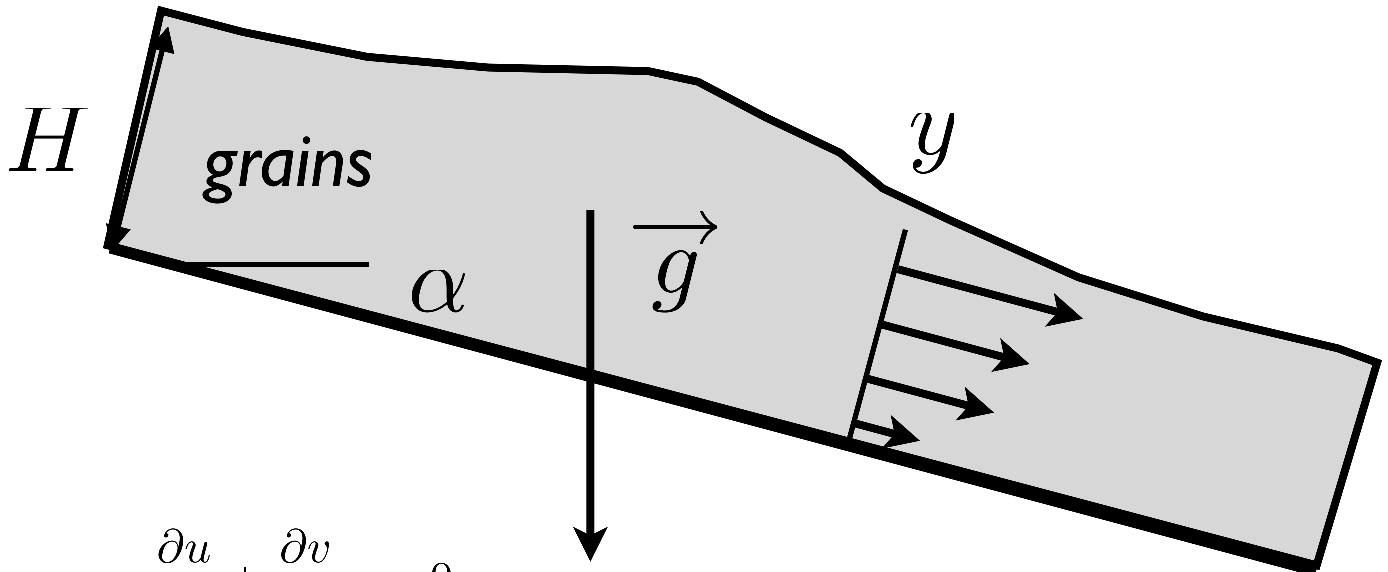


$$\varepsilon = H/L$$

$$\begin{cases} \dfrac{\partial u}{\partial x} + \dfrac{\partial v}{\partial y} = 0 \\ \rho(\dfrac{\partial u}{\partial t} + \dfrac{\partial u^2}{\partial x} + \dfrac{\partial uv}{\partial y}) = -g\rho \sin\alpha - \dfrac{\partial p}{\partial x} + \dfrac{\partial \tau_{xx}}{\partial x} + \dfrac{\partial \tau_{xy}}{\partial y} \\ \rho(\dfrac{\partial v}{\partial t} + \dfrac{\partial uv}{\partial x} + \dfrac{\partial v^2}{\partial y}) = -g\rho \cos\alpha - \dfrac{\partial p}{\partial y} + \dfrac{\partial \tau_{yx}}{\partial x} + \dfrac{\partial \tau_{yy}}{\partial y} \end{cases}$$

$$p = -\rho g \cos\alpha(\eta(x,t) - y)$$

$$\tau_{xy} = \rho g H \sin\alpha \bar{\tau}_{xy}$$

$$\rho U_0^2/L \longleftrightarrow -\frac{\partial p}{\partial x} = -\rho g \frac{\partial \eta}{\partial x}$$

$$\rho U_0^2/(H/\varepsilon) = \rho g \varepsilon.$$

$$\boxed{U_0 = \sqrt{gH}.}$$

# Saint-Venant Savage Hutter

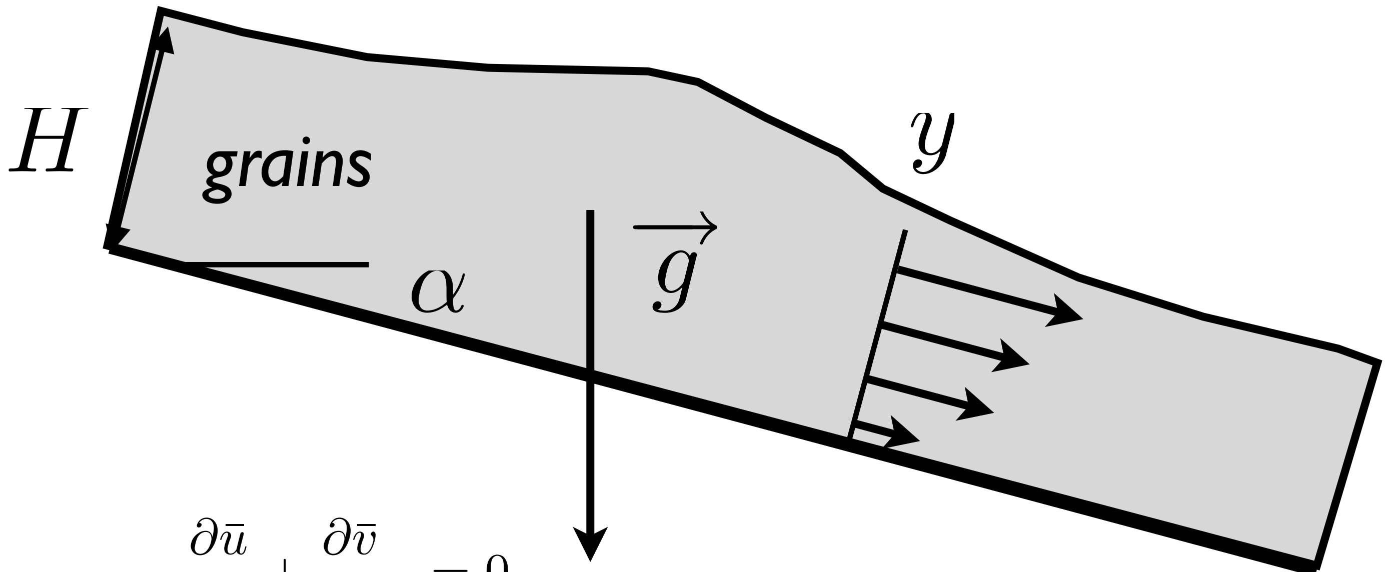


$$\varepsilon = H/L$$

$$\left\{\begin{aligned} \frac{\partial \bar u}{\partial \bar x} + \frac{\partial \bar v}{\partial \bar y} &= 0\\ \varepsilon\left(\frac{\partial \bar u}{\partial \bar t} + \frac{\partial \bar u^2}{\partial \bar x} + \frac{\partial \bar u \bar v}{\partial \bar y}\right) &= -\sin\alpha - \varepsilon\frac{\partial \bar p}{\partial \bar x} + \sin\alpha\varepsilon\frac{\partial \bar\tau_{xx}}{\partial \bar x} + \sin\alpha\frac{\partial \bar\tau_{xy}}{\partial \bar y}\\ \varepsilon^2\left(\frac{\partial \bar v}{\partial \bar t} + \frac{\partial \bar u \bar v}{\partial x} + \frac{\partial \bar v^2}{\partial \bar y}\right) &= -\cos\alpha - \frac{\partial \bar p}{\partial \bar y} + \sin\alpha\varepsilon\frac{\partial \bar\tau_{yy}}{\partial \bar x} + \sin\alpha\frac{\partial \bar\tau_{yx}}{\partial \bar y} \end{aligned}\right.$$

$$p = -\rho g \cos\alpha(\eta(x,t) - y) \qquad \tau_{xy} = \rho g H \sin\alpha \bar\tau_{xy}$$

$$\rho U_0^2/L \longleftrightarrow -\frac{\partial p}{\partial x} = -\rho g \frac{\partial \eta}{\partial x}$$

$$\rho U_0^2/(H/\varepsilon) = \rho g \varepsilon.$$

$$\boxed{U_0 = \sqrt{gH}.}$$

Saint-Venant Savage Hutter

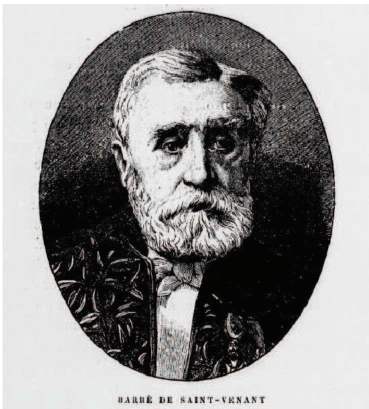

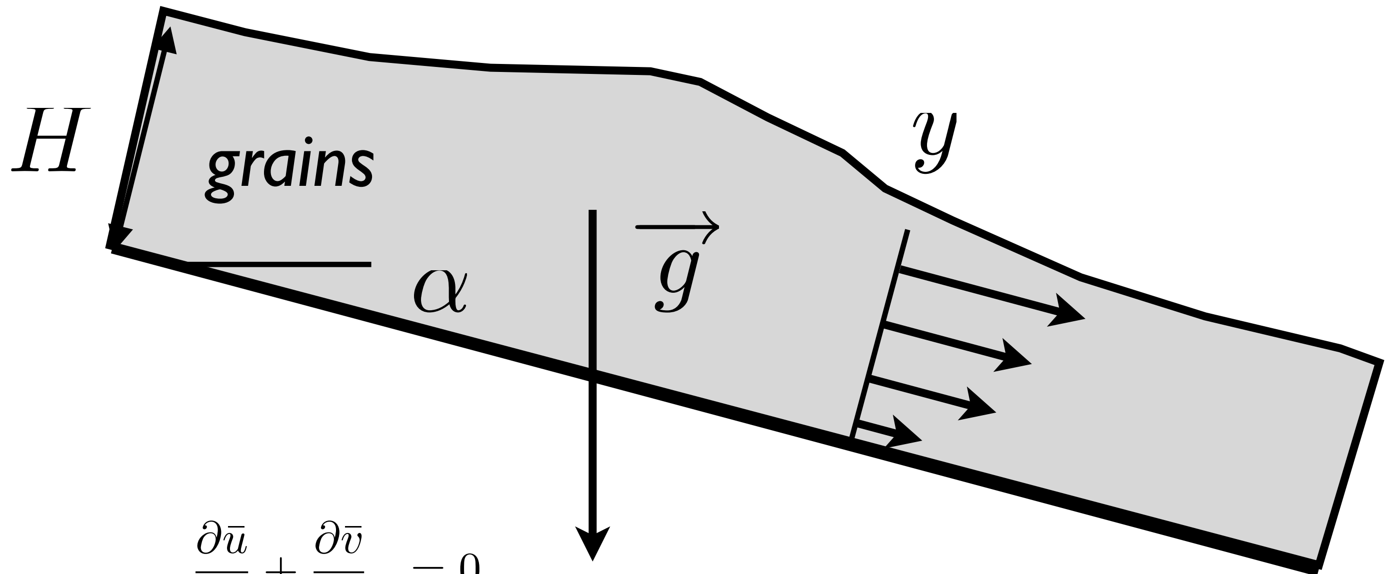


$$\begin{cases} \dfrac{\partial \bar{u}}{\partial \bar{x}} + \dfrac{\partial \bar{v}}{\partial \bar{y}} &= 0 \\ \varepsilon(\dfrac{\partial \bar{u}}{\partial \bar{t}} + \dfrac{\partial \bar{u}^2}{\partial \bar{x}} + \dfrac{\partial \bar{u}\bar{v}}{\partial \bar{y}}) &= -\sin\alpha - \varepsilon \dfrac{\partial \bar{p}}{\partial \bar{x}} + \sin\alpha \dfrac{\partial \bar{\tau}_{xy}}{\partial \bar{y}} \\ 0 &= -\cos\alpha - \dfrac{\partial \bar{p}}{\partial \bar{y}} \end{cases}$$

$$\int dy$$

μ(I) at the wall

$$\frac{\partial h}{\partial t} + \frac{\partial}{\partial x} \int_f^\eta u(x,y,t)dy = 0$$

$$\frac{\partial}{\partial t} \int_f^\eta u(x,y,t)dy + \frac{\partial}{\partial x}(\int_f^\eta u(x,y,t)^2 dy + \cos\alpha \frac{g}{2}(h^2)) = -gh\sin(\alpha) - \cos\alpha g h \frac{d}{dx} f - \mu(I(0))gh\cos(\alpha).$$

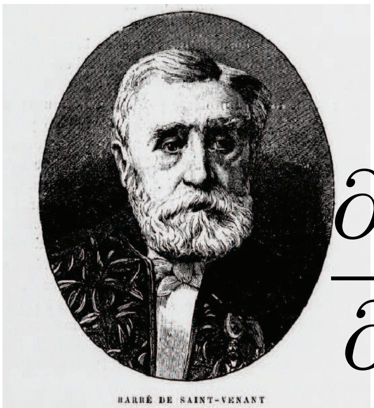

Saint-Venant Savage Hutter

$$\frac{\partial h}{\partial t} + \frac{\partial (Q)}{\partial x} = 0 \quad \frac{\partial Q}{\partial t} + \frac{\partial}{\partial x}(\frac{5Q^2}{4h} + \frac{g}{2}(h^2)) = -gh\mu(I)\frac{Q}{|Q|}$$

# Integral over the layer of grains

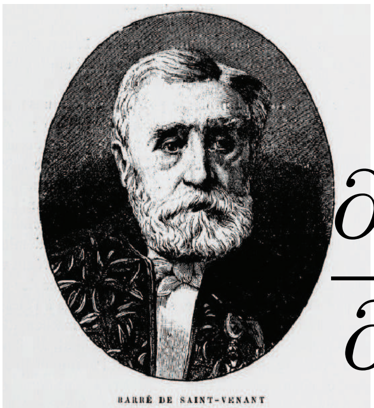


Saint-Venant Savage Hutter *Gerris*

$$\frac{\partial h}{\partial t} + \frac{\partial (Q)}{\partial x} = 0 \quad \frac{\partial Q}{\partial t} + \frac{\partial}{\partial x}(\frac{5Q^2}{4h} + \frac{g}{2}(h^2)) = -gh\mu(I)\frac{Q}{|Q|}$$

*Gerris* is a free finite volume code by Stéphane Popinet

one part of the code is a Shallow Water solver

$$\frac{Q^* - Q^n}{\Delta t} + \frac{\partial}{\partial x}(\frac{Q^2}{h} + \frac{g}{2}(h^2)) = 0 \qquad \frac{Q^{n+1} - Q^*}{\Delta t} = -gh^*\mu(I^*)\frac{Q^{n+1}}{|Q^*|}$$

Audusse et al.

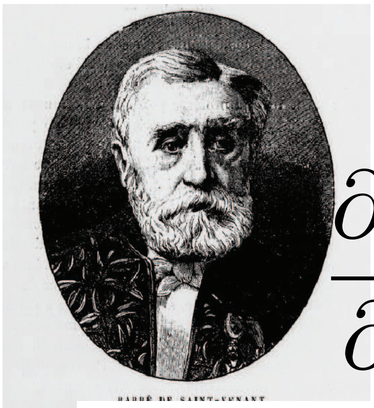

Saint-Venant Savage Hutter *Gerris*

$$\frac{\partial h}{\partial t} + \frac{\partial (Q)}{\partial x} = 0 \qquad \frac{\partial Q}{\partial t} + \frac{\partial}{\partial x}\left(\frac{5Q^2}{4h} + \frac{g}{2}(h^2)\right) = -gh\mu(I)\frac{Q}{|Q|}$$

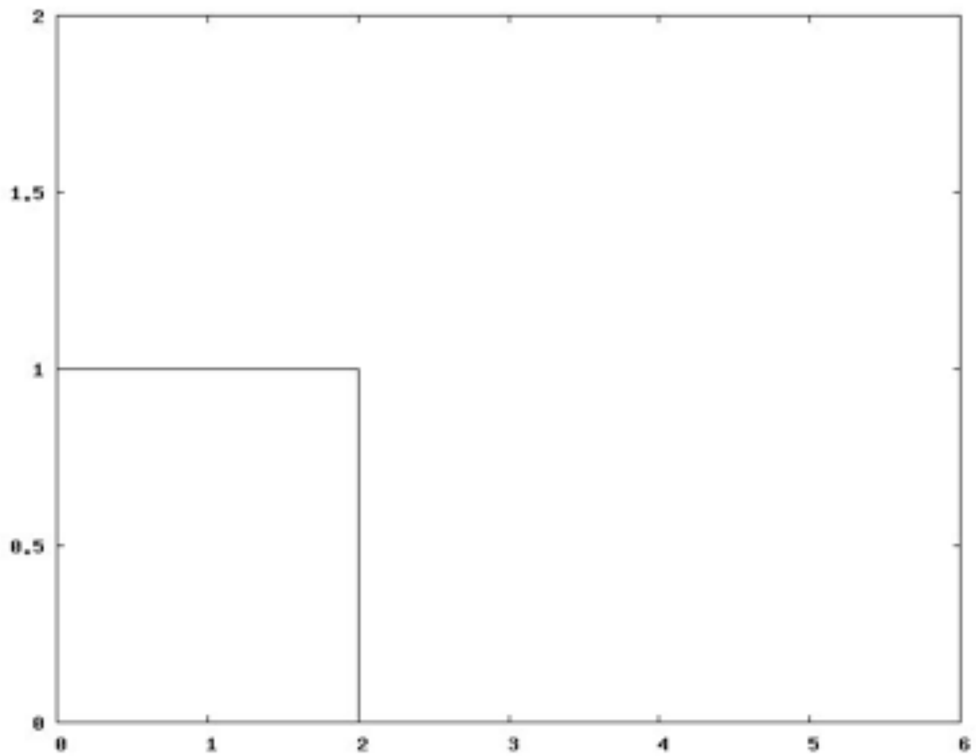


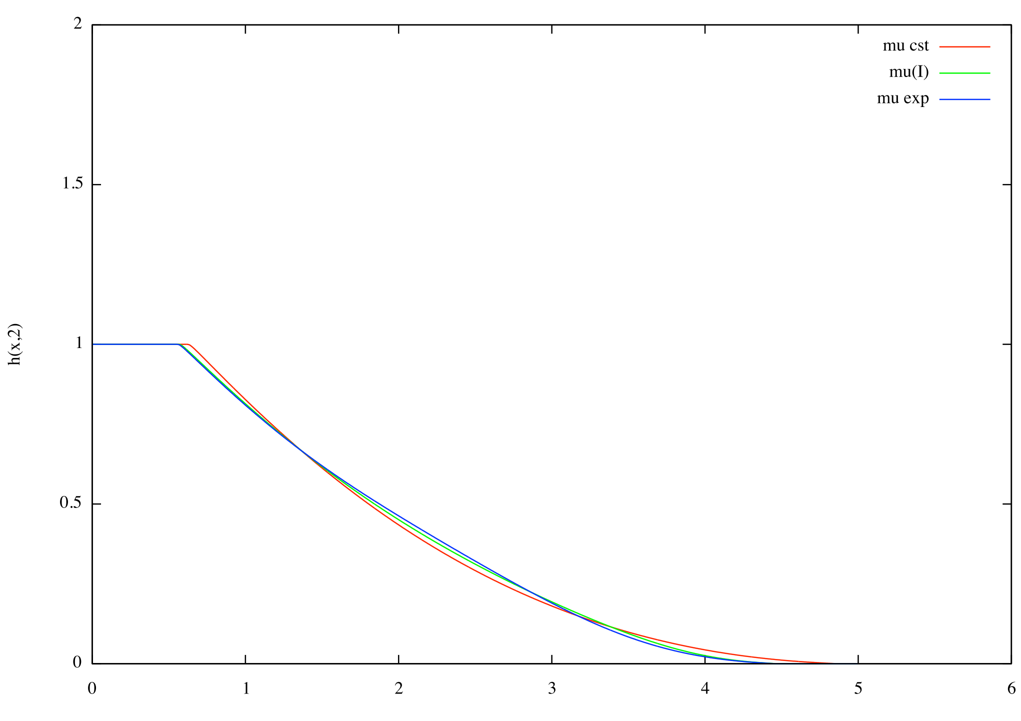


$$\mu(I) = \mu_s$$

$$\mu(I) = \mu_s + \frac{\Delta\mu}{\frac{I_0}{I} + 1}$$

$$\mu(I) = \mu_s + \Delta\mu e^{-\beta/I}$$

mu = 0.45
mu = (0.4 + 0.26/(0.4/In +1))
mu = (0.4 + 0.26*exp(-0.136/In))

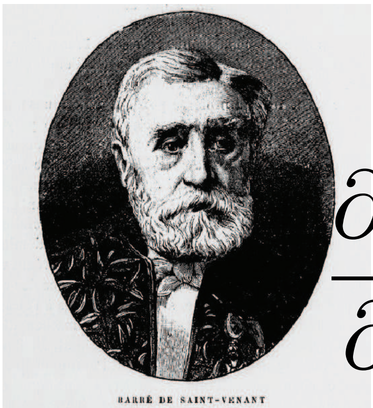


Saint-Venant Savage Hutter *Gerris*

$$\frac{\partial h}{\partial t} + \frac{\partial (Q)}{\partial x} = 0 \quad \frac{\partial Q}{\partial t} + \frac{\partial}{\partial x}\left(\frac{5Q^2}{4h} + \frac{g}{2}(h^2)\right) = -gh\mu(I)\frac{Q}{|Q|}$$

valid by hypothesis for small aspect ratio

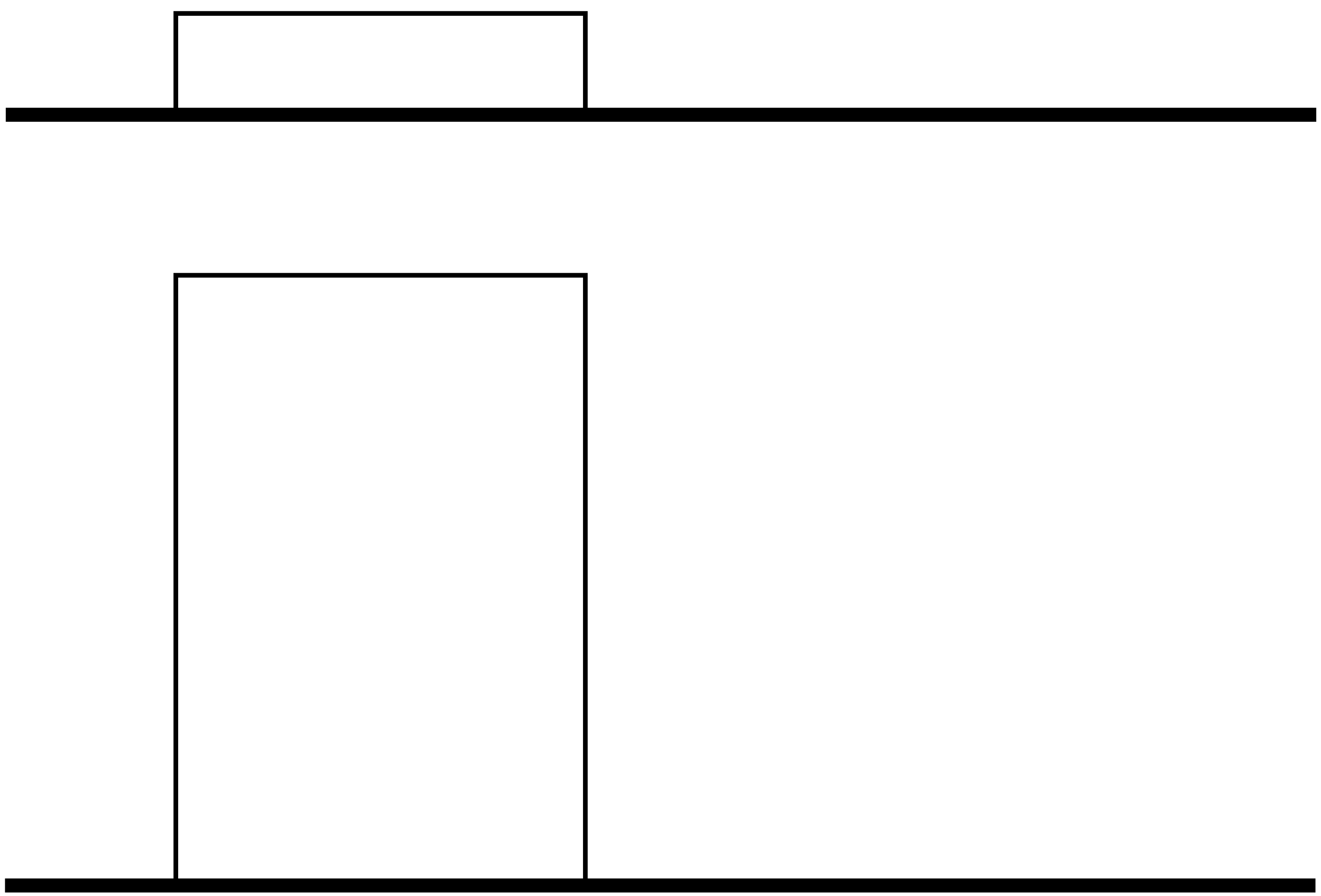

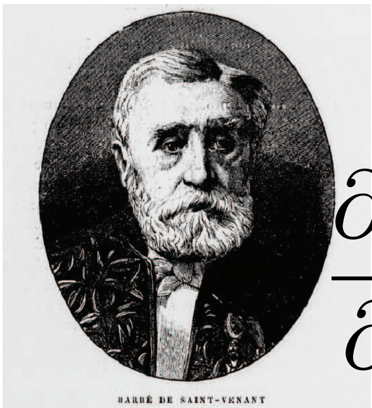

Saint-Venant Savage Hutter *Gerris*

$$\frac{\partial h}{\partial t} + \frac{\partial (Q)}{\partial x} = 0 \quad \frac{\partial Q}{\partial t} + \frac{\partial}{\partial x}\left(\frac{5Q^2}{4h} + \frac{g}{2}(h^2)\right) = -gh\mu(I)\frac{Q}{|Q|}$$

add a source term corresponding to pluviation

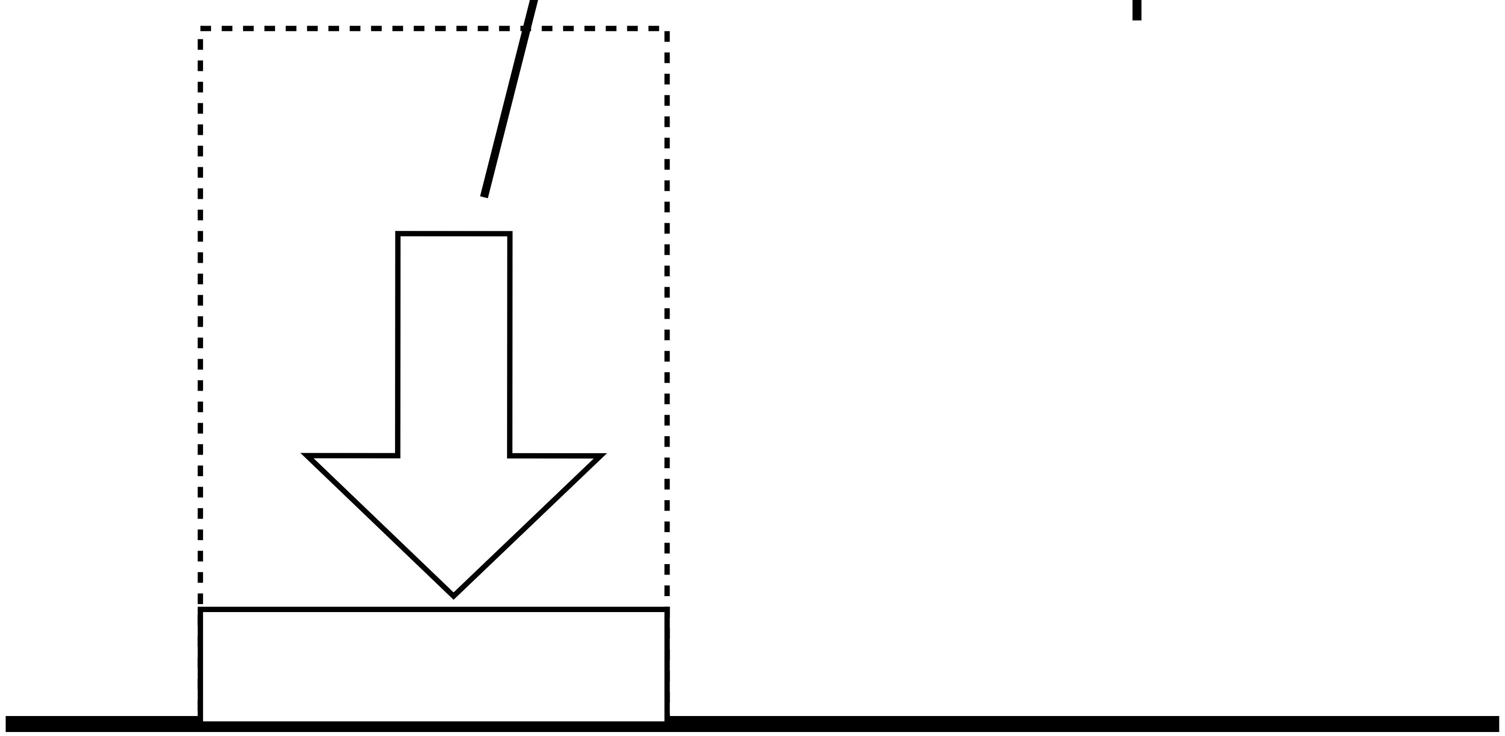

Saint-Venant Savage Hutter *Gerris* better description of the run-out

no pluviation

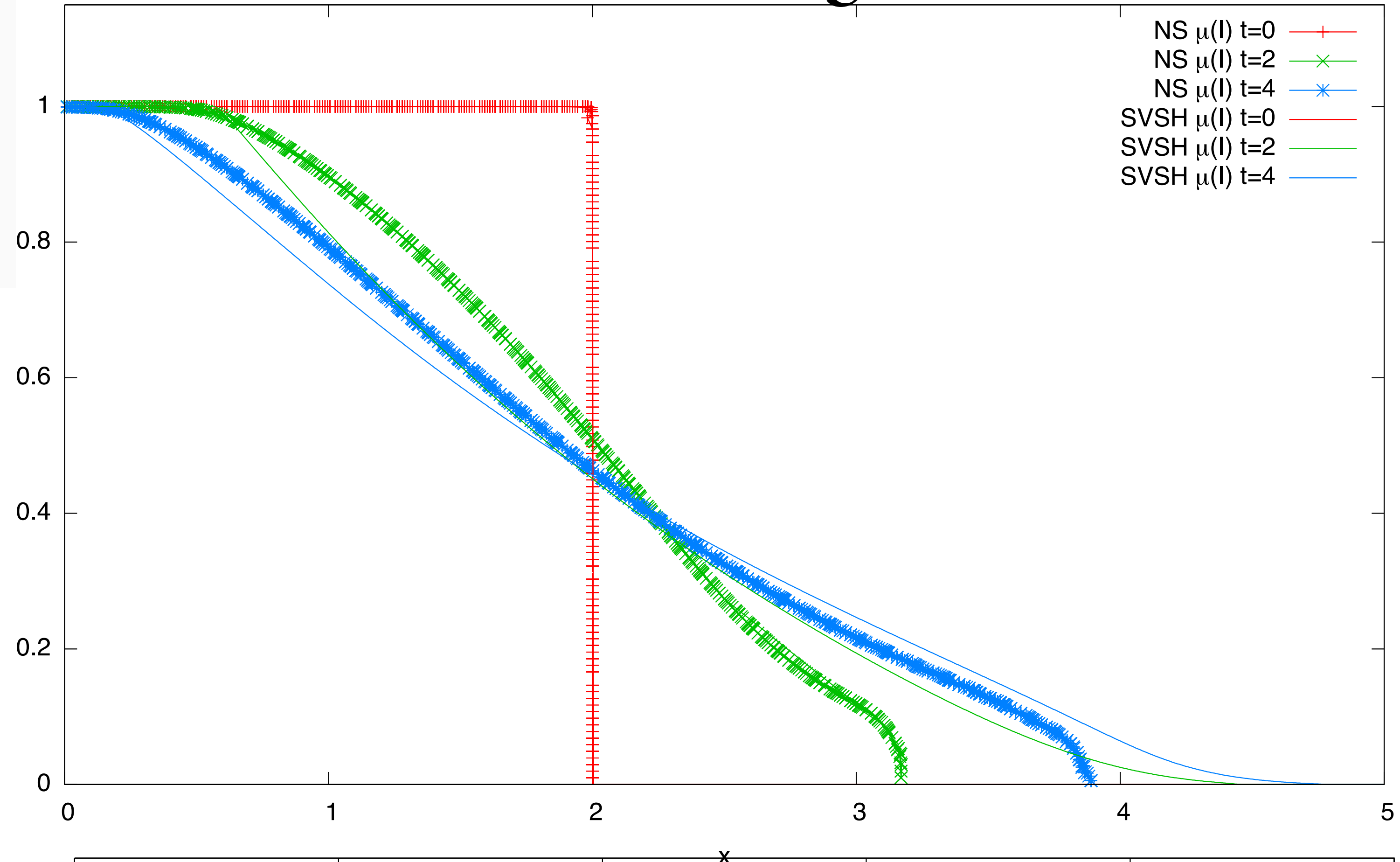


pluviation

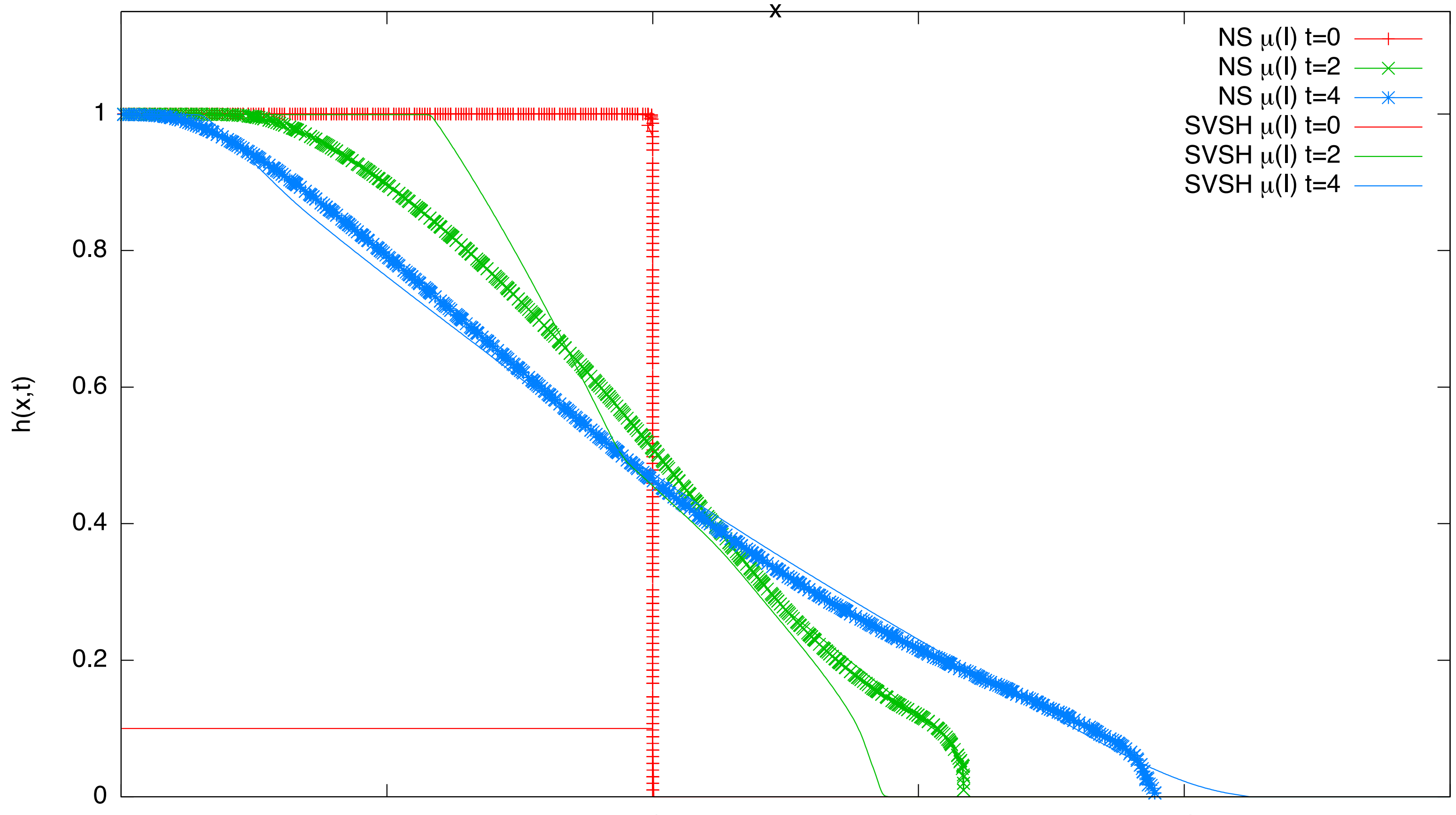


L. Satron, J. Hinch (DAMTP), A. Mangeney (IPGP), E. Larieu (IMFT)

# Saint-Venant Savage Hutter *Gerris*

better description of the run-out

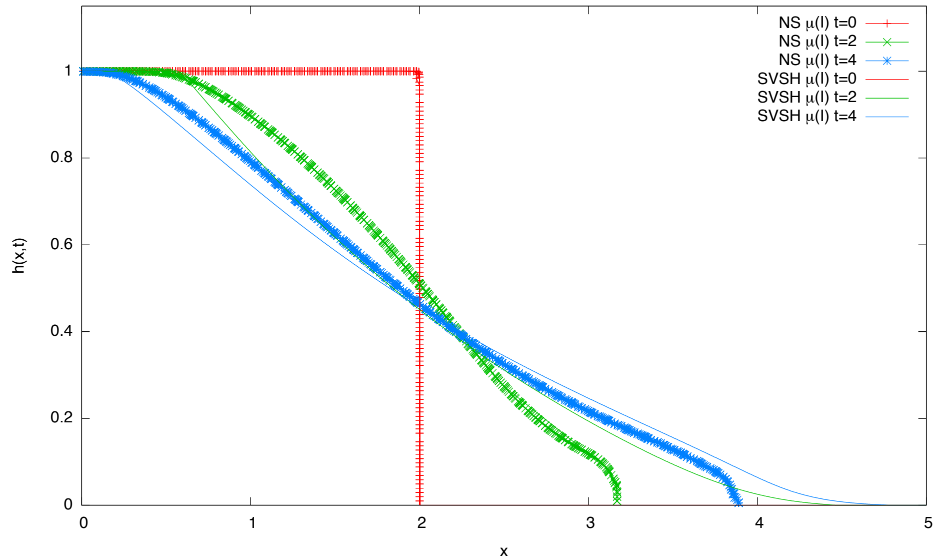


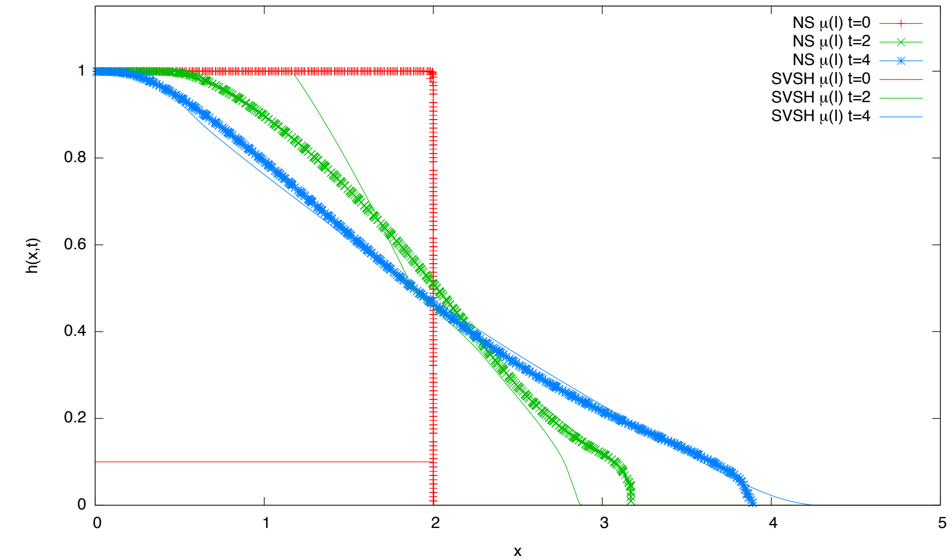


no pluviation

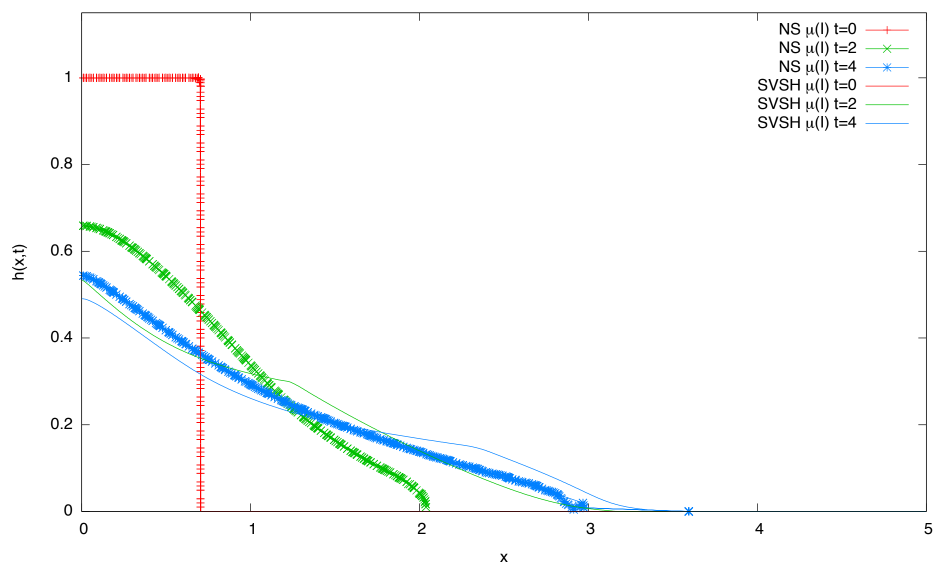


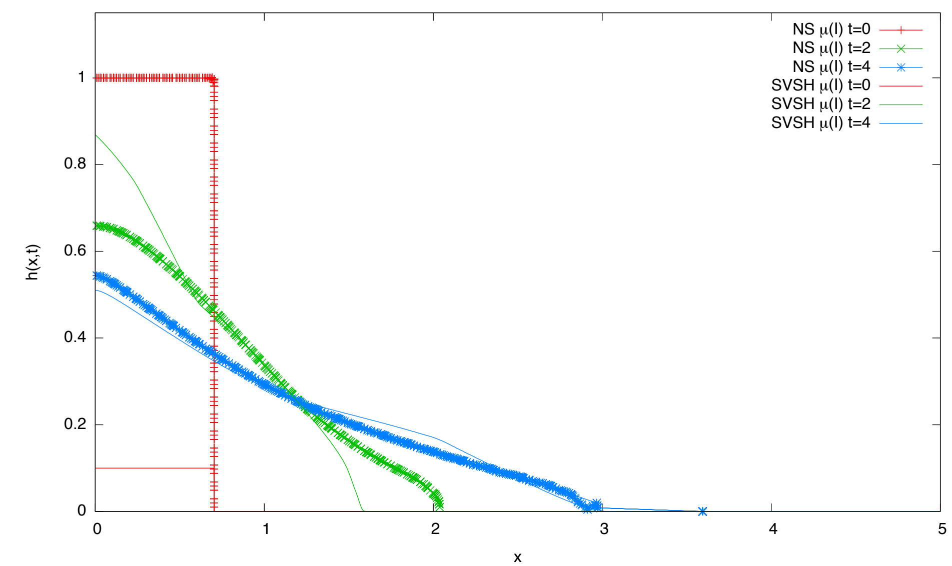


pluviation

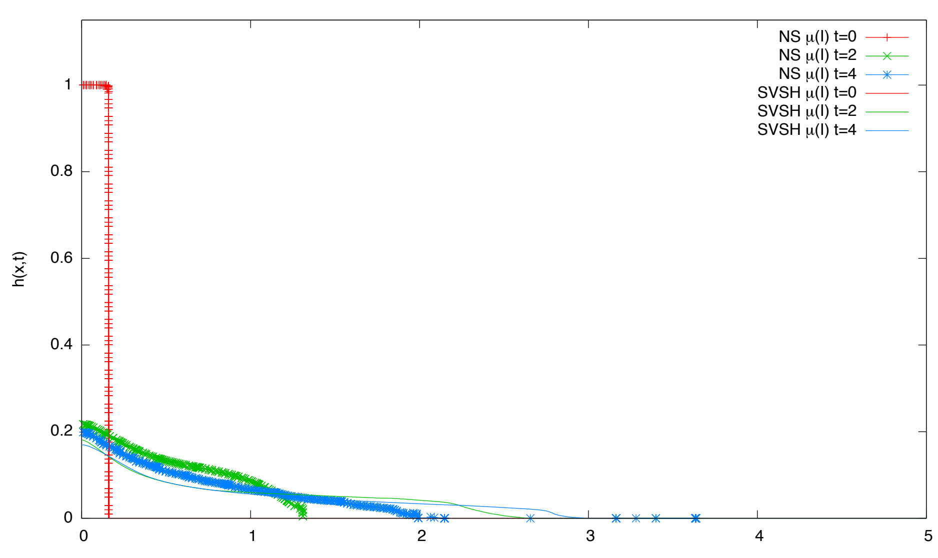


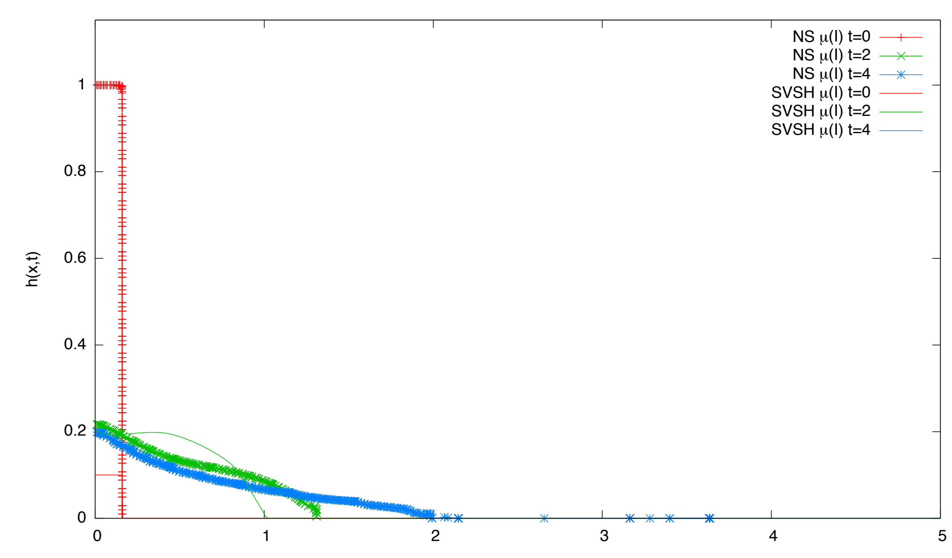


L. Satron, J. Hinch (DAMTP), A. Mangeney (IPGP), E. Larieu (IMFT)

Saint-Venant Savage Hutter *Gerris*

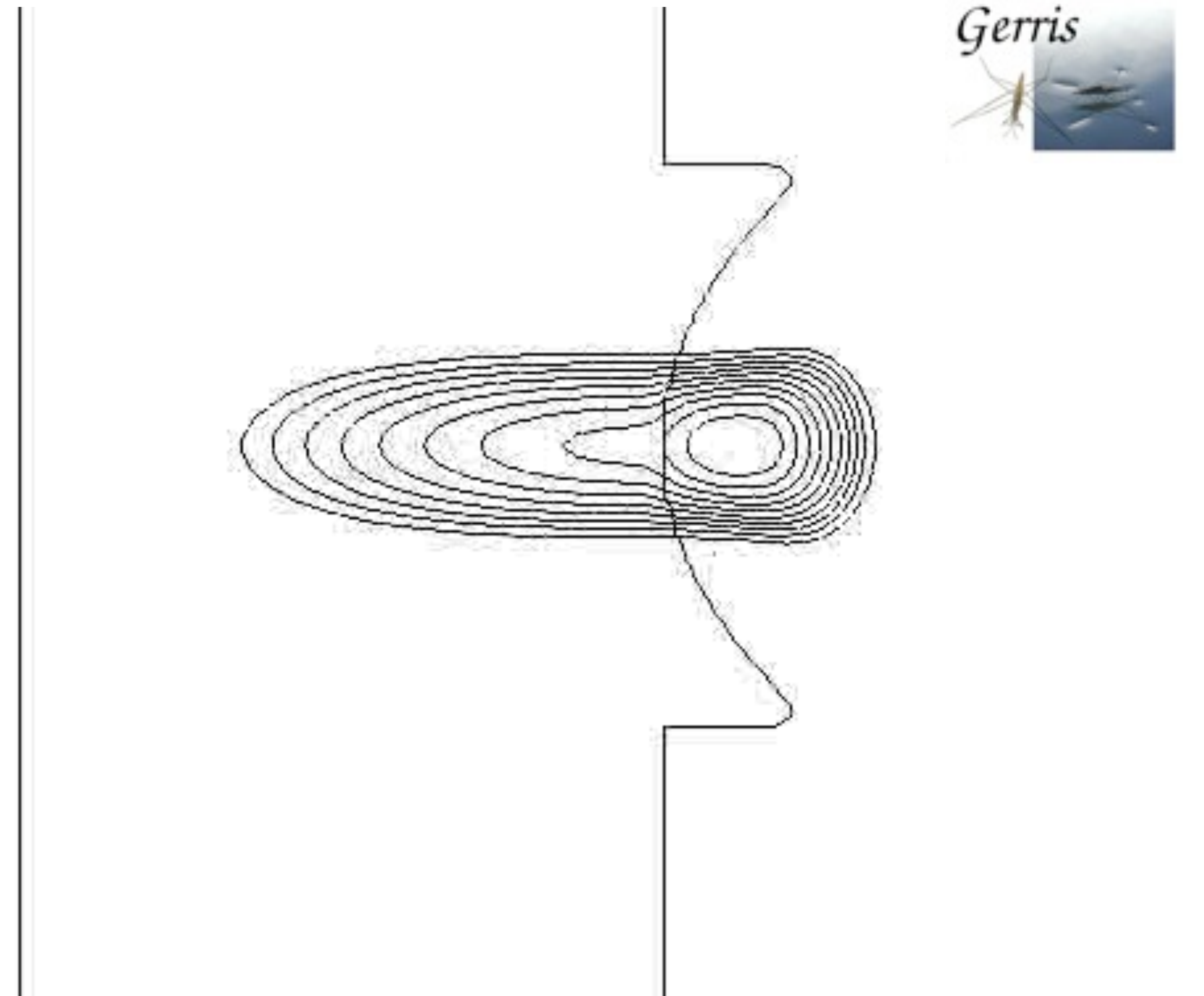


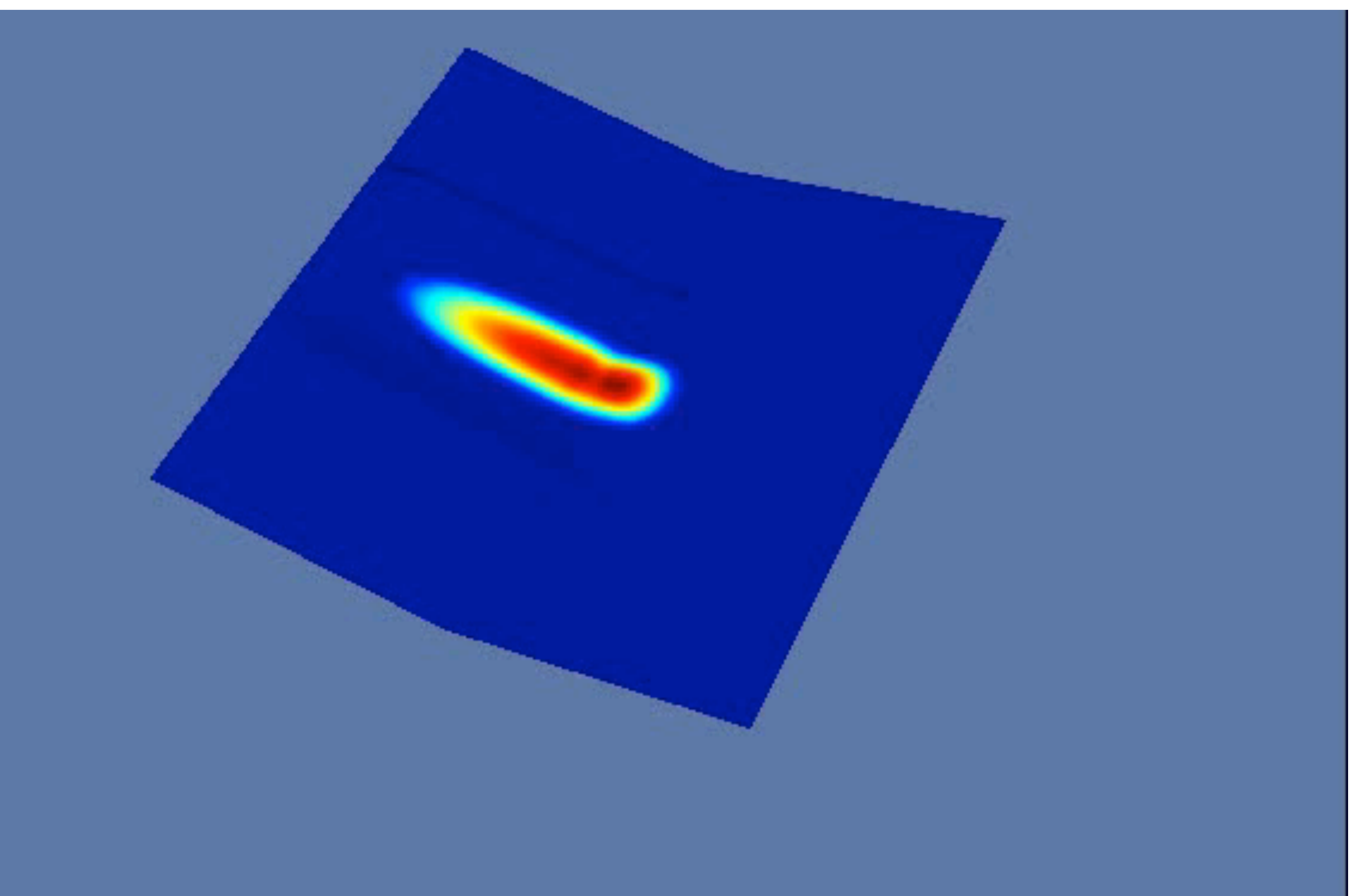

# Saint-Venant Savage Hutter *Gerris*

WIELAND, J. M. N. T. GRAY AND K. HUTTER 1999

Marina Pirulli, Marie-Odile Bristeau Anne Mangeney, Claudio Scavia 2006

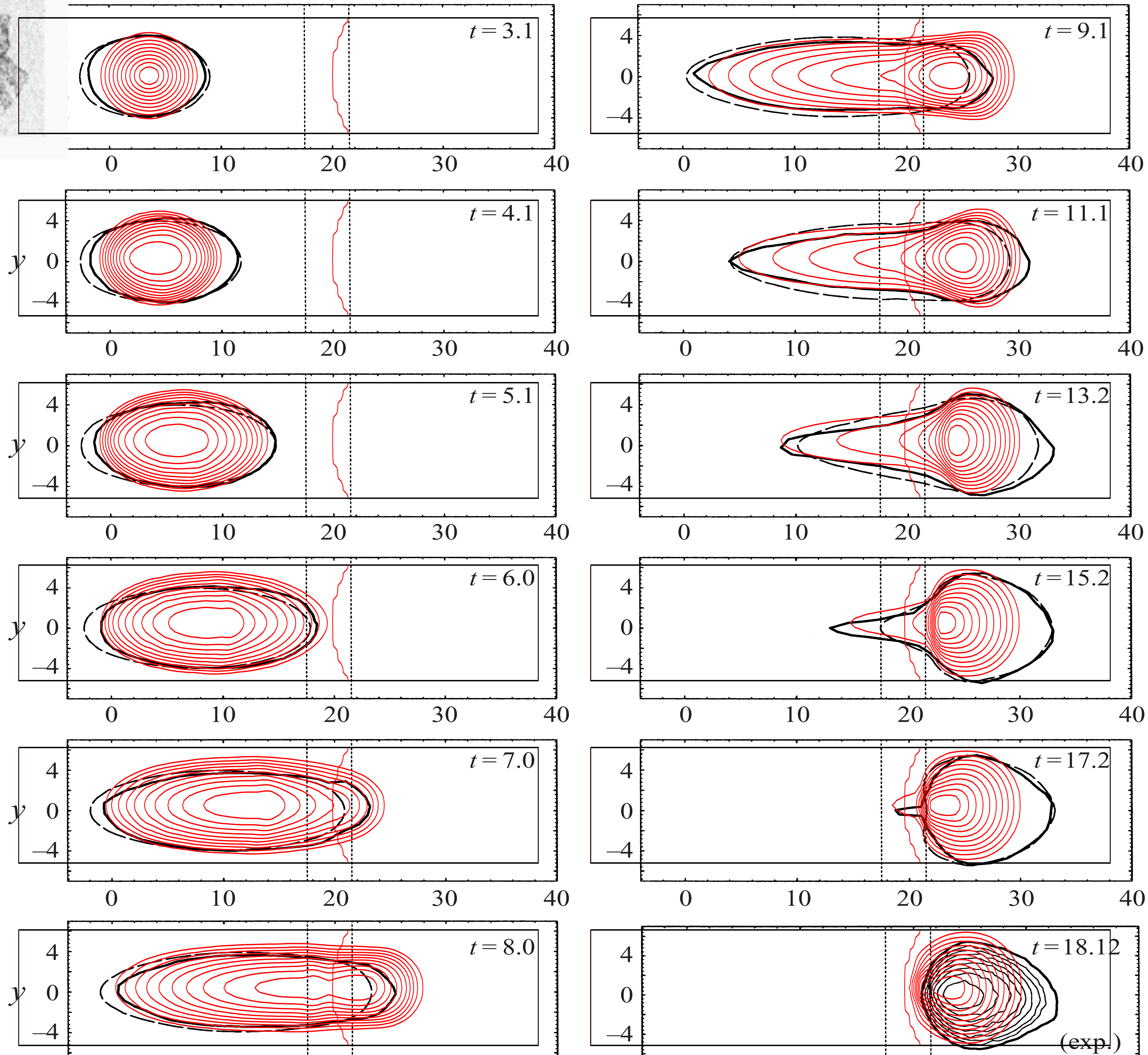

M. Pirulli et al. / Environmental Modelling & Software xx (2006) 1–18

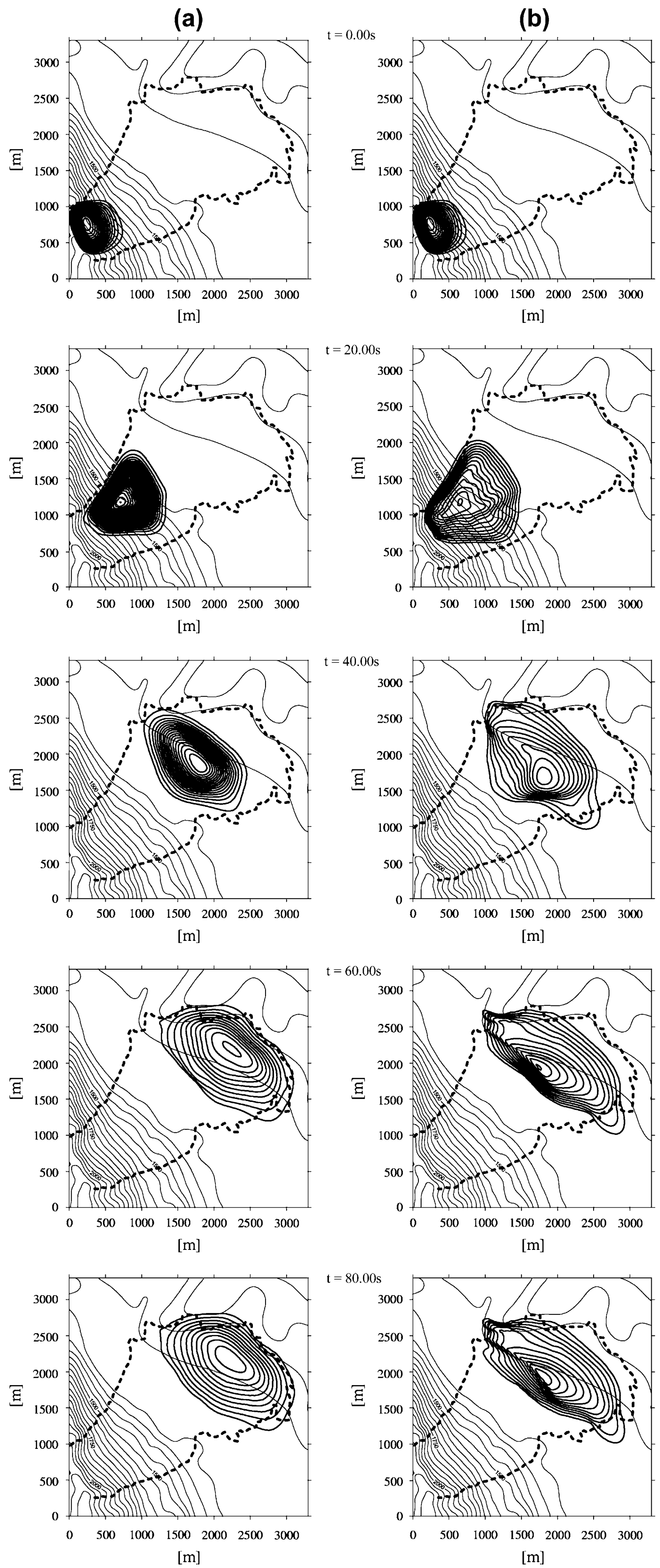


Fig. 24. Analysis of the Frank slide with RASH$^{3D}$. Plan of the simulated flow position at 20 s intervals (0 s–20 s–40 s–60 s–80 s) in condition of (a) anisotro
and (b) isotropy of normal stresses. The flow depth contours are at 3 m intervals. The sliding surface contours are at 50 m intervals. The dashed line indicated t
extent of the real event.

H x L = 1000m x 2500m

150m initial 16 m for the train



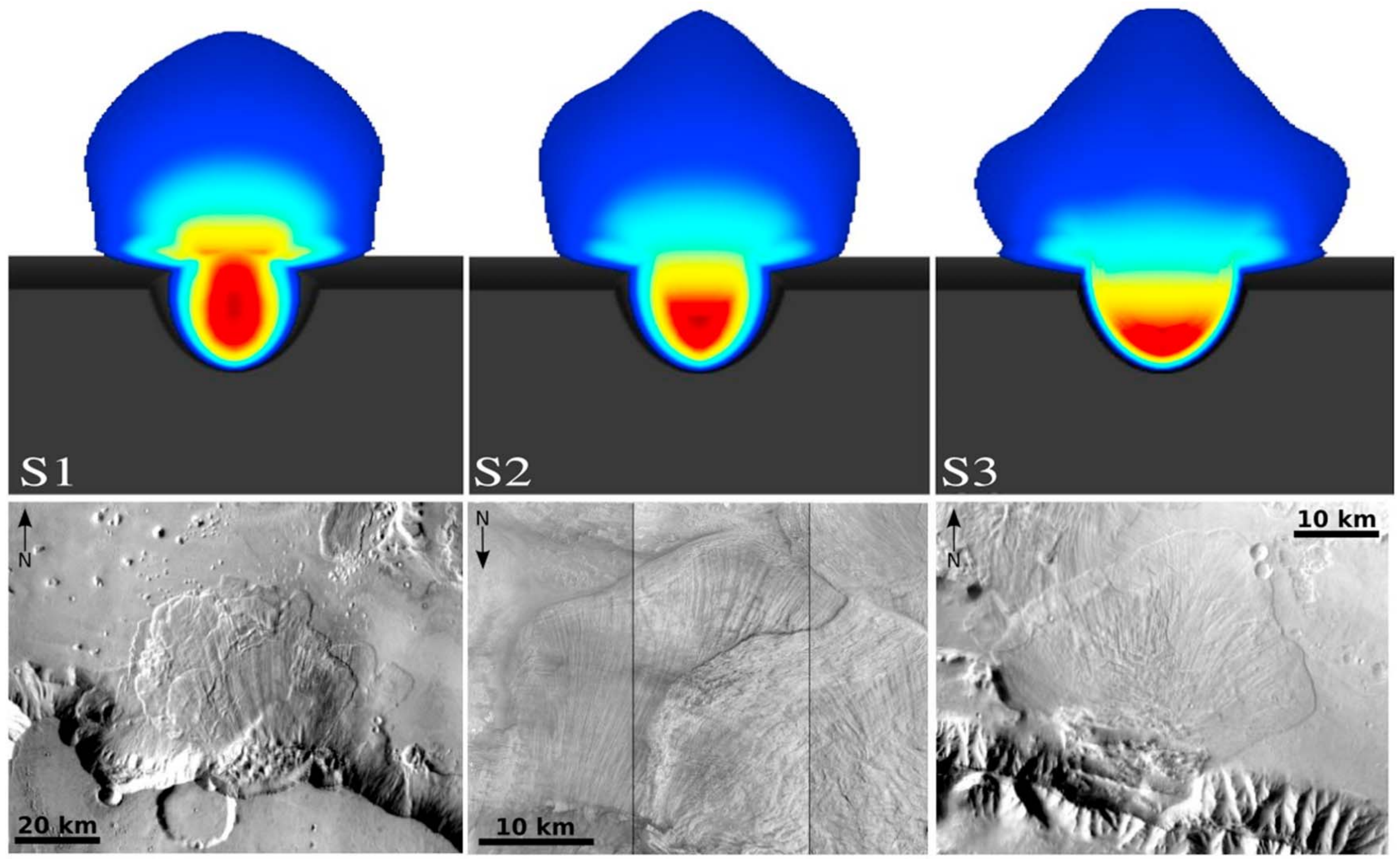


**Figure 6.** (top) Deposits of simulated landslides obtained for each scar geometry $S_i$ using $\delta$ = 10°. (bottom) Martian landslides observed on THEMIS IR present similar deposit shapes, respectively, from left to right: Ganges Chasma, East Ius Chasma, and Coprates Chasma.

# outline

- what is a granular fluid? some images
- the μ(I) friction law obtained from experiments and discrete simulation
- the viscosity associated to the μ(I) friction law
- the Saint Venant Savage Hutter Hyperbolic model
- implementing the μ(I) friction law in Navier Stokes
- Examples of flows: focusing on the granular column collapse (limits of Saint Venant Savage Hutter Hyperbolic model)

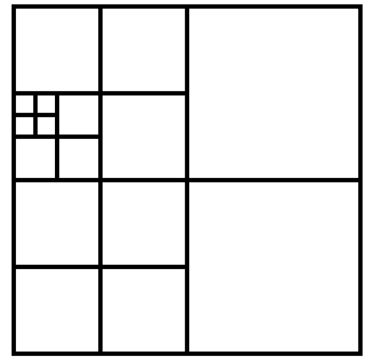

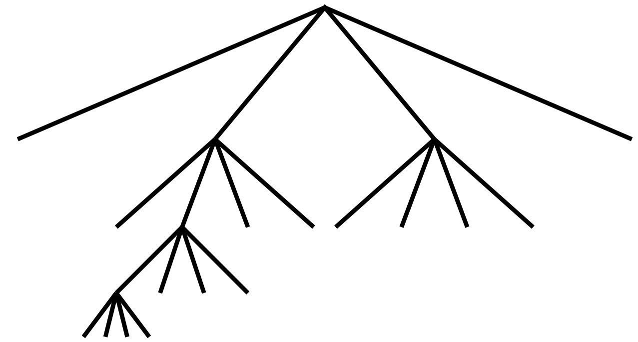


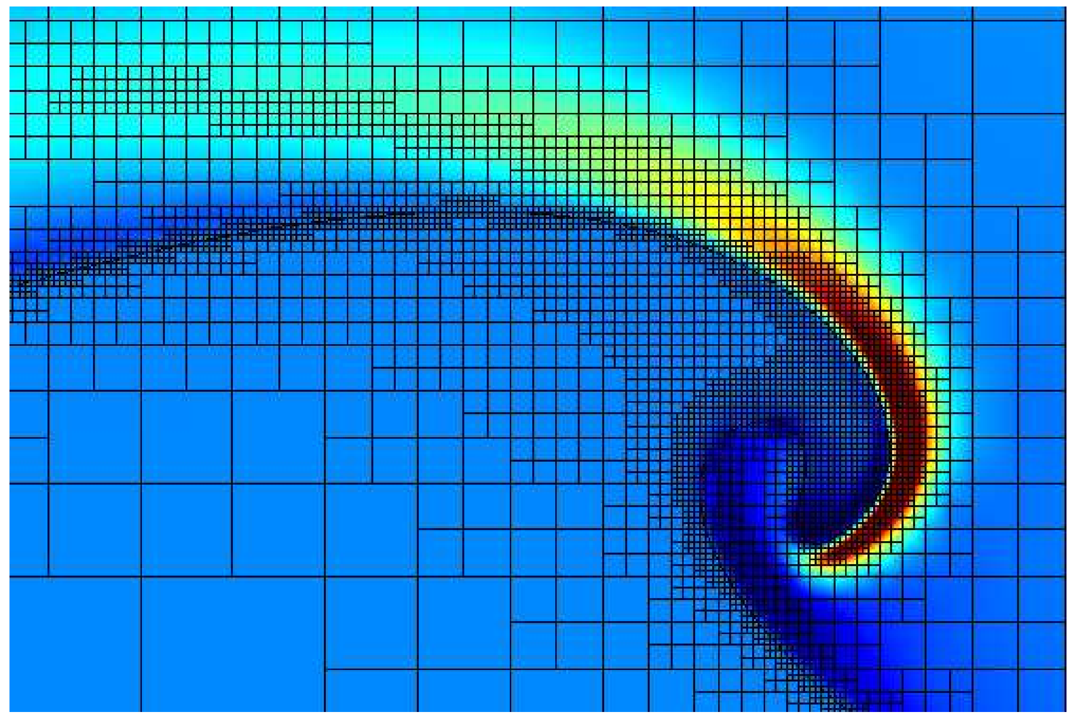

- *Gerris* is a finite volume code by Stéphane Popinet NIWA

one part of the code is a Navier Stokes solver

- automatic mesh adaptation
- Volume Of Fluid method for two phase flows
- free on sourceforge

# rheology; defining a viscosity

$$\mu(I) = \mu_1 + \frac{\mu_2 - \mu_1}{I_0/I + 1}$$

$$\eta \frac{\partial u}{\partial y} = \mu(I) P$$

local equilibrium

$$\eta = \frac{\mu\left(\frac{d \frac{\partial u}{\partial y}}{\sqrt{P/\rho}}\right) P}{\frac{\partial u}{\partial y}}$$

construction of a viscosity

P. Jop, Y. Forterre, O. Pouliquen, (2006) "A rheology for dense granular flows", Nature 441, pp. 727-730

# implementation in *Gerris* flow solver?

$$\mu(I) = \mu_1 + \frac{\mu_2 - \mu_1}{I_0/I + 1}$$

$$D_2 = \sqrt{D_{ij}D_{ij}} \qquad\qquad D_{ij} = \frac{u_{i,j} + u_{j,i}}{2}$$

construction of a viscosity based on the *D*2 invariant and redefinition of *I*

$$\eta = \min(\eta_{max}, \max\left(\frac{\mu(I)}{\sqrt{2}D_2}p\ ,\ 0\right)) \qquad I = d\sqrt{2}D_2/\sqrt{(|p|/\rho)}.$$

- the «min» limits viscosity to a large value
- always flow, even slow

Boundary Conditions: no slip and *P=0* at the interface

# implementation in *Gerris* flow solver?

$$\mu(I) = \mu_1 + \frac{\mu_2 - \mu_1}{I_0/I + 1}$$

$$D_2 = \sqrt{D_{ij} D_{ij}} \qquad D_{ij} = \frac{u_{i,j} + u_{j,i}}{2}$$

construction of a viscosity based on the *D*2 invariant and redefinition of *I*

$$\eta = \min(\eta_{max}, \max\left(\frac{\mu(I)}{\sqrt{2}D_2} p\ ,\ 0\right)) \qquad I = d\sqrt{2}D_2/\sqrt{(|p|/\rho)}.$$

$$\nabla \cdot \mathbf{u} = 0, \;\; \rho\left(\frac{\partial \mathbf{u}}{\partial t} + \mathbf{u} \cdot \nabla \mathbf{u}\right) = -\nabla p + \nabla \cdot (2\eta \mathbf{D}) + \rho g,$$

$$\frac{\partial c}{\partial t} + \nabla \cdot (c\mathbf{u}) = 0, \;\; \rho = c\rho_1 + (1-c)\rho_2, \;\; \eta = c\eta_1 + (1-c)\eta_2$$

The granular fluid is covered by a passive light fluid (it allows for a zero pressure boundary condition at the surface, bypassing an up to now difficulty which was to impose this condition on a unknown moving boundary).

Boundary Conditions: no slip and *P=0* at the top

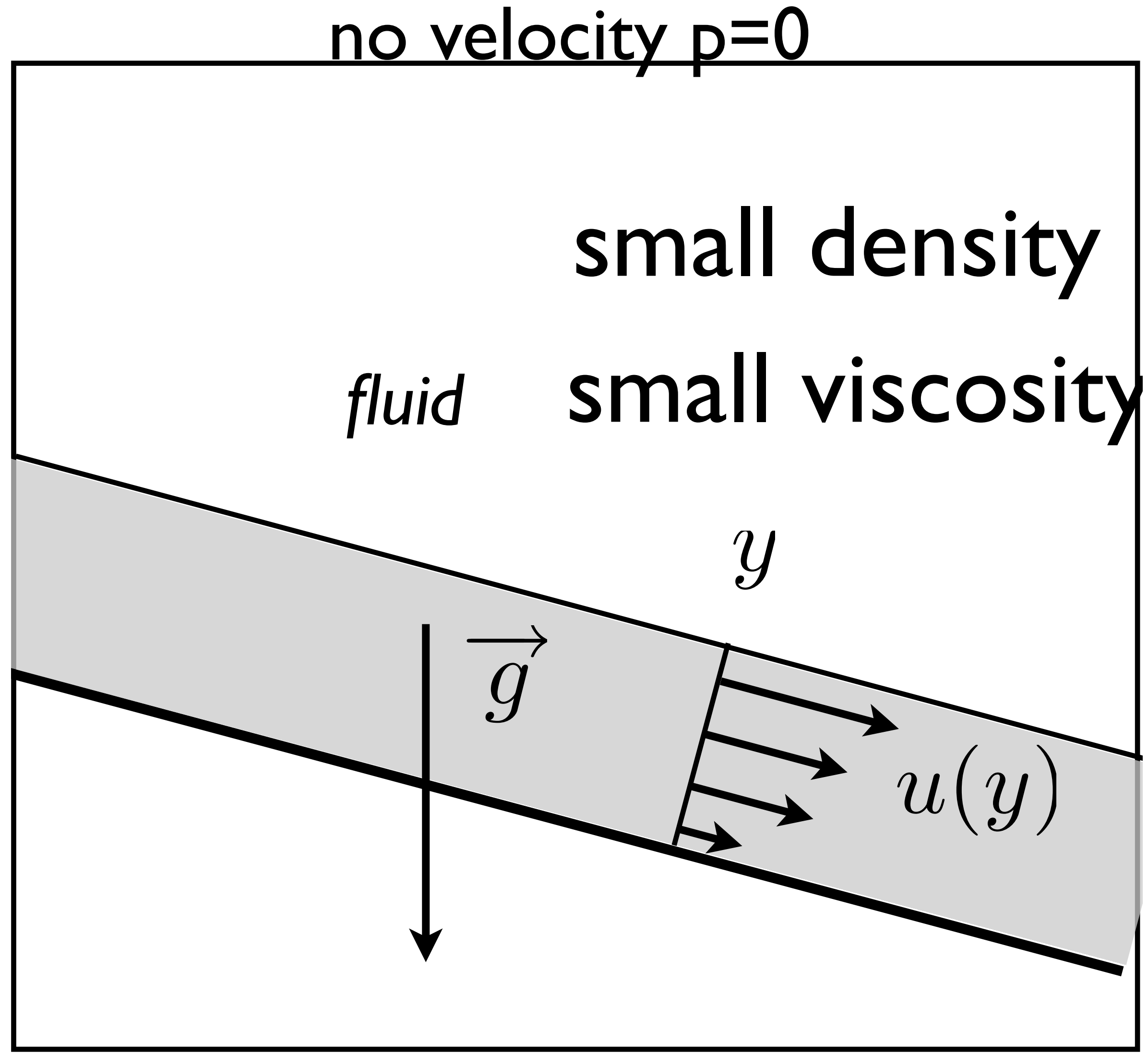


$$\frac{\partial c}{\partial t} + \nabla \cdot (c\mathbf{u}) = 0, \quad \rho = c\rho_1 + (1-c)\rho_2, \quad \eta = c\eta_1 + (1-c)\eta_2$$

The granular fluid is covered by a passive light fluid (it allows for a zero pressure boundary condition at the surface, bypassing an up to now difficulty which was to impose this condition on a unknown moving boundary).

# Boundary Conditions: no slip and *P=0* at the top

# Projection Method

$$\rho_{n+\frac{1}{2}}\left(\frac{\mathbf{u}_*-\mathbf{u}_n}{\Delta t}+\mathbf{u}_{n+\frac{1}{2}}\cdot\boldsymbol{\nabla}\mathbf{u}_{n+\frac{1}{2}}\right)=\boldsymbol{\nabla}\cdot(\eta_{n+\frac{1}{2}}\mathbf{D}_*)-\boldsymbol{\nabla}p_{n-\frac{1}{2}},$$
$$\mathbf{u}_{n+1}=\mathbf{u}_*-\frac{\Delta t}{\rho_{n+\frac{1}{2}}}(\boldsymbol{\nabla}p_{n+\frac{1}{2}}-\boldsymbol{\nabla}p_{n-\frac{1}{2}}),$$
$$\boldsymbol{\nabla}\cdot\mathbf{u}_{n+1}=0.$$


## multigrid solver for Laplacien of pressure

$$\boldsymbol{\nabla}\cdot\left(\frac{\Delta t}{\rho_{n+\frac{1}{2}}}\boldsymbol{\nabla}p_{n+\frac{1}{2}}\right)=\boldsymbol{\nabla}\cdot\left(\mathbf{u}_*+\frac{\Delta t}{\rho_{n+\frac{1}{2}}}\boldsymbol{\nabla}p_{n-\frac{1}{2}}\right)$$

## implicit for u*

$$\frac{\rho_{n+\frac{1}{2}}}{\Delta t}\mathbf{u}_\star-\frac{1}{2}\nabla\cdot(\eta_{n+\frac{1}{2}}\nabla\mathbf{u}_\star) \quad = \quad \rho_{n+\frac{1}{2}}\left[\frac{\mathbf{u}_n}{\Delta t}-\mathbf{u}_{n+\frac{1}{2}}\cdot\nabla\mathbf{u}_{n+\frac{1}{2}}\right]-\nabla p_{n-\frac{1}{2}}+\frac{1}{2}\nabla\mathbf{u}_n^T\nabla\eta_{n+\frac{1}{2}}.$$

## VOF reconstruction

$$\frac{c_{n+\frac{1}{2}}-c_{n-\frac{1}{2}}}{\Delta t}+\nabla\cdot(c_n\mathbf{u}_n)=0$$

# outline

- what is a granular fluid? some images
- the μ(I) friction law obtained from experiments and discrete simulation
- the viscosity associated to the μ(I) friction law
- the Saint Venant Savage Hutter Hyperbolic model
- implementing the μ(I) friction law in Navier Stokes
- Examples of flows: focusing on the granular column collapse (limits of Saint Venant Savage Hutter Hyperbolic model)

# Test of the code: «Bagnold» avalanche

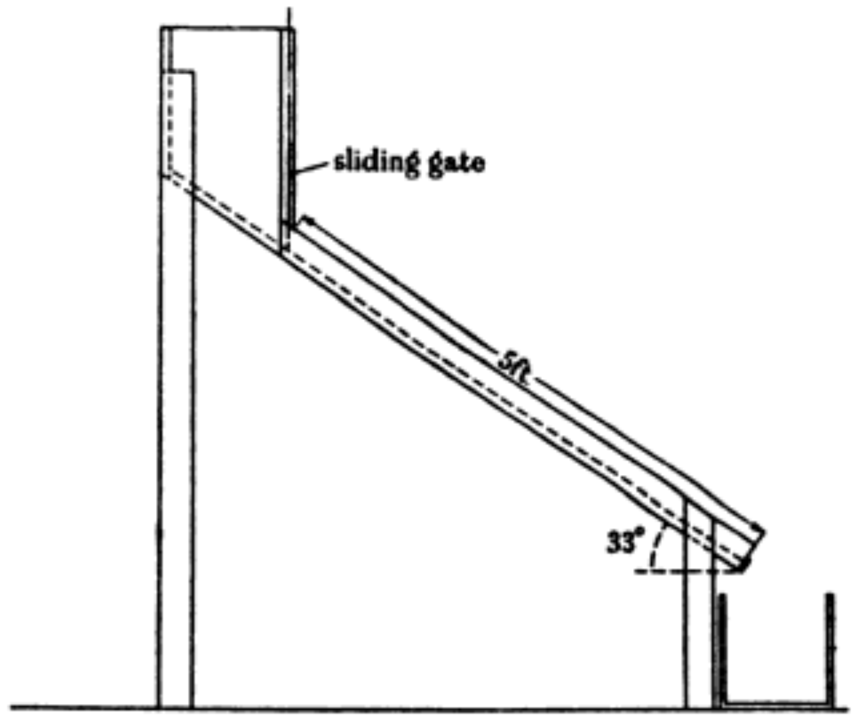


kind of Nuβelt solution

$$T \propto \sigma(\lambda D)^2 \, (dU/dy)^2$$

$$U = \frac{2}{3} \times 0.165 \, (g \sin \beta)^{1/2} \, \frac{y'^{3/2}}{D} \, ,$$

Bagnold 1954

TABLE 1.

| flow height Y (cm) | measured speed (cm/sec) | speed, from (9) (cm/sec) | ratio |
|---|---|---|---|
| 0.5 | 17.2 | 26.4 | 1.53 |
| 0.65 | 27.5 | 38.8 | 1.41 |
| 0.75 | 30.0 | 48.0 | 1.6 |
| 0.9 | 39.0 | 63.0 | 1.61 |

http://www.boker.org.il/meida/negev/desert_biking/bagnold/tsoar_paper.htm

# Test of the code: «Bagnold» avalanche

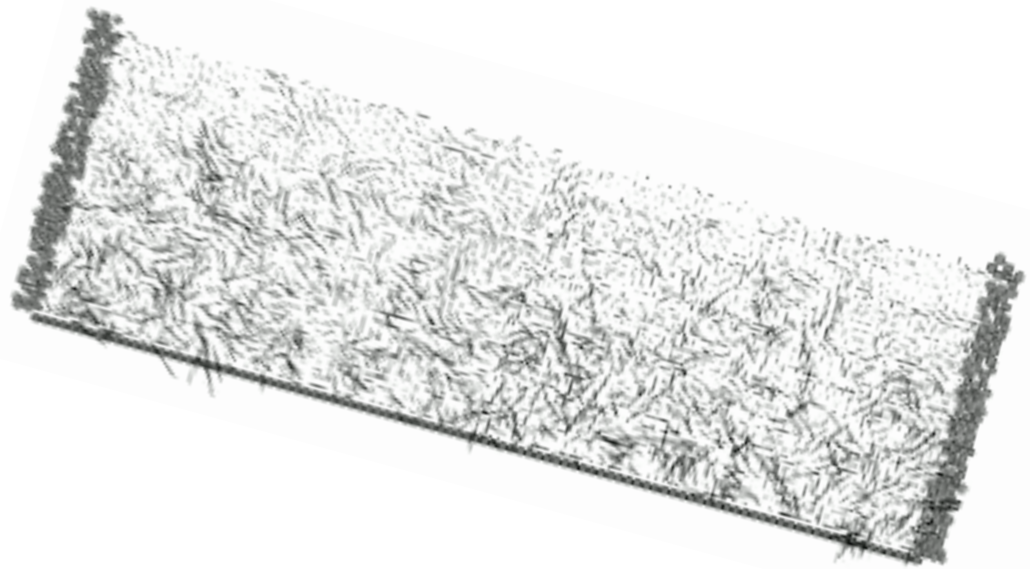

kind of Nuβelt solution

Contact Dynamic simulation Lydie Staron

# Test of the code: «Bagnold» avalanche

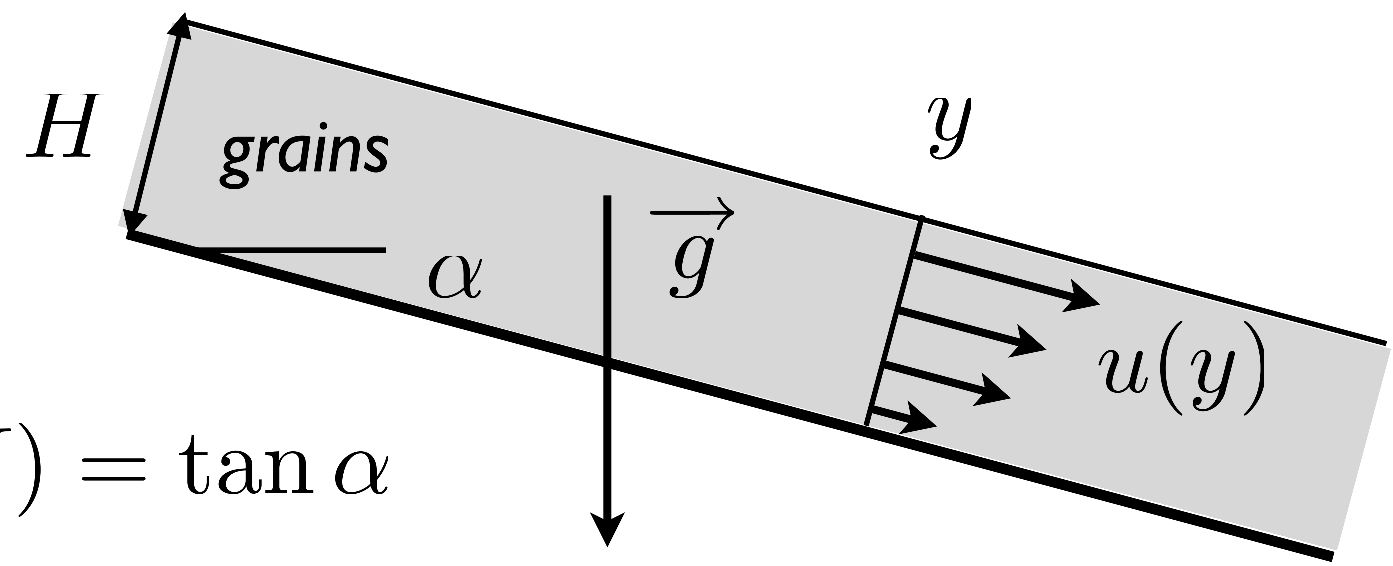


$$\mu(I) = \tan\alpha$$

$$u = \frac{2}{3} I_\alpha \sqrt{gd\cos\alpha \frac{H^3}{d^3}} \left(1 - \left(1 - \frac{y}{H}\right)^{3/2}\right),$$

$$v = 0, \quad p = \rho g H \left(1 - \frac{y}{H}\right)\cos\alpha.$$

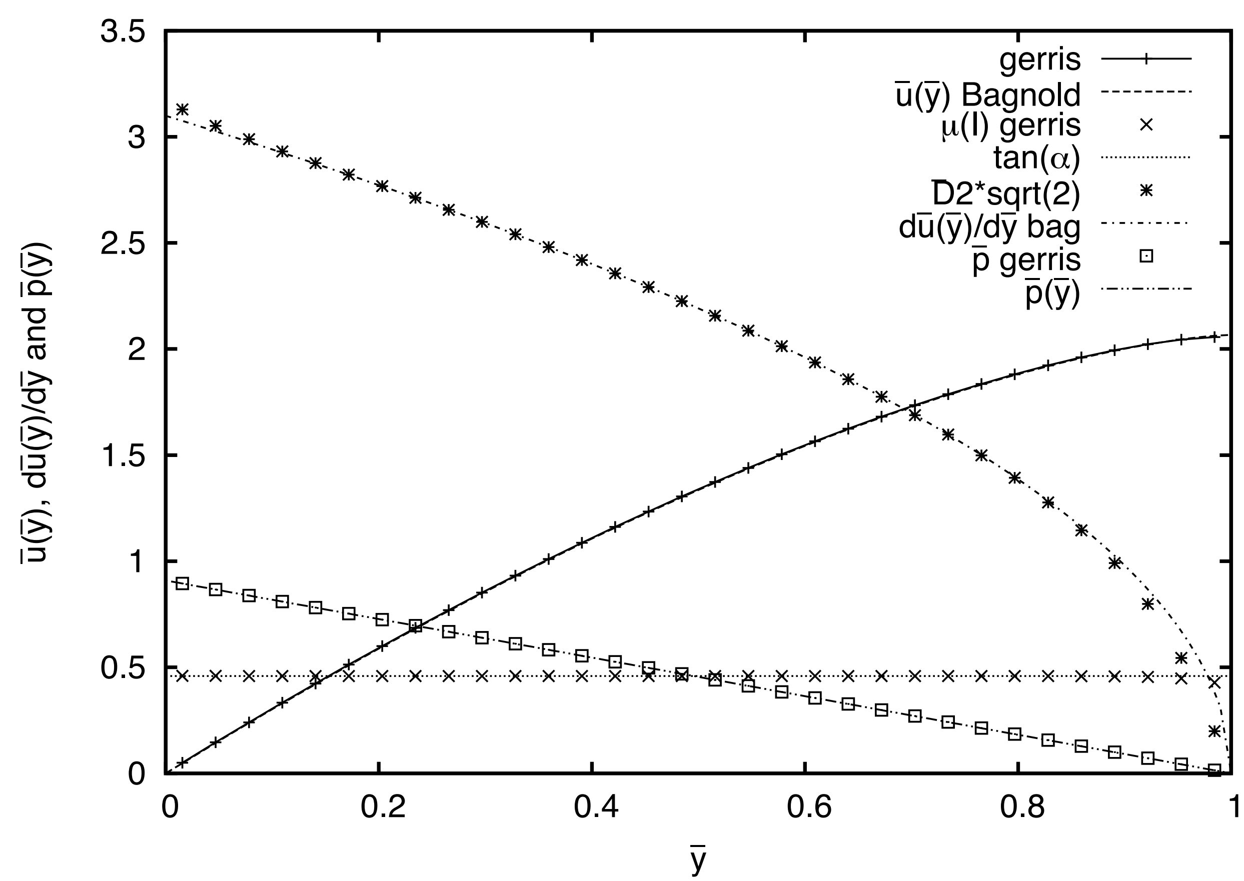

# Test of the code: «Bagnold» avalanche

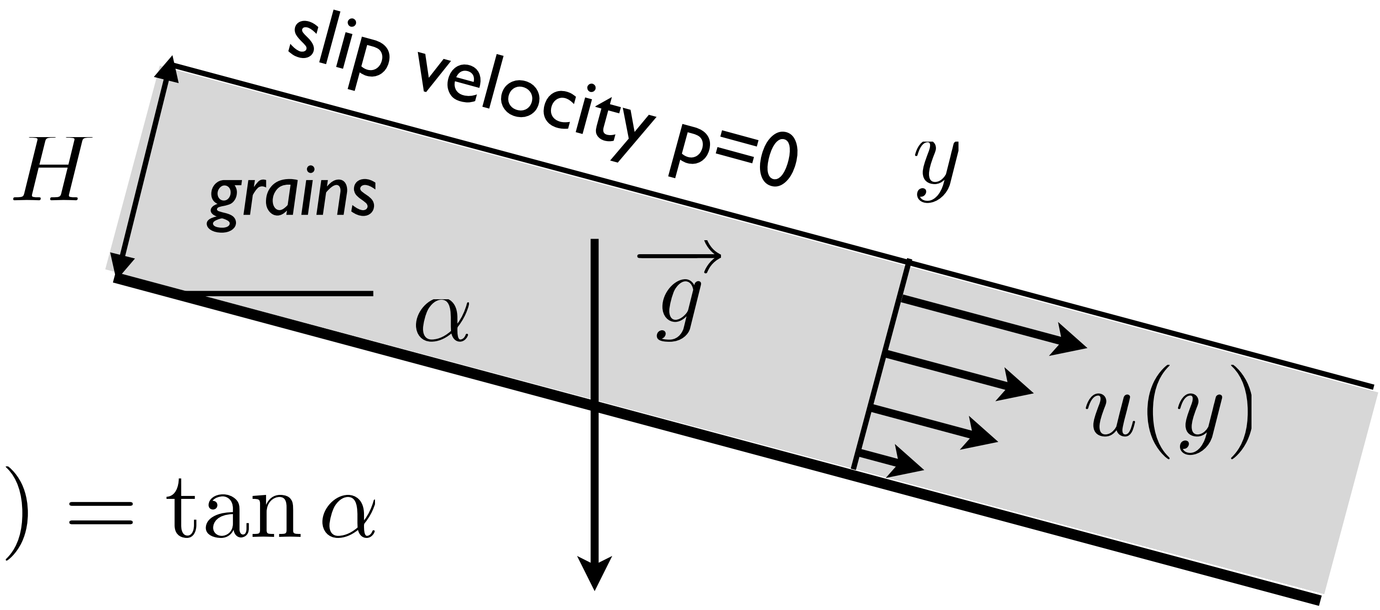


$$\mu(I) = \tan\alpha$$

$$u = \frac{2}{3} I_\alpha \sqrt{gd\cos\alpha\frac{H^3}{d^3}}\left(1-\left(1-\frac{y}{H}\right)^{3/2}\right),$$

$$v = 0, \quad p = \rho g H\left(1-\frac{y}{H}\right)\cos\alpha.$$

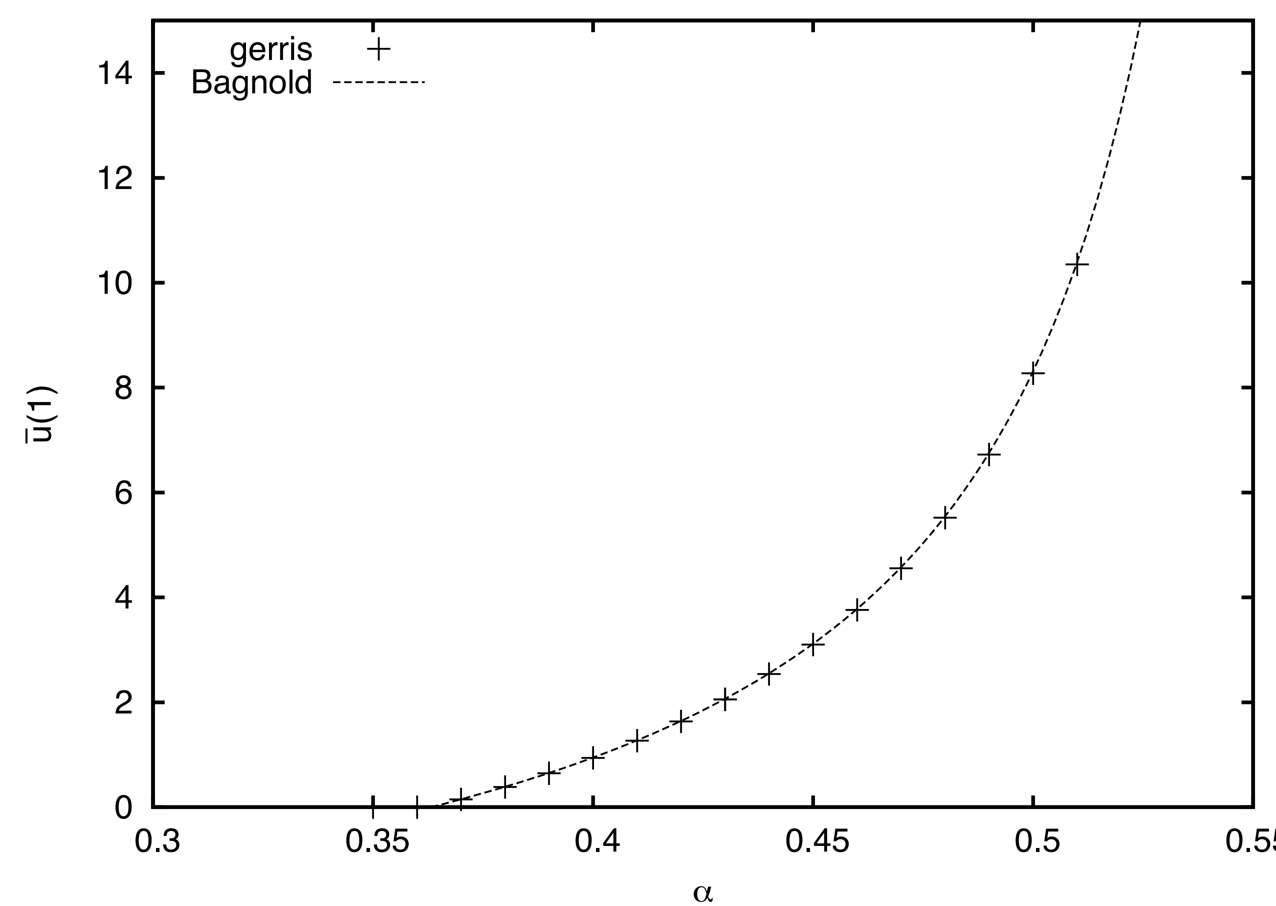

# Test of the code: «Bagnold» avalanche

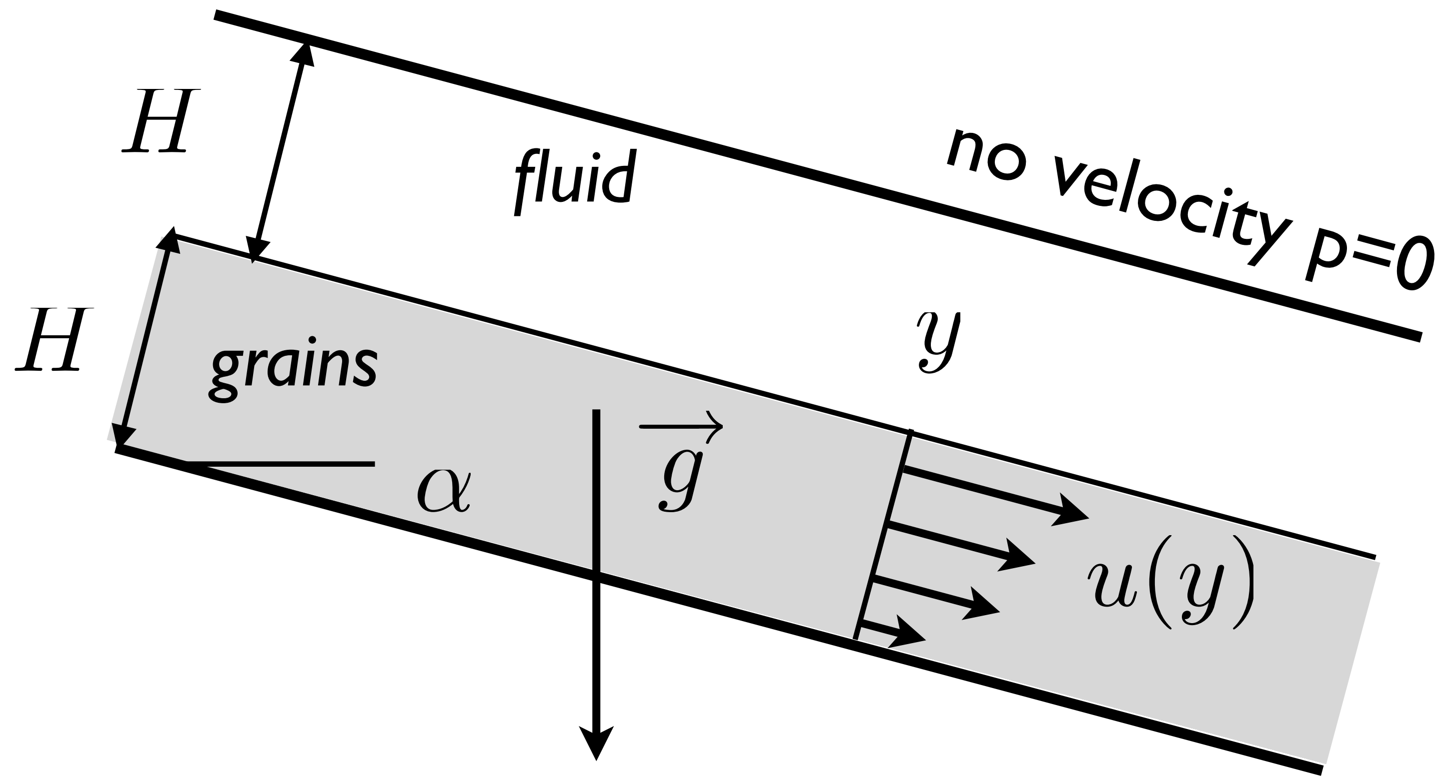


$$u(y) = \frac{(2H - y)\,(\rho_f g y \sin\alpha - 2\tau_0)}{2\mu_f}$$

$$d\frac{\partial u}{\partial y} = \max\left[\sqrt{p_0/\rho + gH\left(1 - \frac{y}{H}\right)\cos\alpha} \times \mu^{-1}\left(\frac{\tau_0 + \rho g H\left(1 - \frac{y}{H}\right)\sin\alpha}{p_0 + \rho g H\left(1 - \frac{y}{H}\right)\cos\alpha}\right), 0\right].$$

$$u(H^-) - u(H^+) = 0$$

# Test of the code: «Bagnold» avalanche

change of density of the fluid

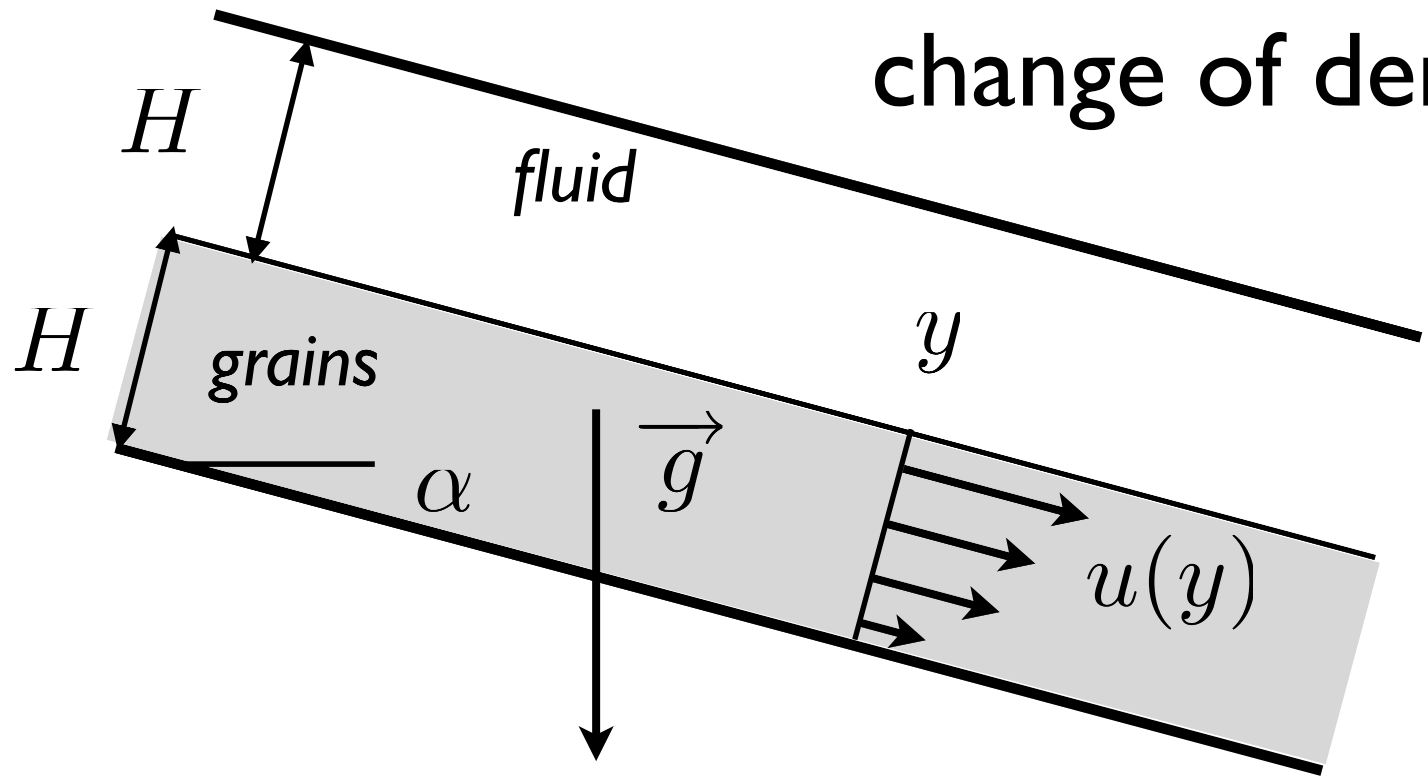


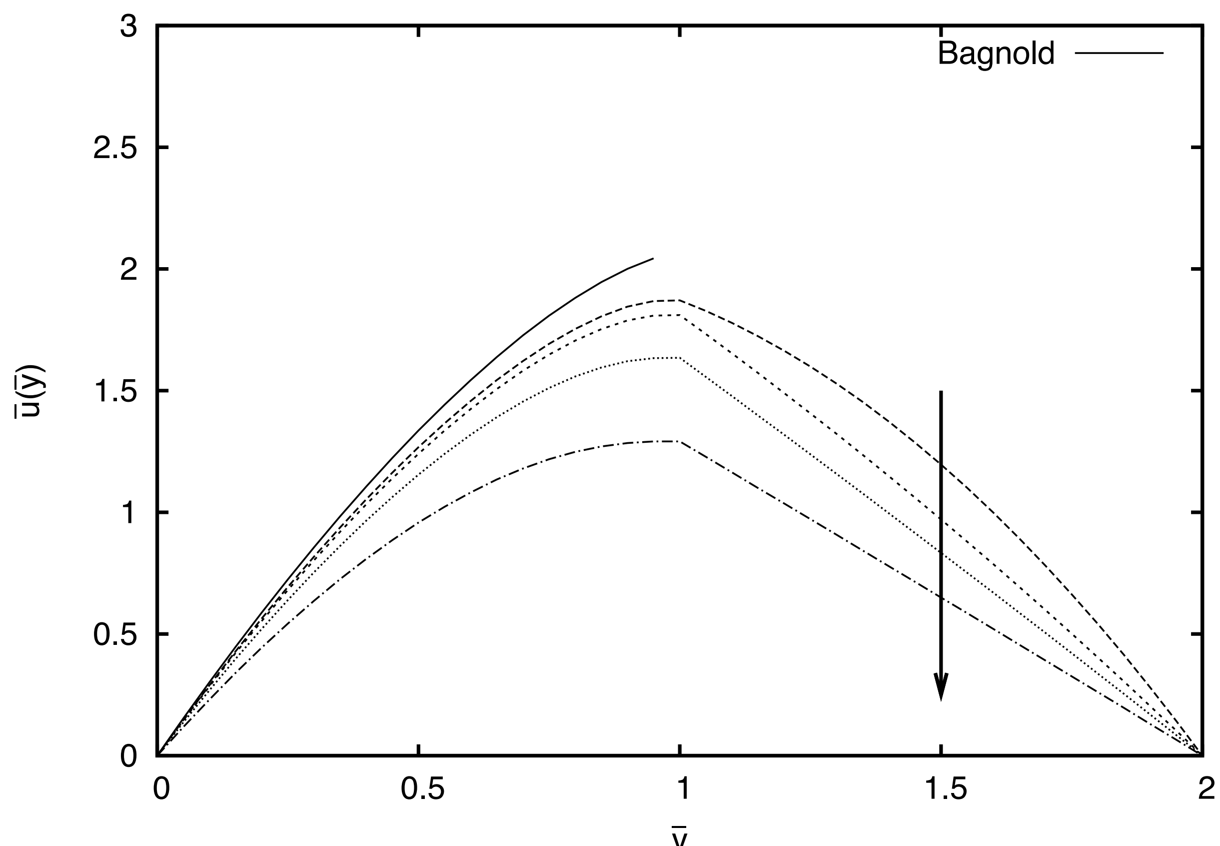

# Test of the code: «Bagnold» avalanche

## change of viscosity of the fluid

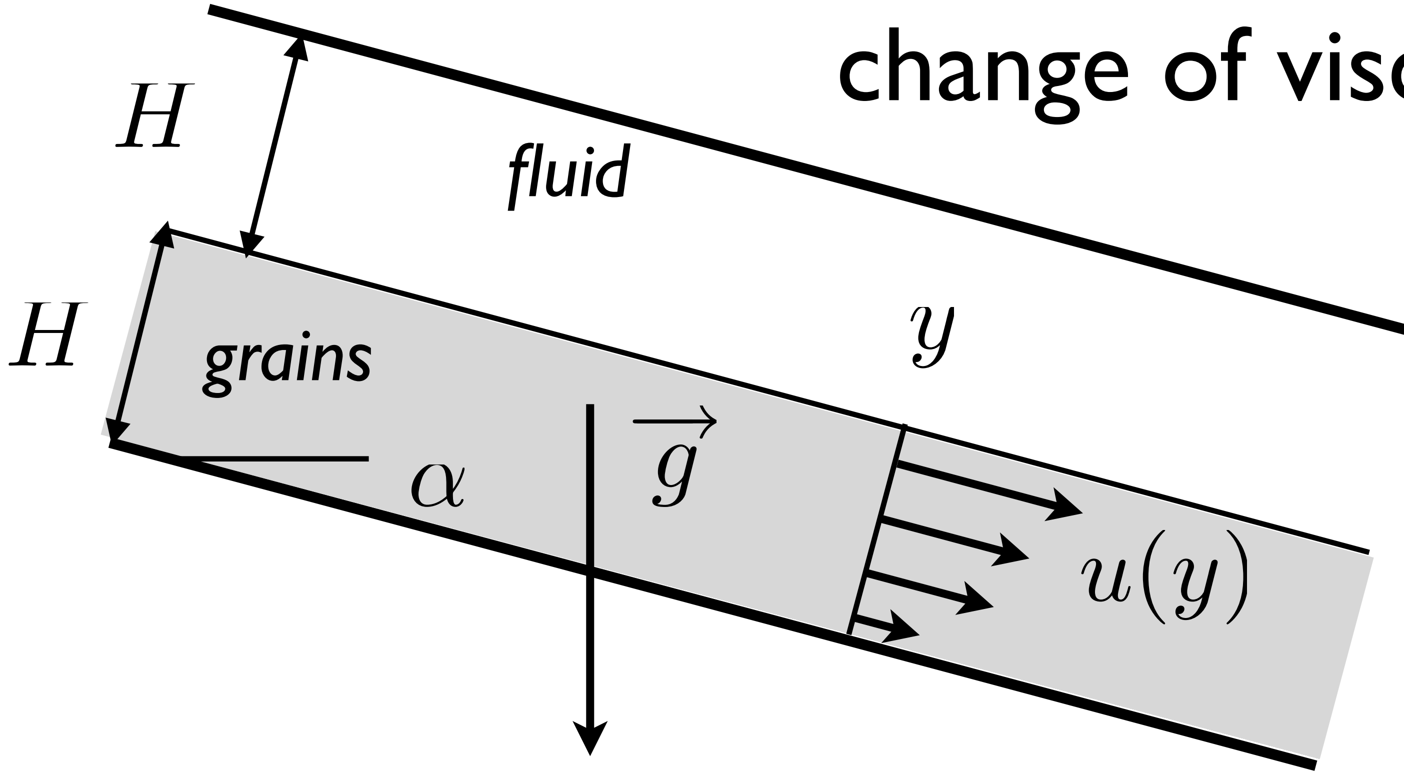


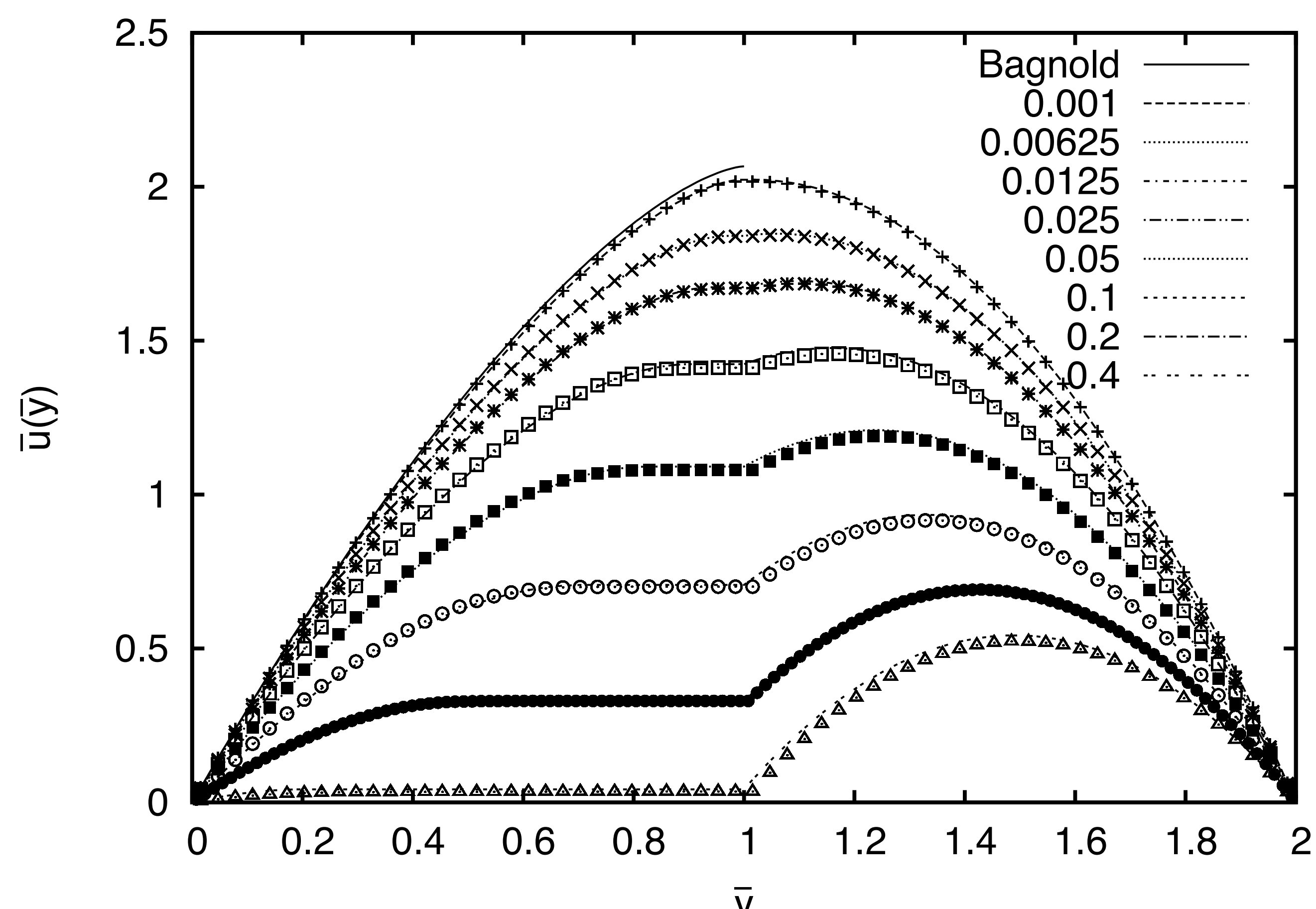

The sand pit problem: quickly remove the bucket of sand

http://www.mylot.com/w/photokeywords/pail.asp

# Granular Column Collapse

E. Lajeunesse A. Mangeney-Castelnau and J. P. Vilotte PoF 204

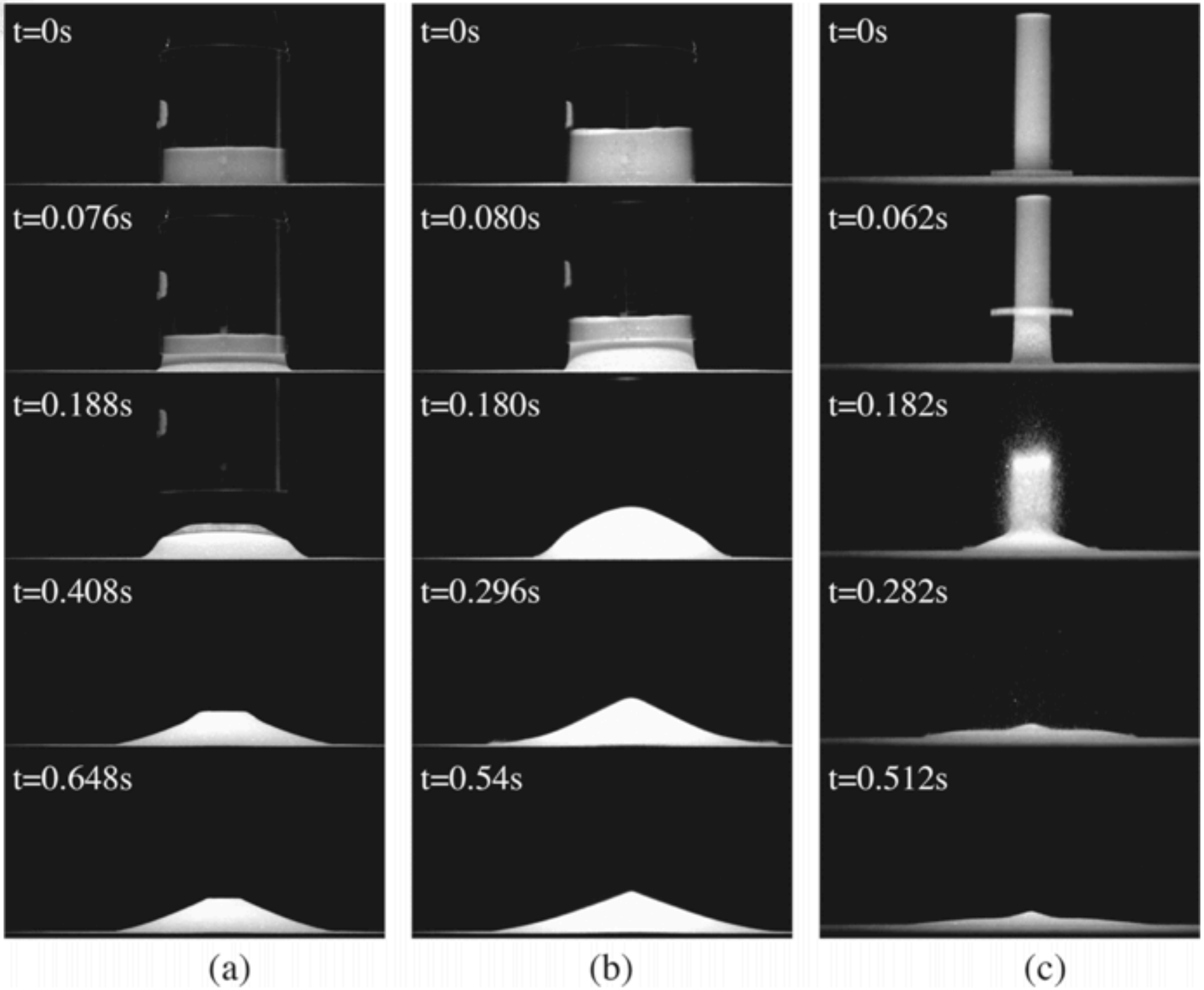


The sand pit problem: quickly remove the bucket of sand

http://www.mylot.com/w/photokeywords/pail.asp

# Collapse of columns

a=0.37

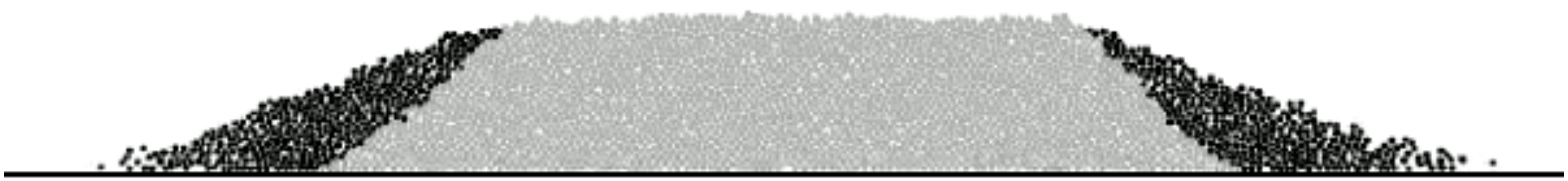

Contact Dynamic simulation Lydie Staron

# Collapse of columns

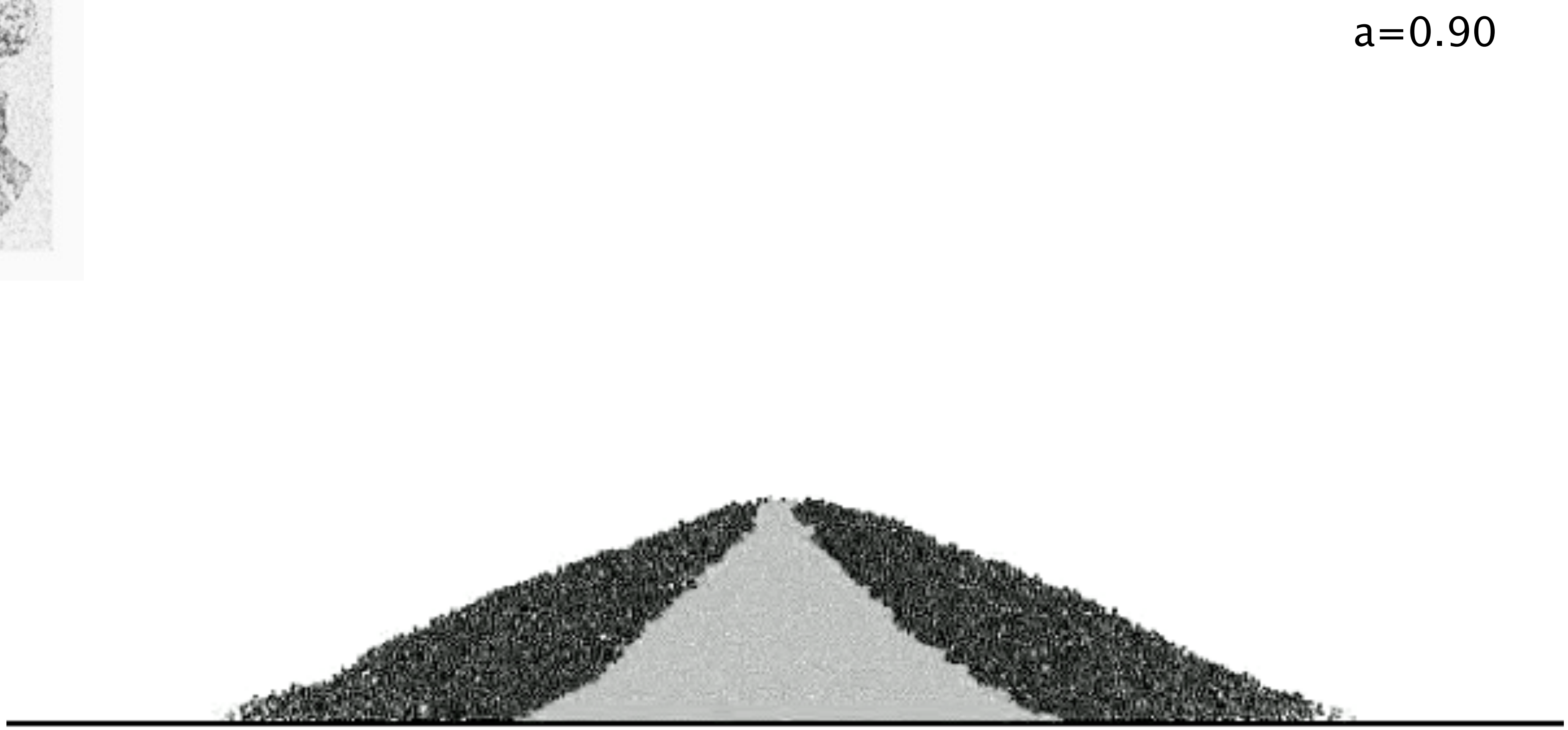


Contact Dynamic
simulation Lydie Staron

# Collapse of columns simulation *Gerris μ(I)*

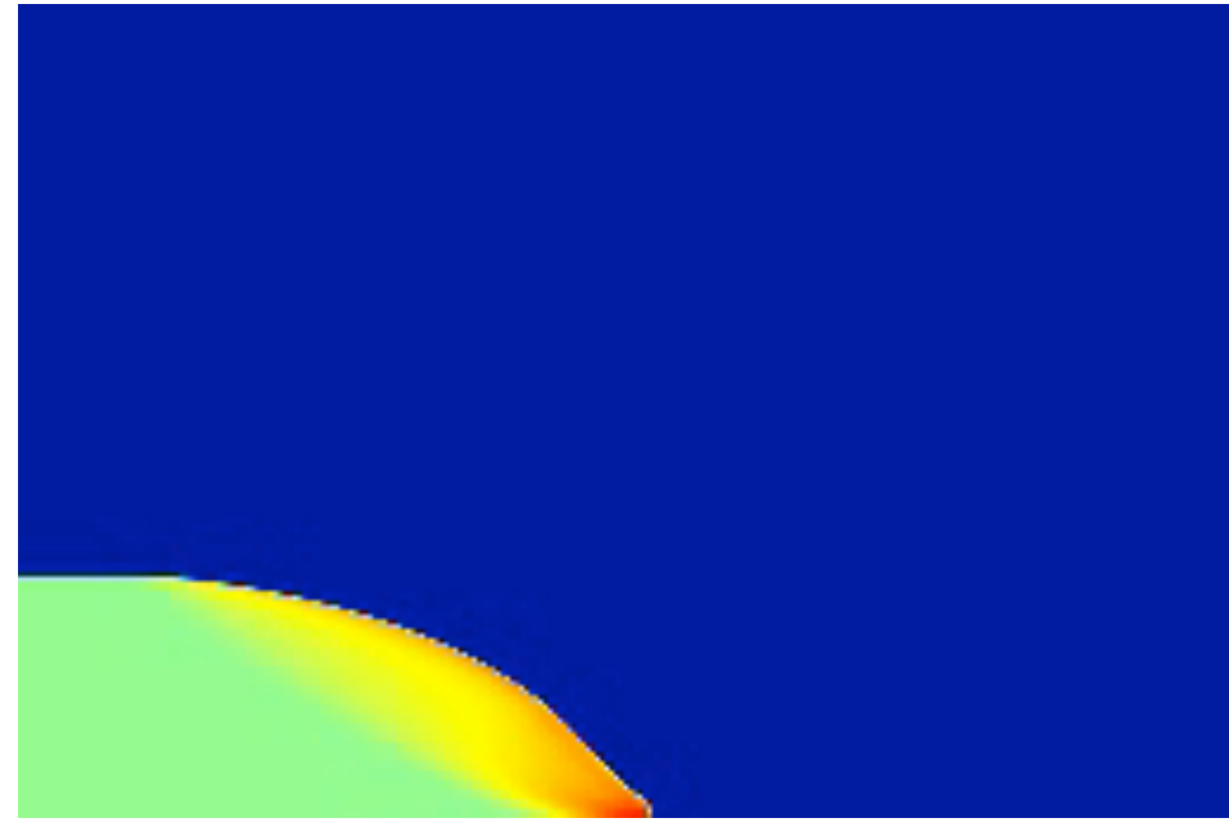

Collapse of columns of aspect ratio 0.5 comparison of Discrete Simulation Contact Method and Navier Stokes gerris, shape at time 0, 1, 2, 3, 4 and position of the front of the avalanche as function of time (time measured with $\sqrt{H_0/g}$ and space with $aH_0$ )

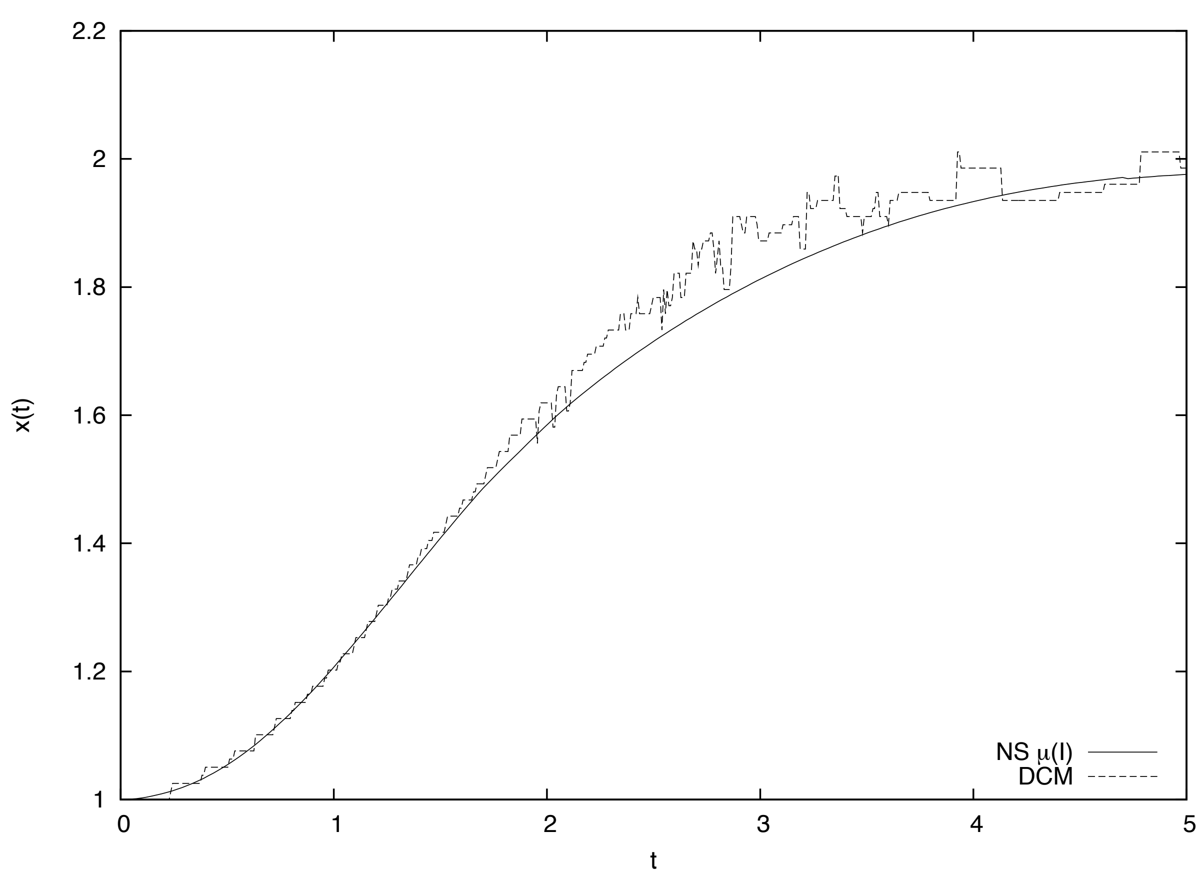


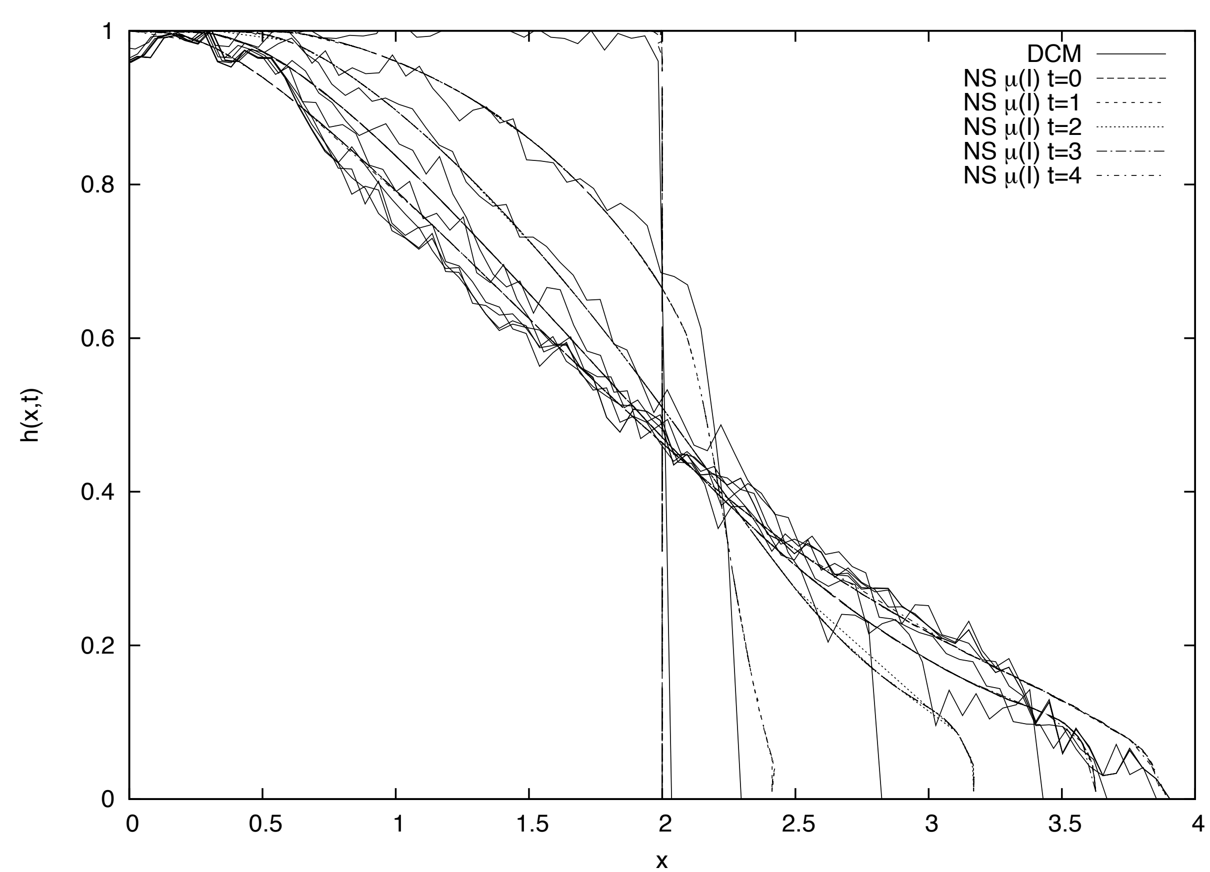

# Collapse of columns   simulation *Gerris* μ(I)

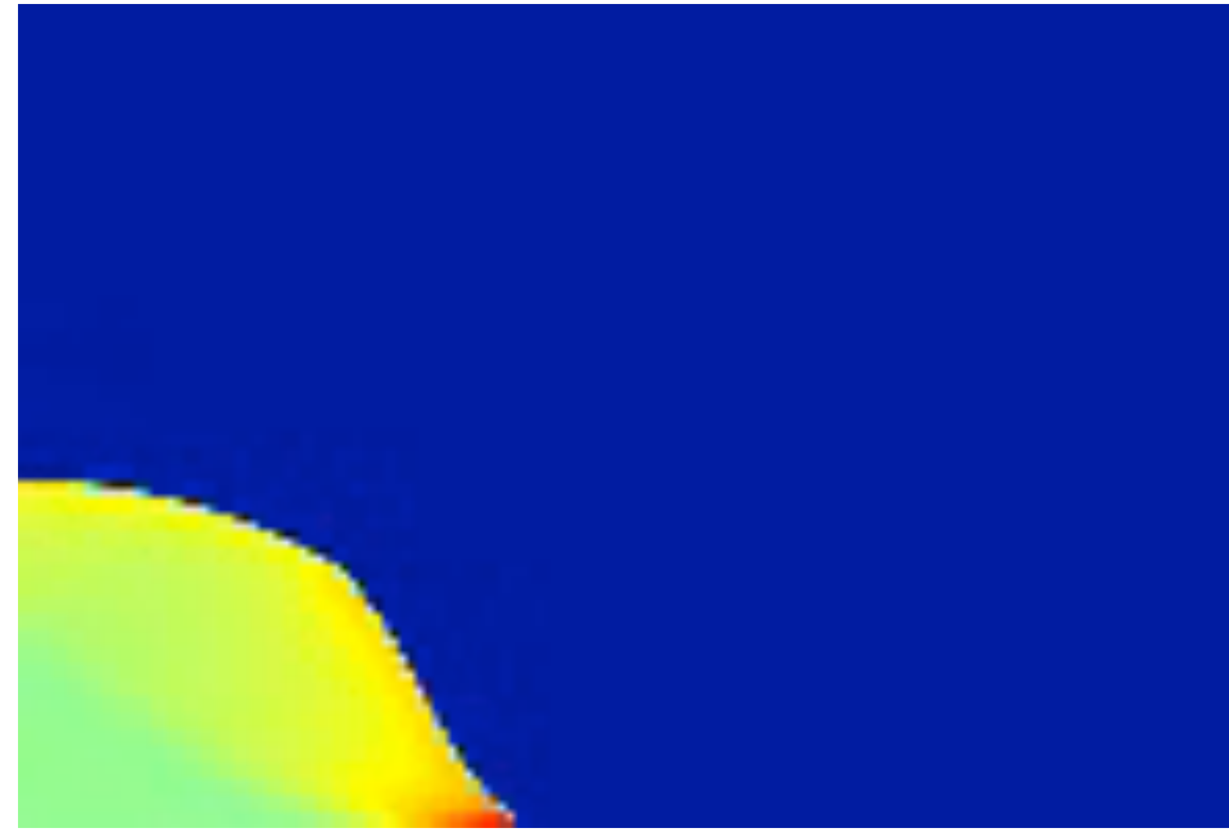

Collapse of columns of aspect ratio 1.42 comparison of Discrete Simulation Contact Method and Navier Stokes gerris, shape at time 0, 1, 2, 3, 4 and position of the front of the avalanche as function of time  (time measured with $\sqrt{H_0/g}$ and space with $aH_0$ )

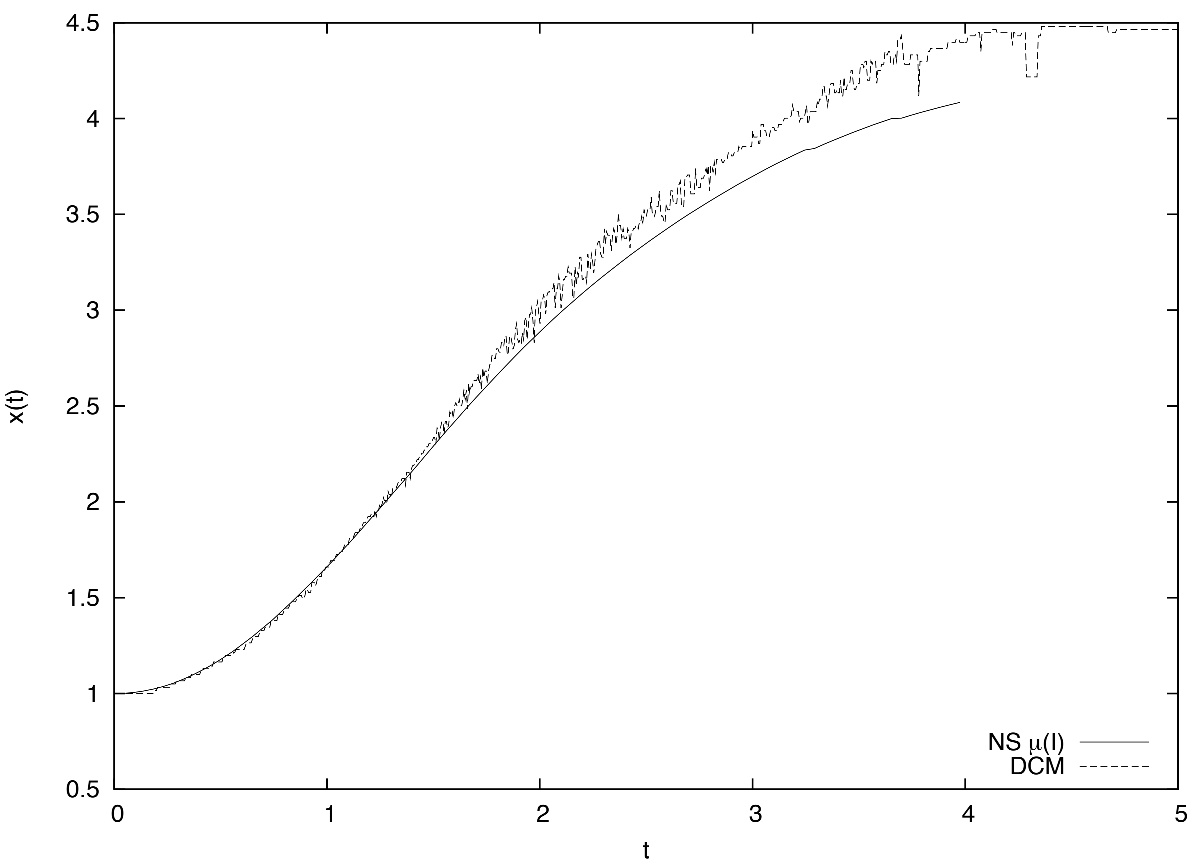


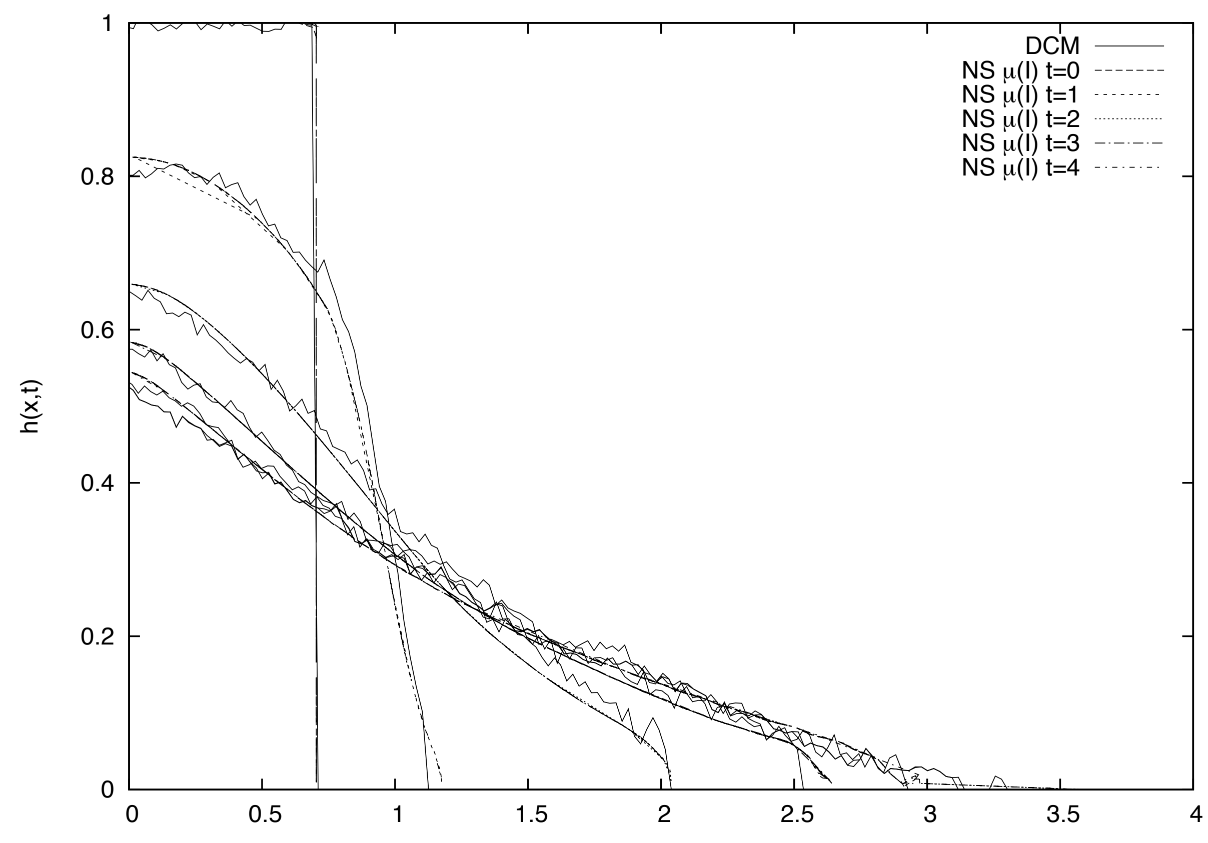

# Collapse of columns simulation *Gerris μ(I)*

Collapse of columns of aspect ratio 6.26 comparison of Discrete Simulation Contact Method and Navier Stokes gerris, shape at time 0, 1, 2, 3, 4 and position of the front of the avalanche as function of time (time measured with $\sqrt{H_0/g}$ and space with $aH_0$ )

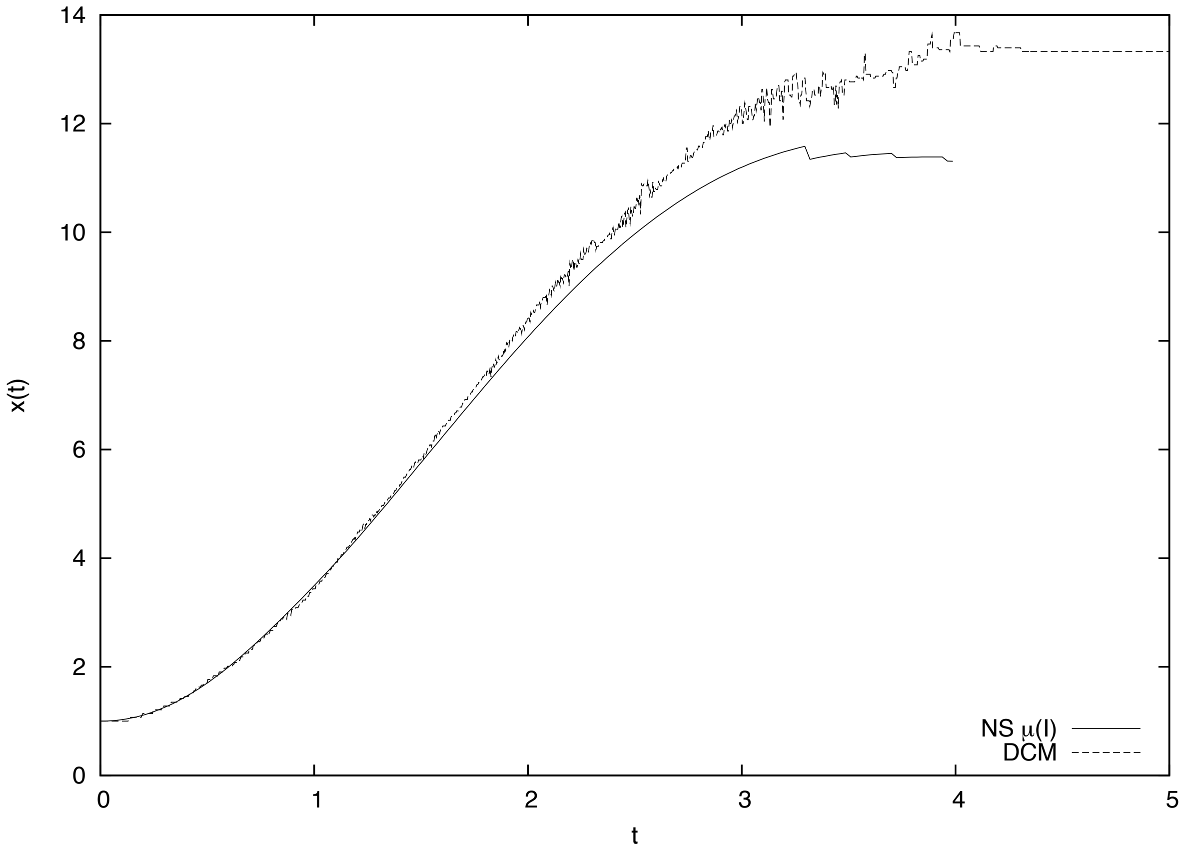


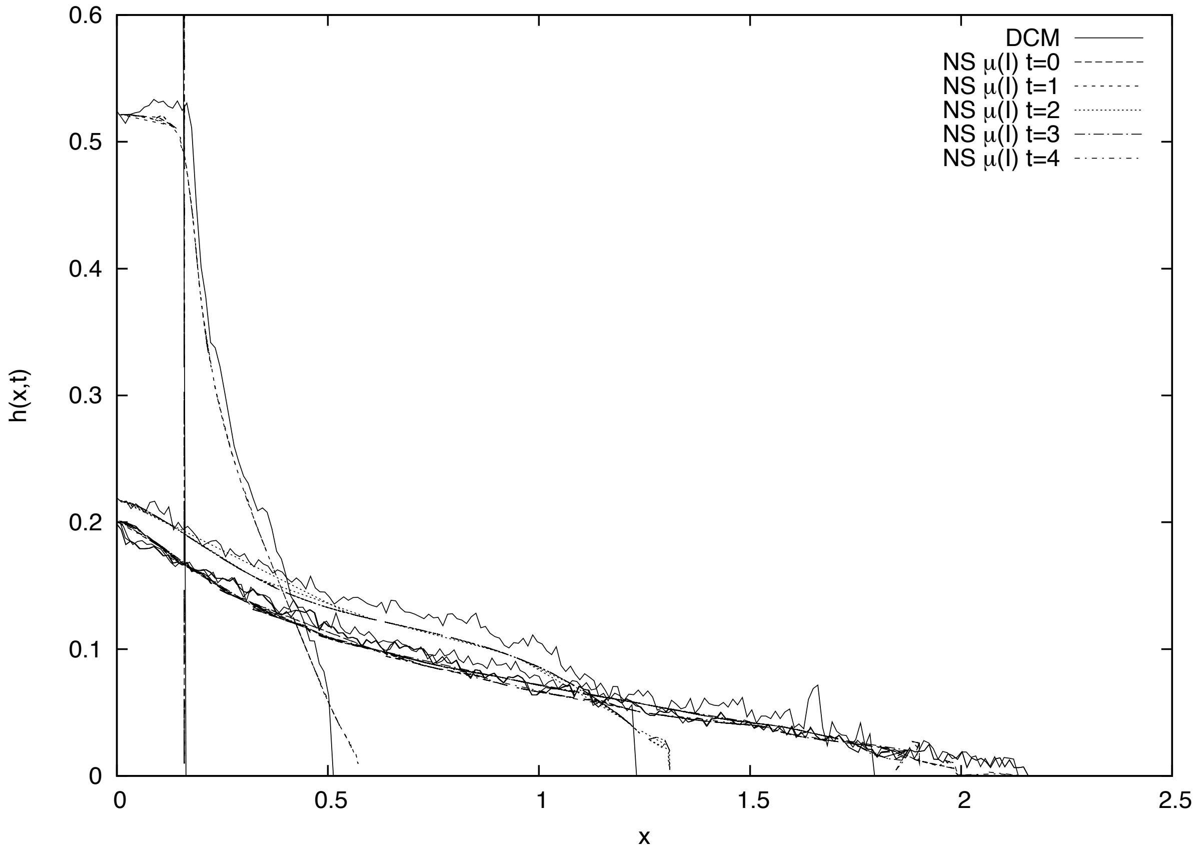

# Collapse of columns simulation *Gerris μ(I)*

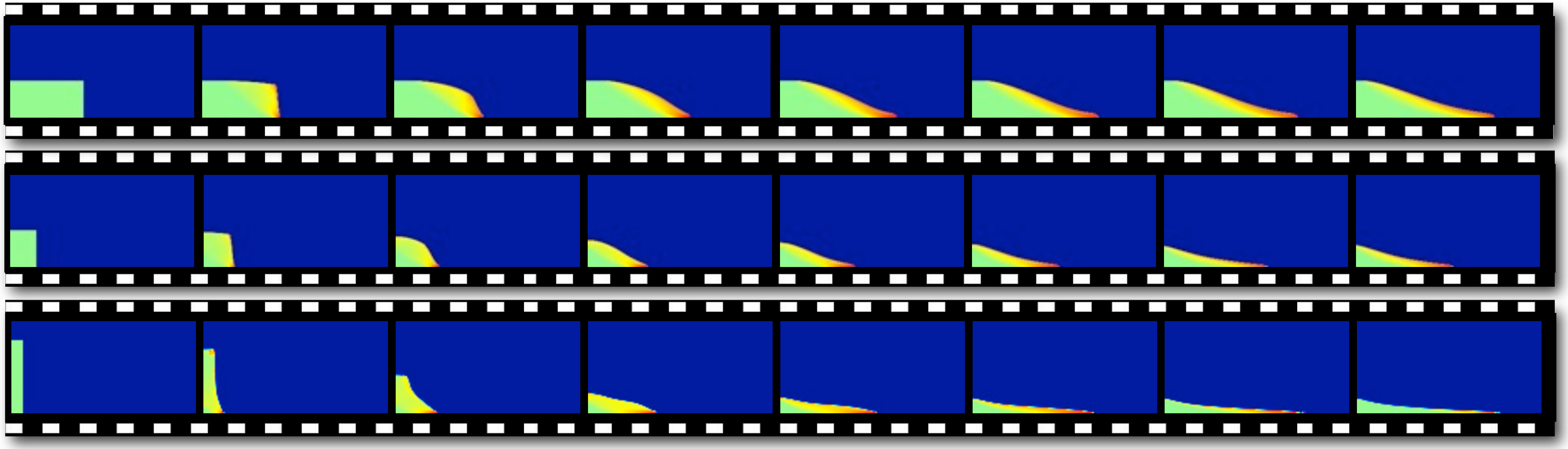

Snapshots of collapse of three columns of aspect ration 0.5 1.42 and 6.26 (top to bottom)

# Collapse of columns simulation *Gerris* $\mu(I)$

## optimisation

$$\mu(I) = \mu_s + \frac{\Delta\mu}{\frac{I_0}{I} + 1}$$

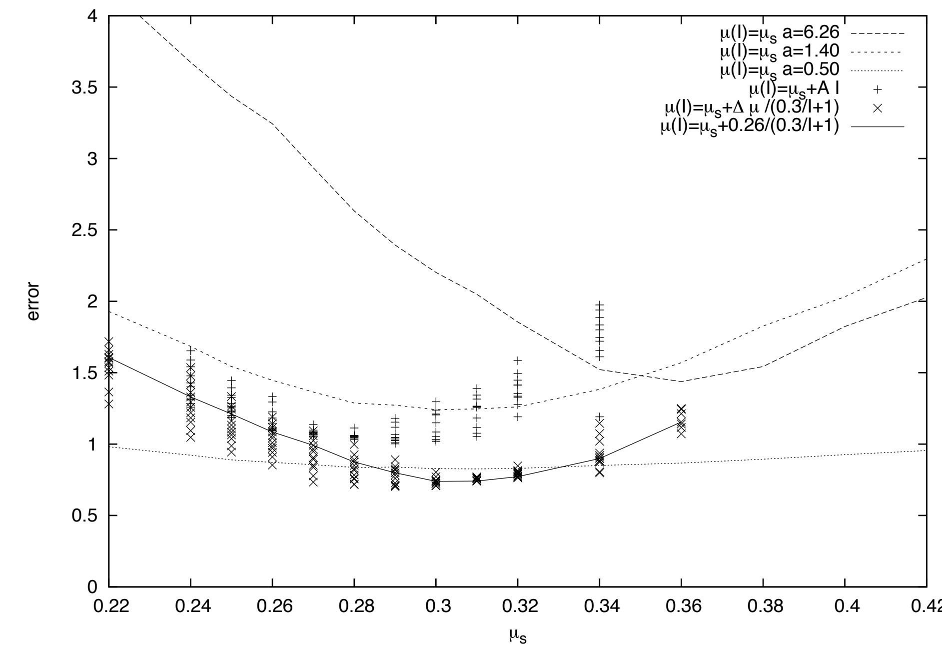


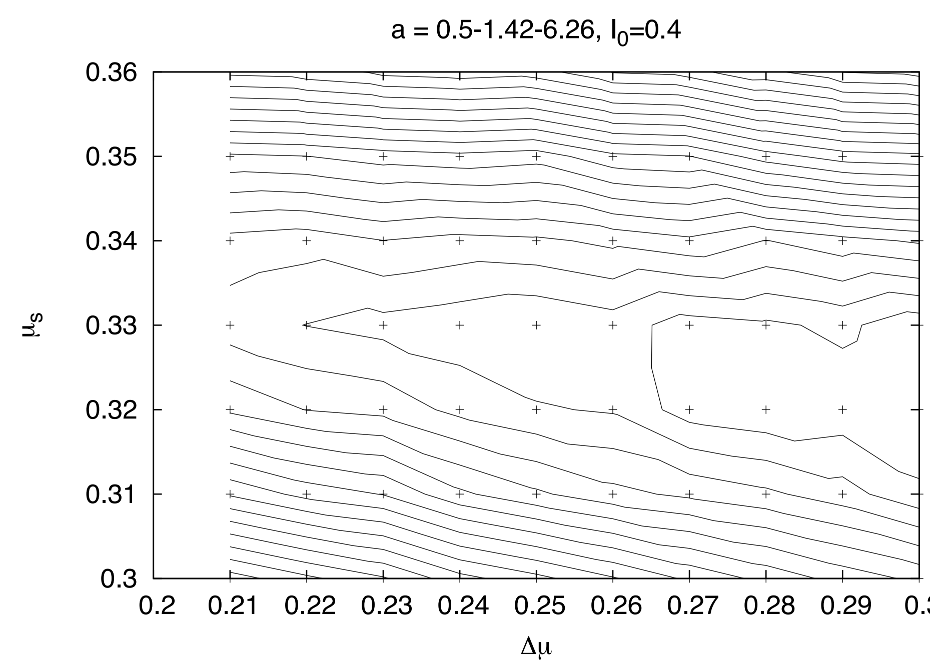


final values $\mu_s = 0.32 \; \Delta\mu = 0.28 \; I_0 = 0.4$

# Collapse of columns   simulation *Gerris* $\mu(I)$

$a = 0.5$   DCM vs *Gerris* $\mu(I)$

# Collapse of columns simulation *Gerris μ(I)*

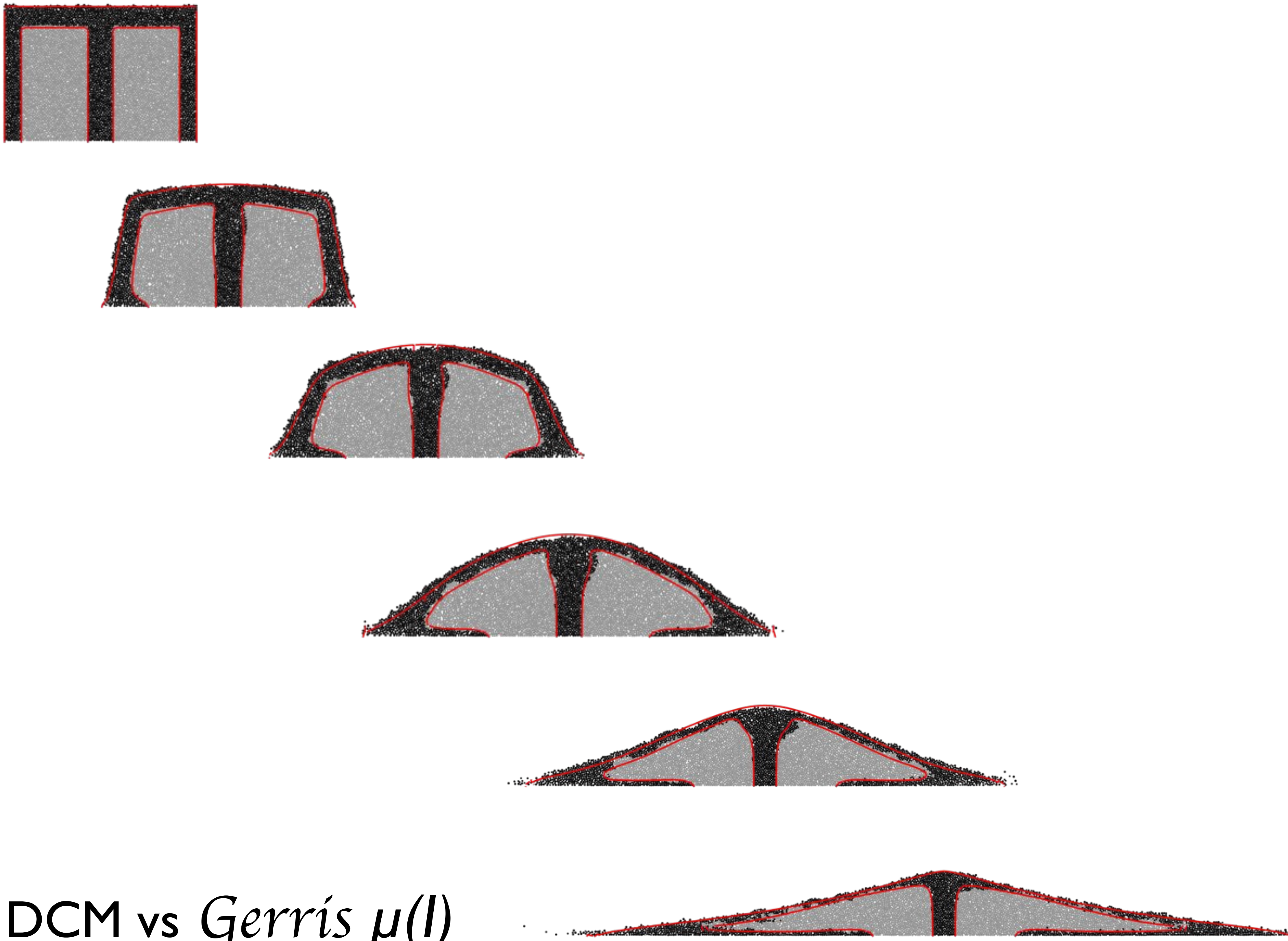

$a = 1.42$ DCM vs *Gerris μ(I)*

# Collapse of columns  simulation *Gerris* $\mu(I)$

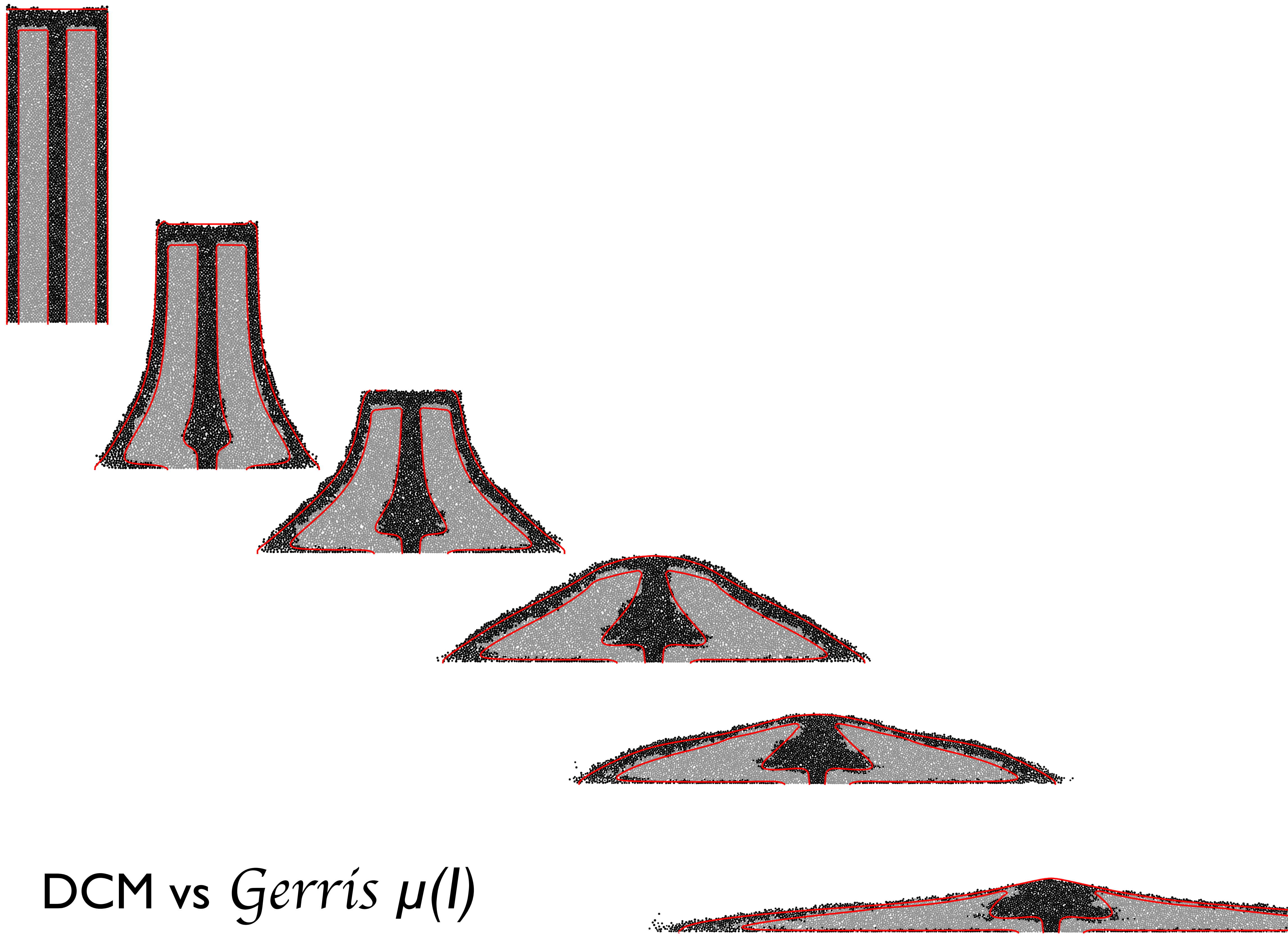

$a = 6.6$ DCM vs *Gerris* $\mu(I)$

# Collapse of columns simulation *Gerris* $\mu(I)$

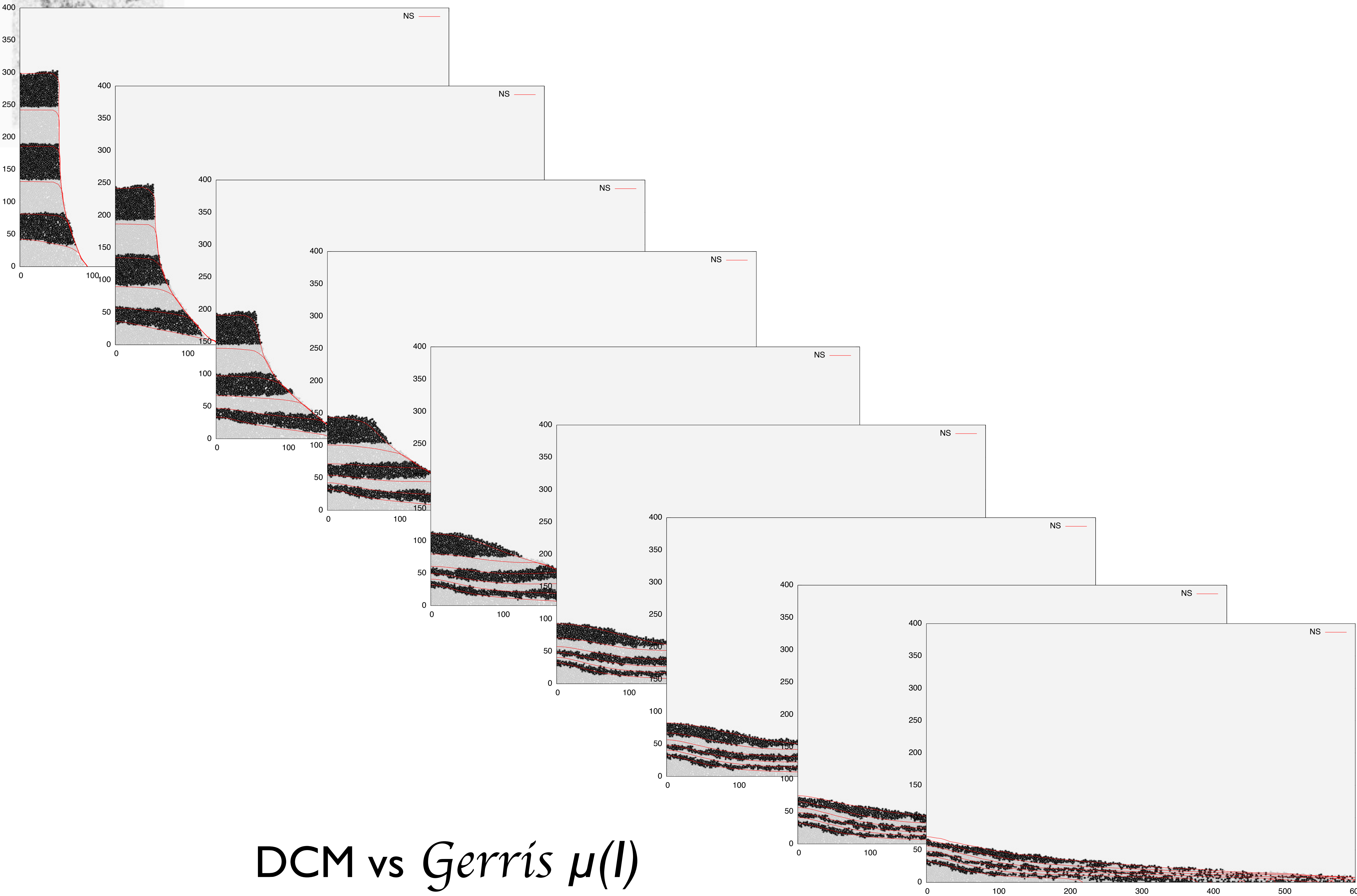


DCM vs *Gerris* $\mu(I)$

# Collapse of columns simulation *Gerris μ(I)*

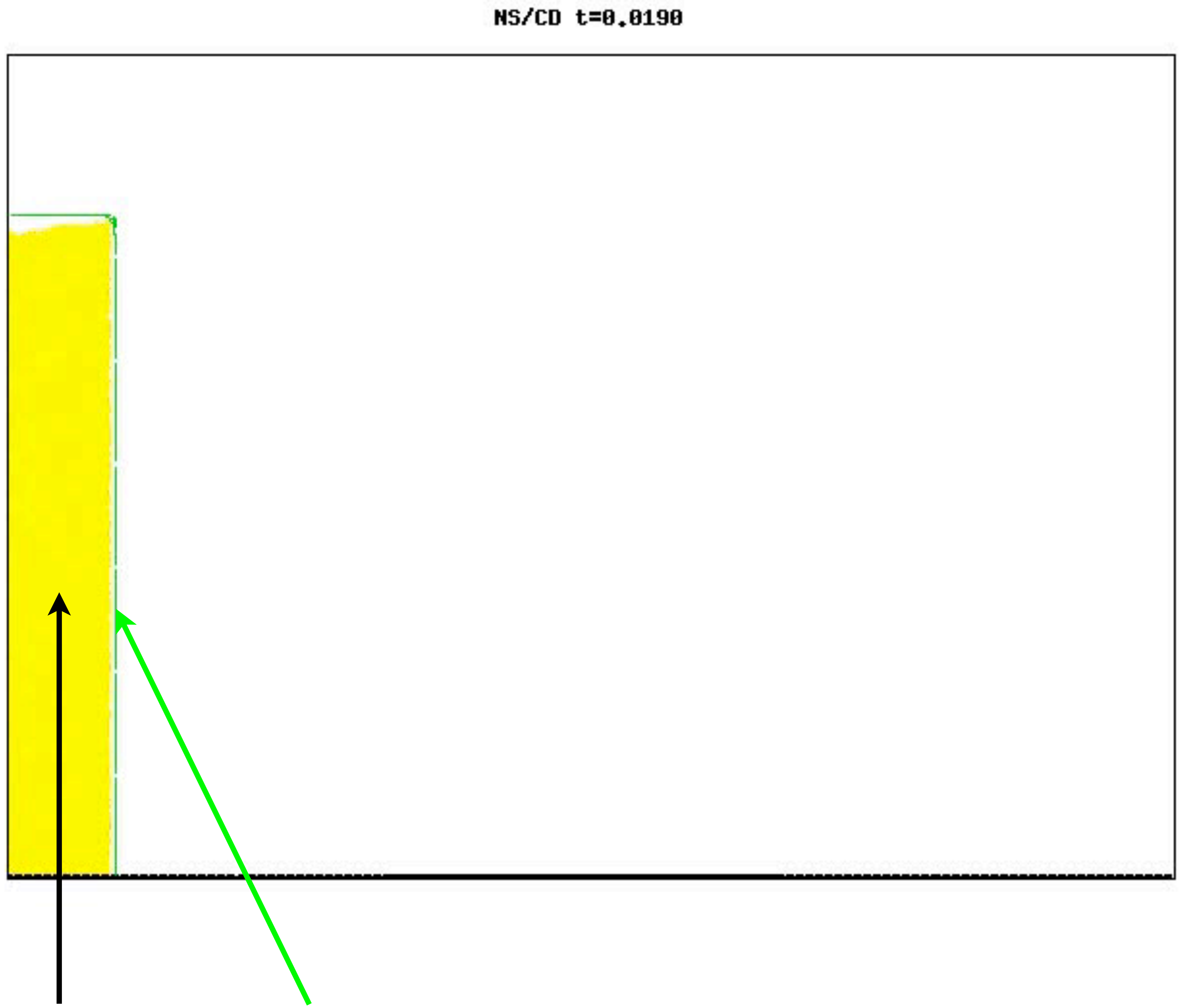


DCM vs *Gerris μ(I)*

# Collapse of columns simulation *Gerris μ(I)*

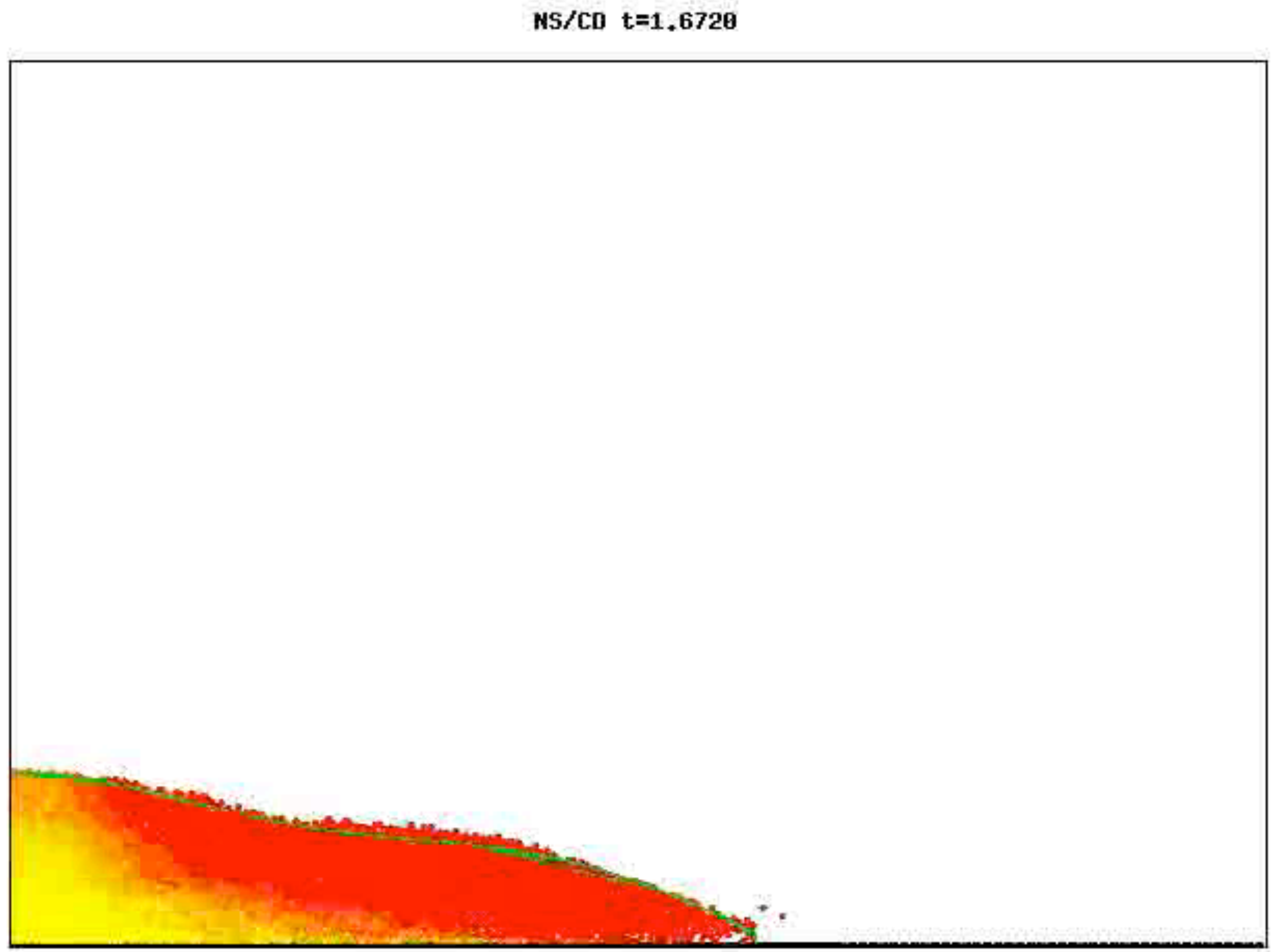


DCM vs *Gerris μ(I)*

# Collapse of columns simulation *Gerris μ(I)*

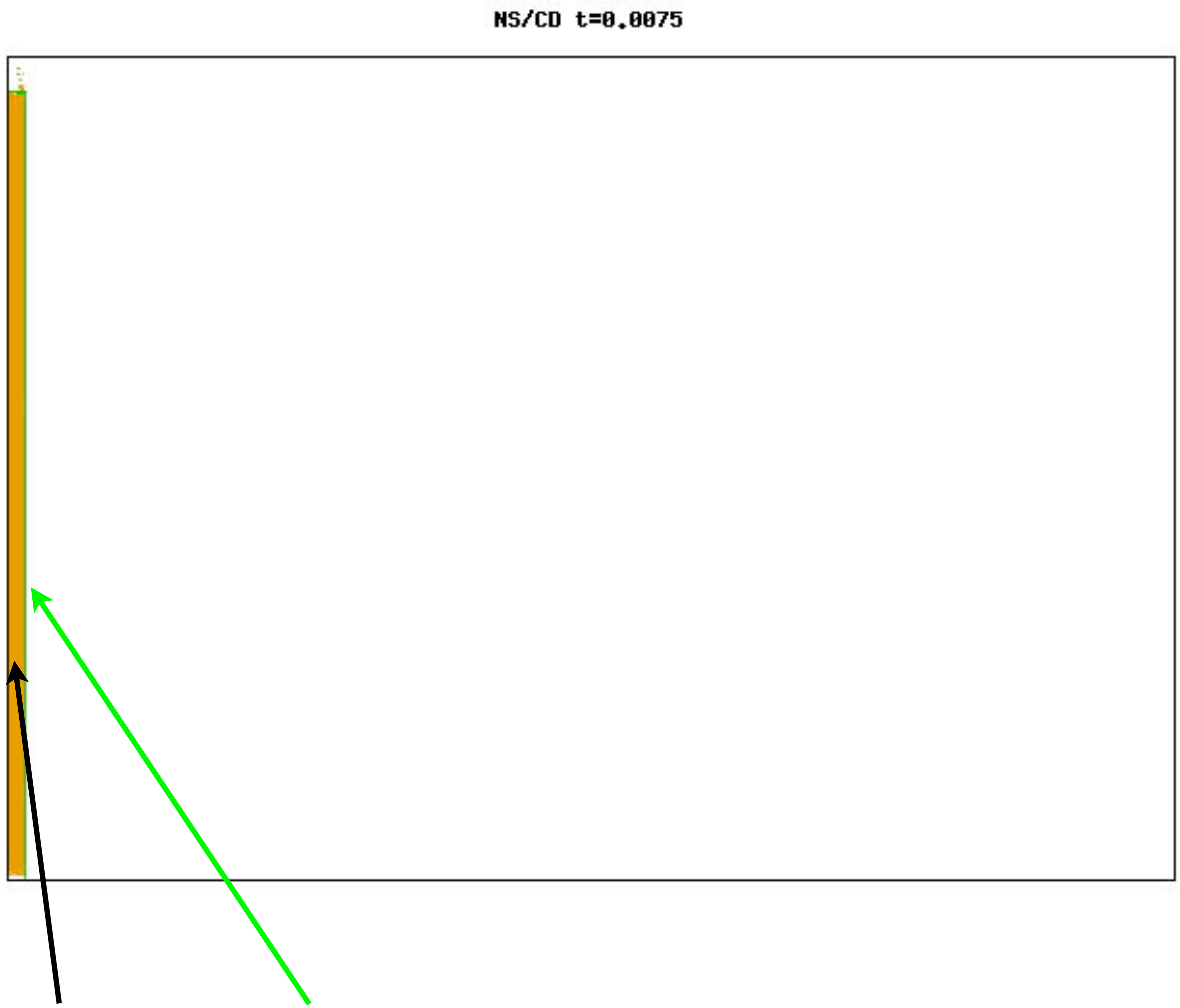


DCM vs *Gerris μ(I)*

# Collapse of columns simulation *Gerris μ(I)*

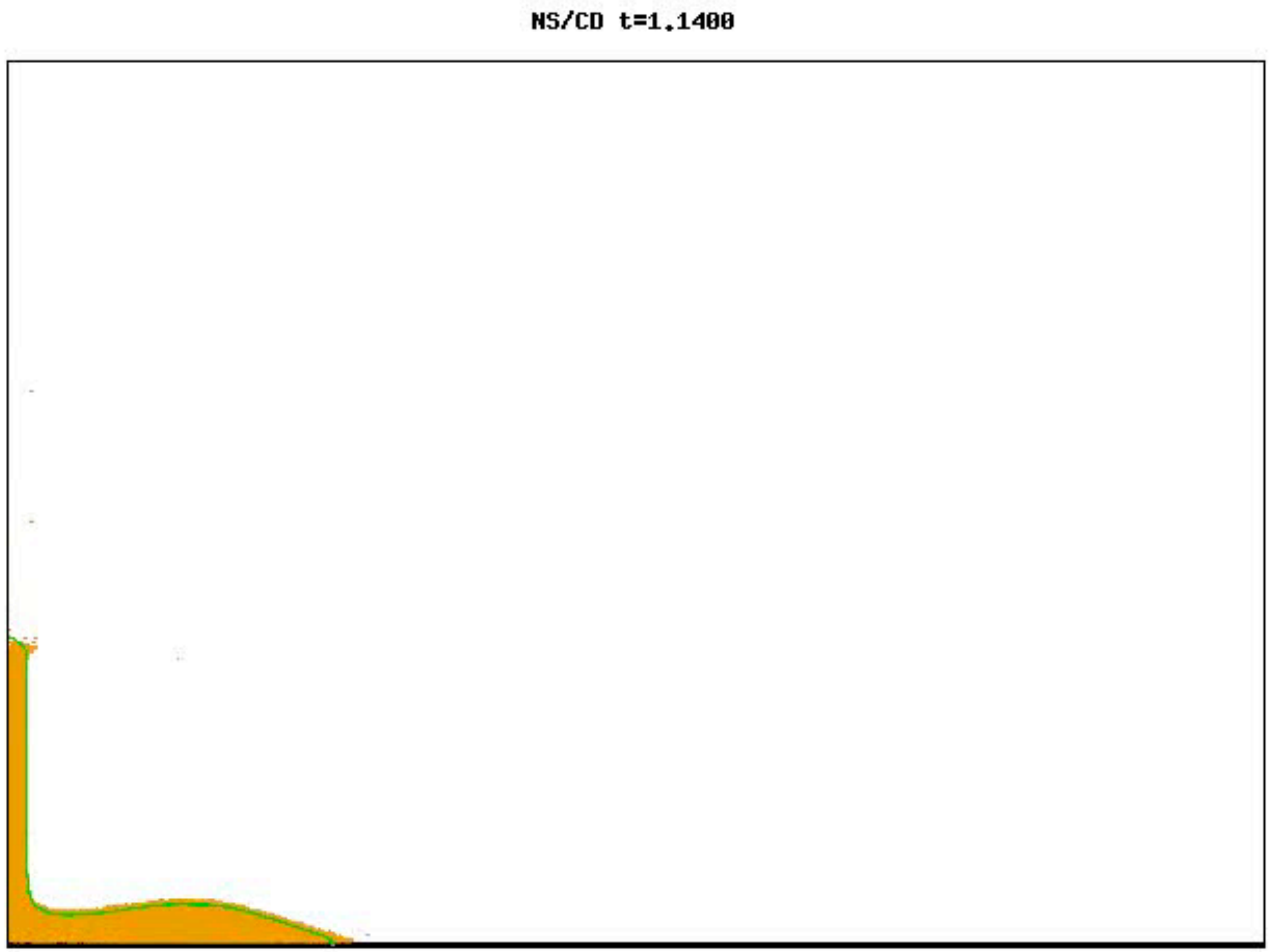


DCM vs *Gerris μ(I)*

# Collapse of columns simulation *Gerris* μ(I)

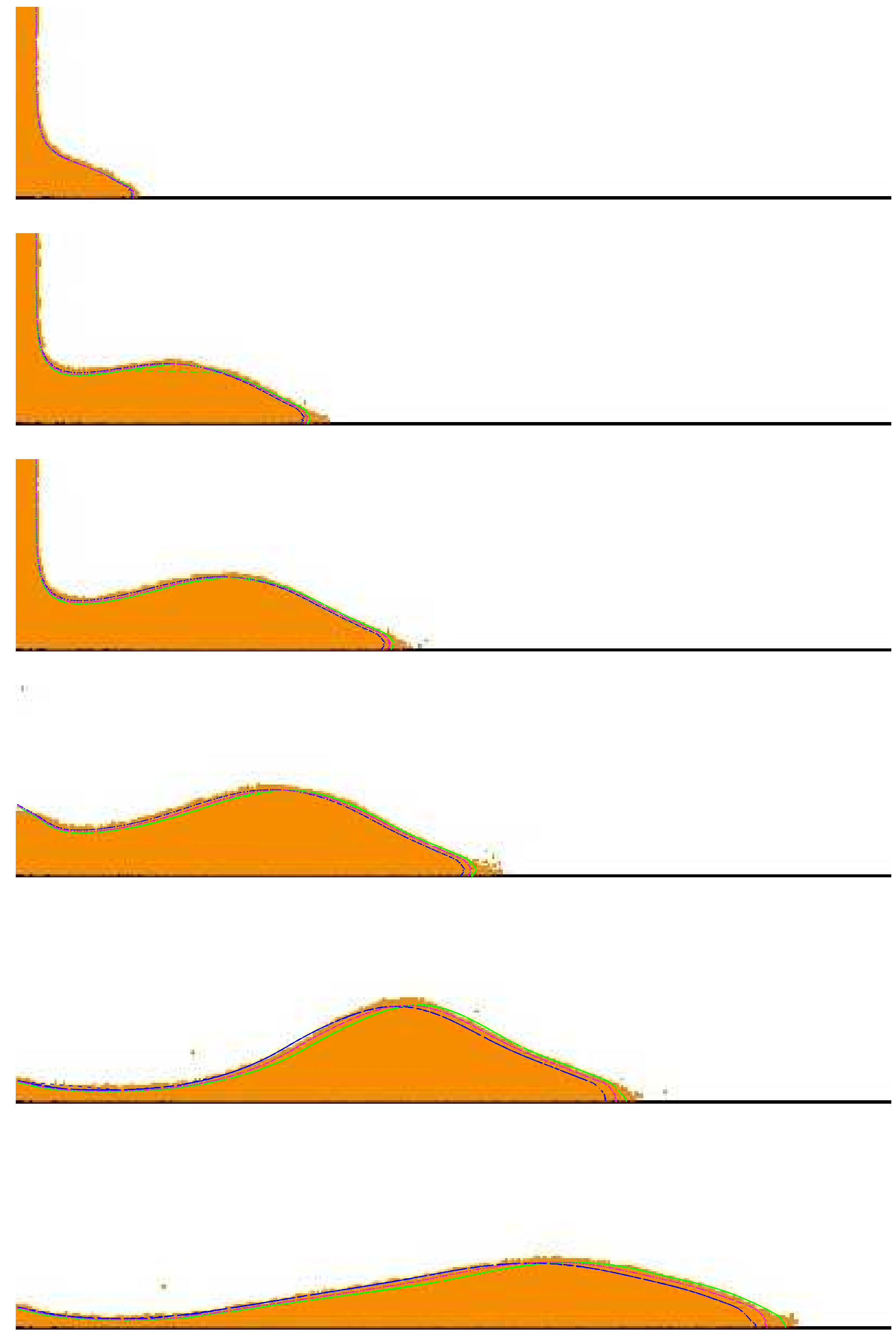

Figure 10: Strip representing a series of snapshots ($t = 0.5, 1.0, 1.2, 1.4, 1.7$, and $2.0$) of a column collapse with aspect ratio $a = 68$. The most advanced curve (in green) corresponds to $\mu_s = 0.3$ $\Delta mu = 0.26$ and $I_0 = 0.30$. the less advanced (in blue) $\mu_s = 0.32$ $\Delta mu = 0.28$ and $I_0 = 0.30$ fits better the end of the heap. The curve in between (in cyan) corresponds to $\mu_s = 0.32$ $\Delta mu = 0.28$ and $I_0 = 0.40$ and fits better the top of the surge.

DCM vs *Gerris* μ(I)

- comparaison of velocity profiles

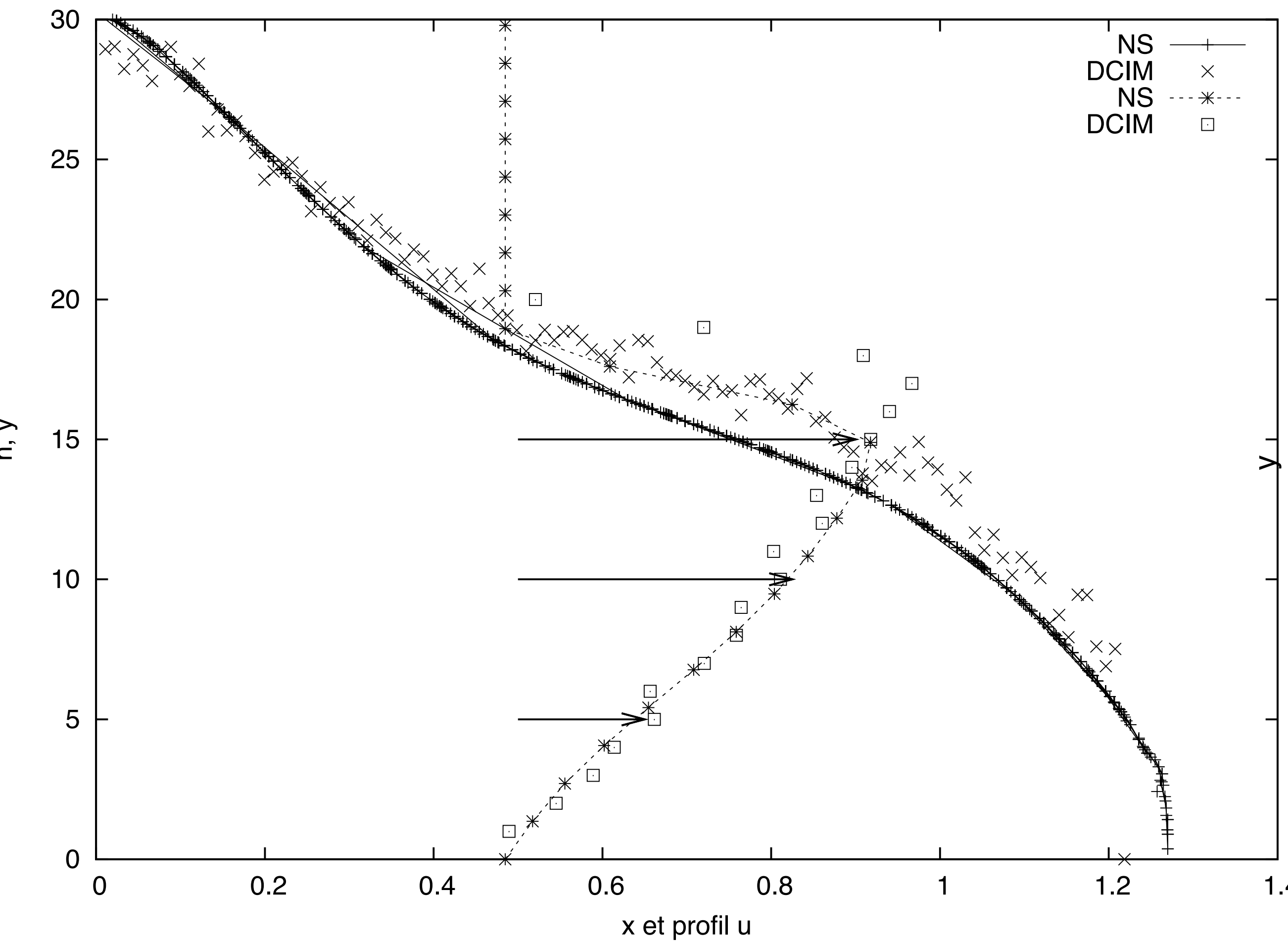


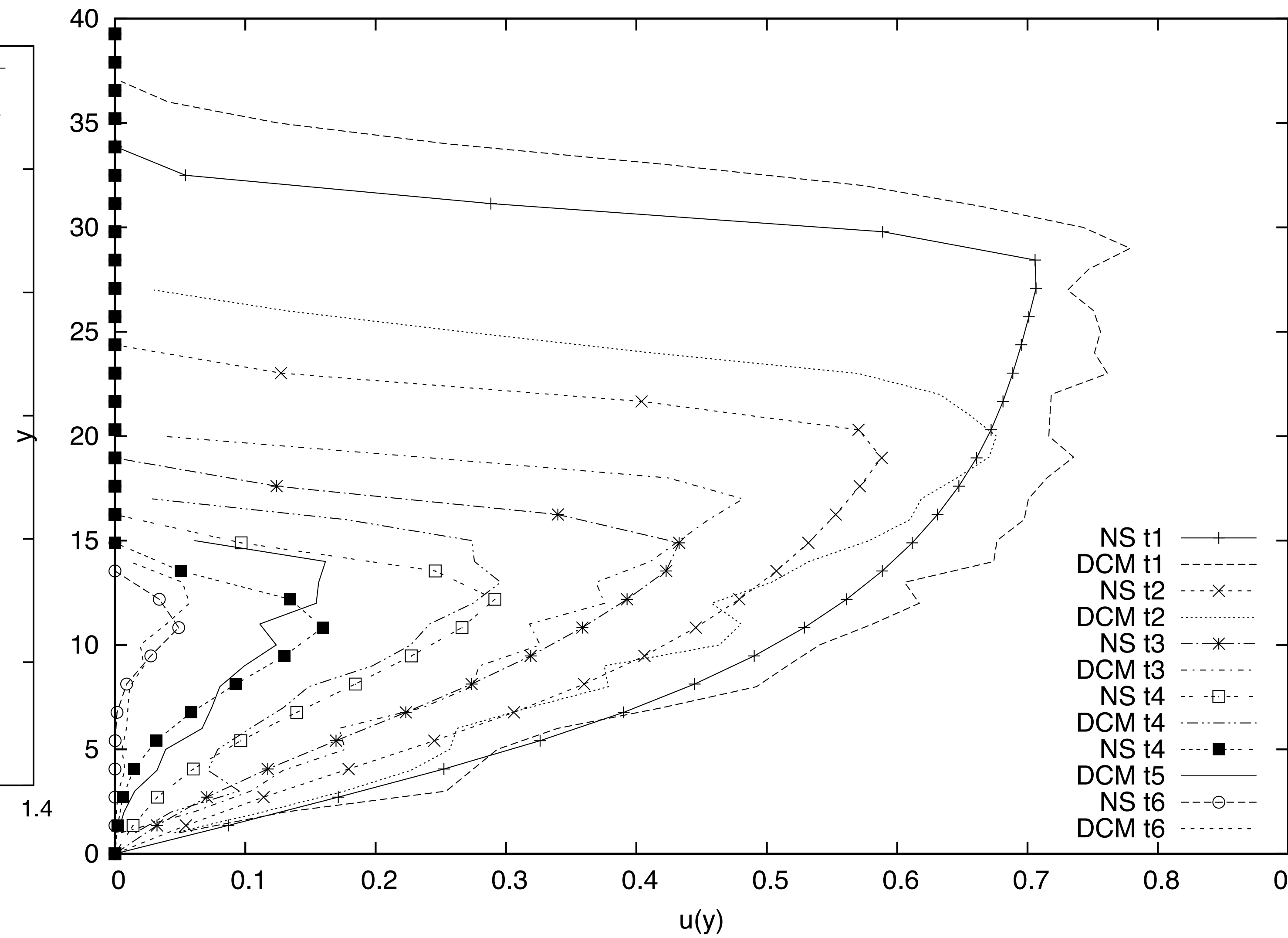


DCM vs *Gerris* $\mu(I)$

- comparaison of velocity profiles

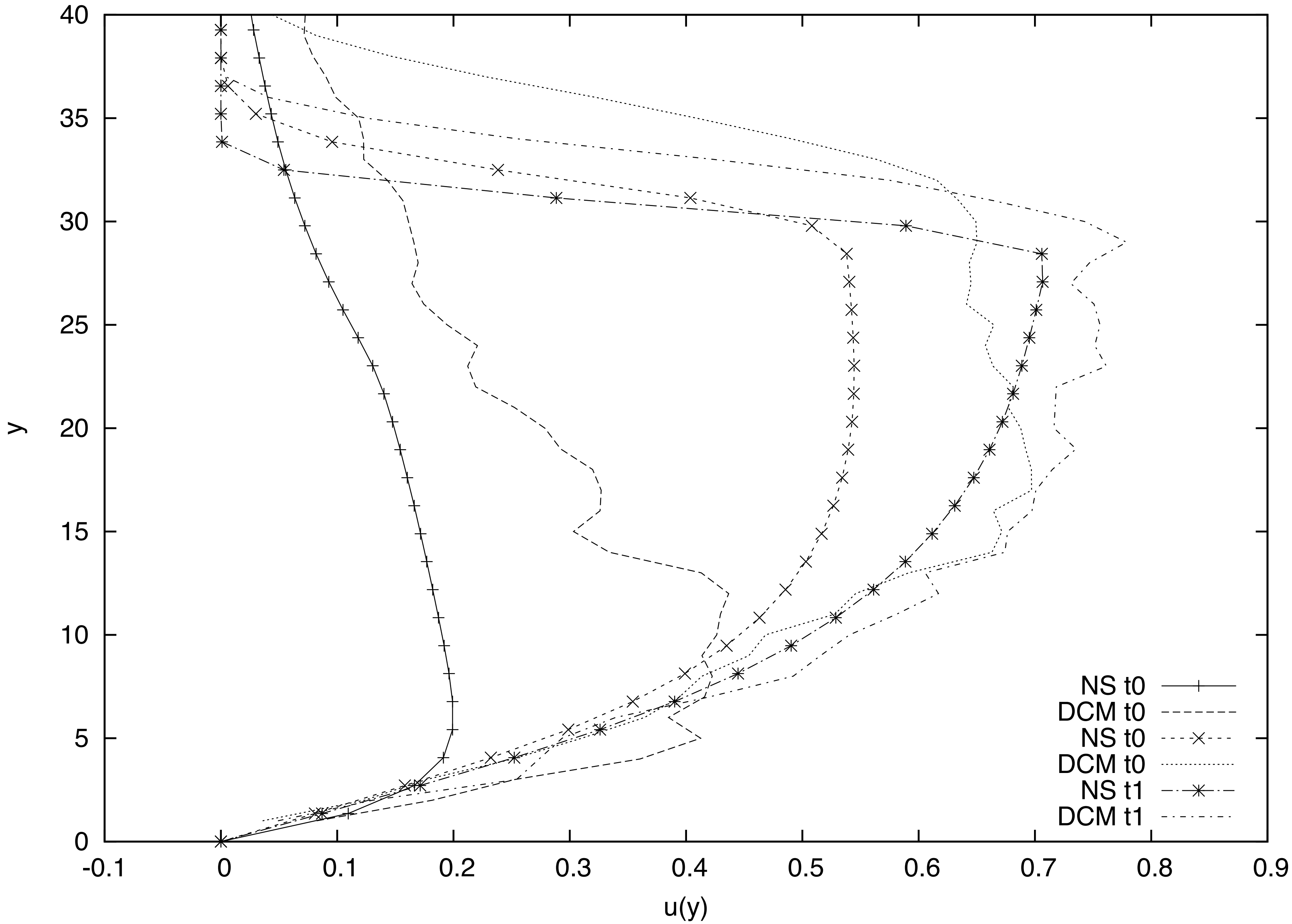


DCM vs *Gerris μ(I)*

# • comparaison of velocity profiles

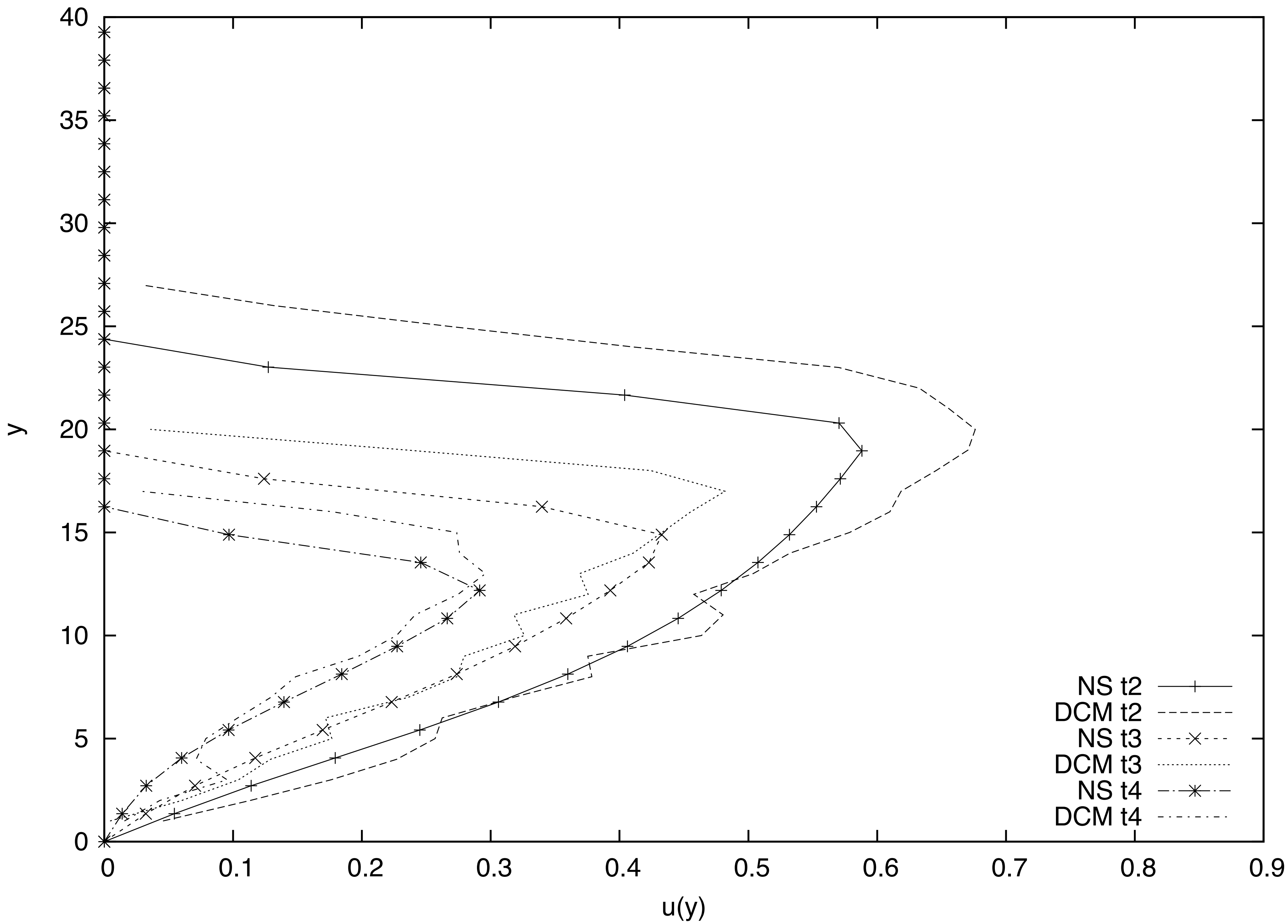


DCM vs *Gerris μ(I)*

- comparaison of velocity profiles

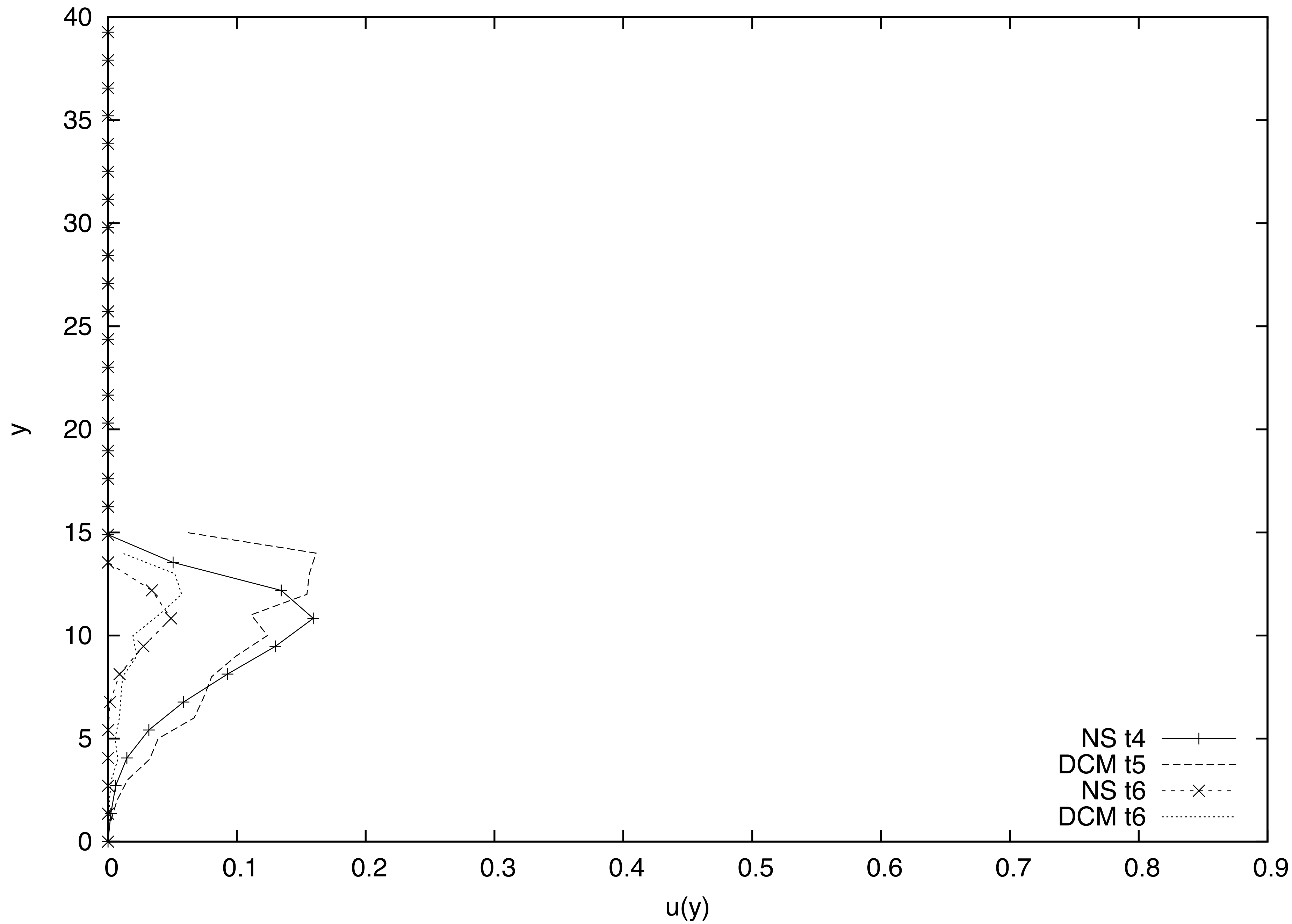


DCM vs *Gerris* $\mu(I)$

# Collapse of columns simulation *Gerris μ(I)*

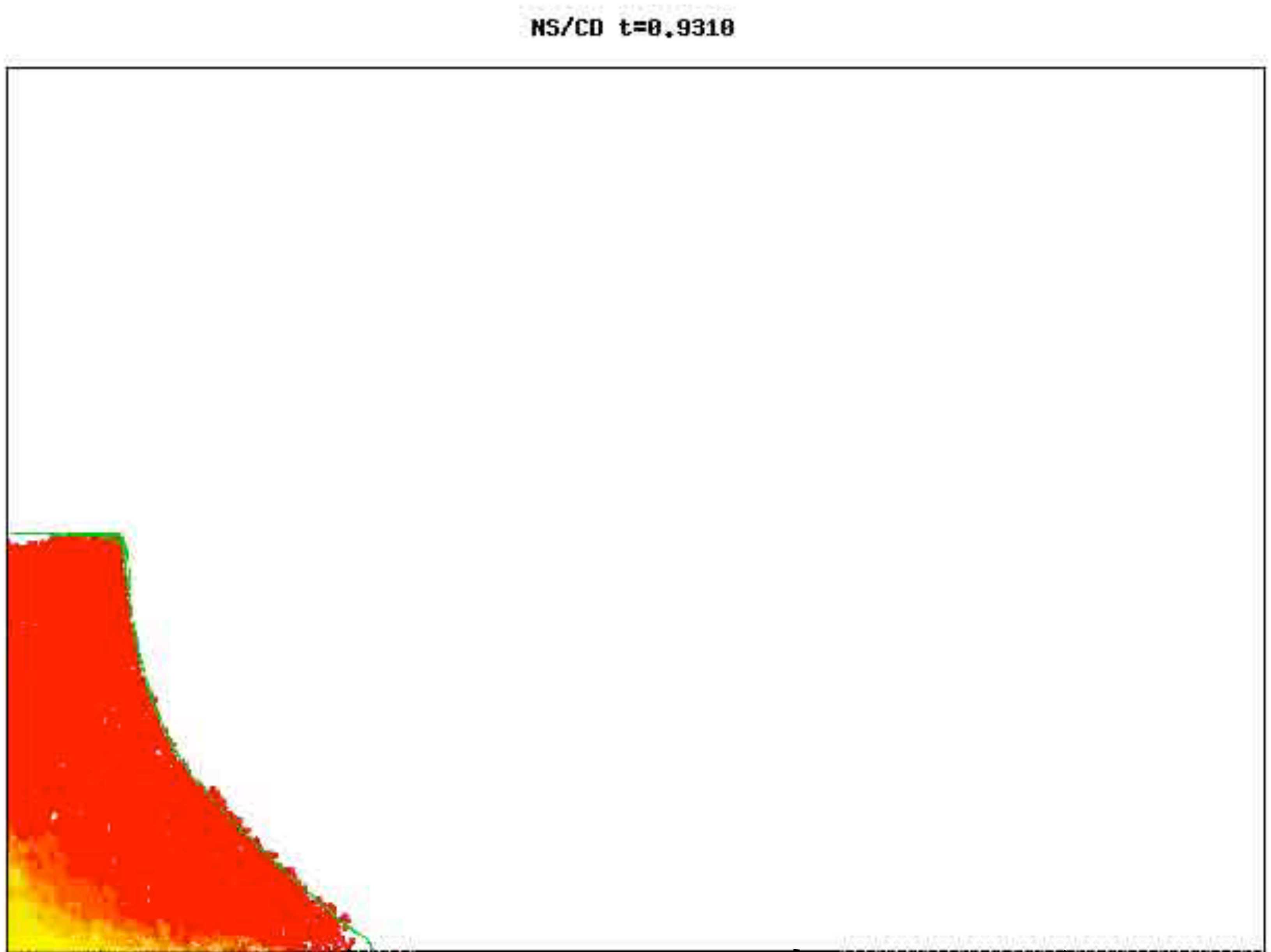


at the tip, a=6.6 t=1.33 2 2.66

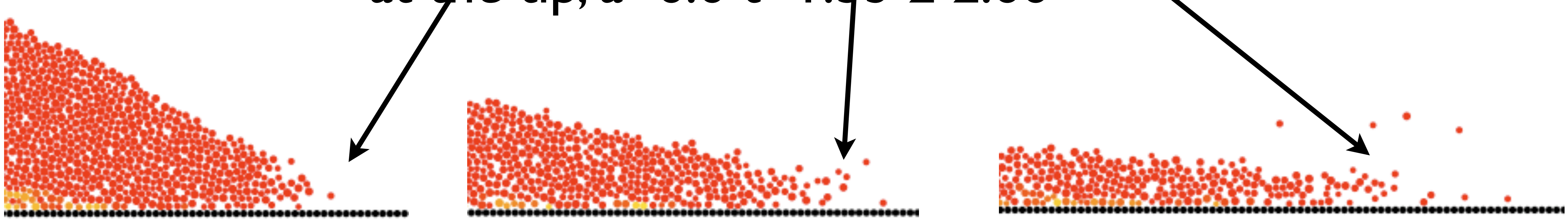

DCM vs *Gerris μ(I)*

E Lajeunesse J. B. Monnier and G. M. Homsy PoF 05

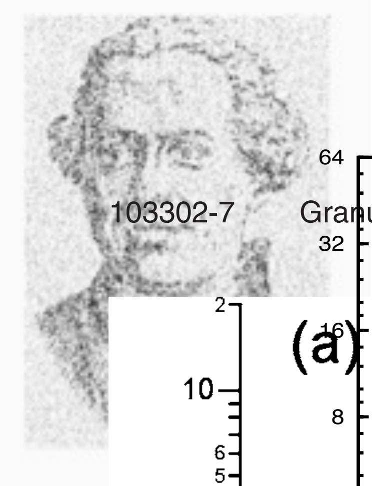



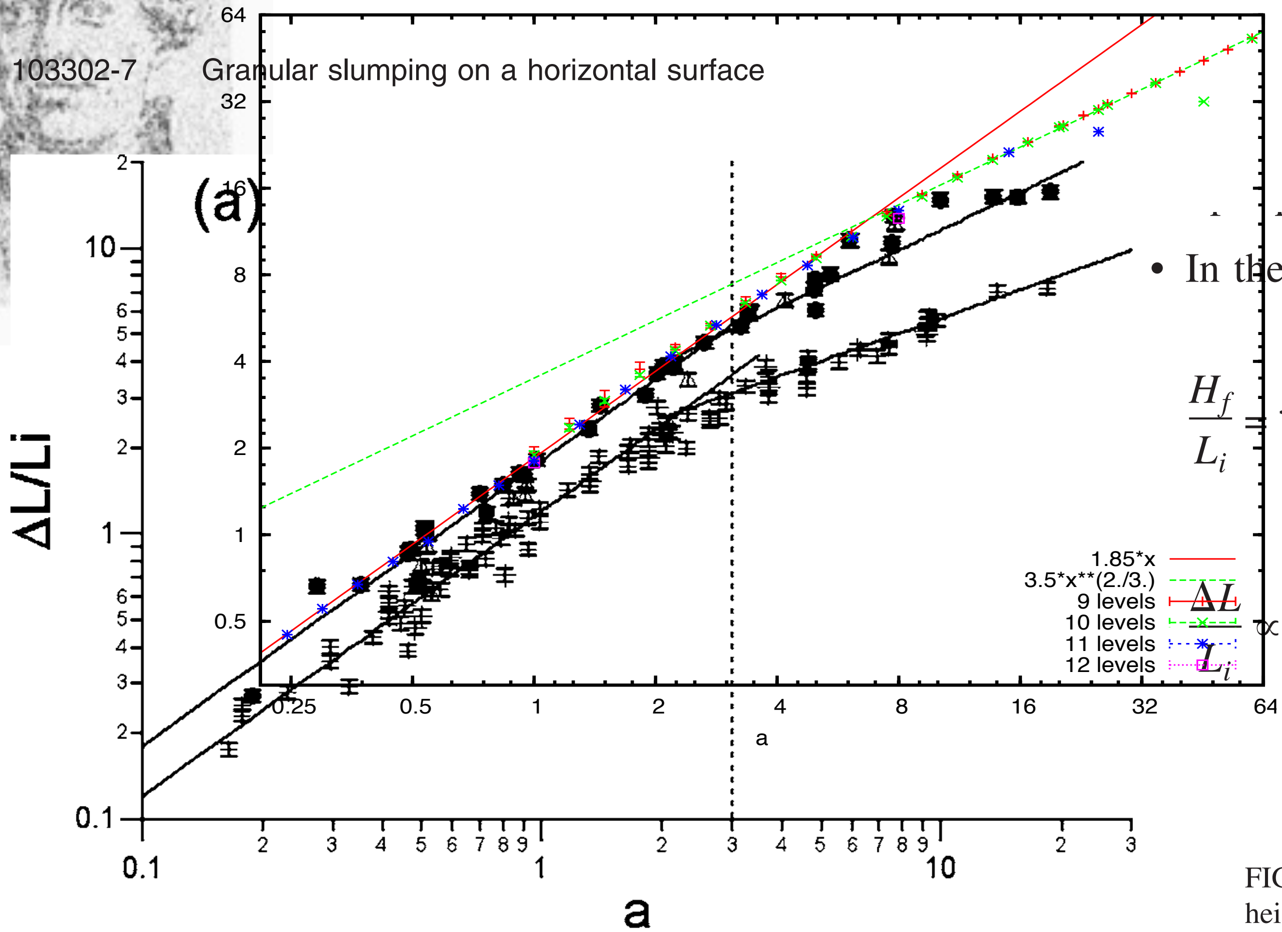


- In the axisymmetric geometry

$$\frac{H_f}{L_i} = \begin{cases} a & a \lesssim 0.74, \\ 0.74 & a \gtrsim 0.74, \end{cases}$$

$$\frac{\Delta L}{L_i} \propto \begin{cases} a & a \lesssim 3, \\ a^{1/2} & a \gtrsim 3. \end{cases}$$

- In the rectangular channel:

$$\frac{H_f}{L_i} \propto \begin{cases} a & a \lesssim 0.7, \\ a^{1/3} & a \gtrsim 0.7, \end{cases}$$

$$\frac{\Delta L}{L_i} \propto \begin{cases} a & a \lesssim 3, \\ a^{2/3} & a \gtrsim 3. \end{cases}$$

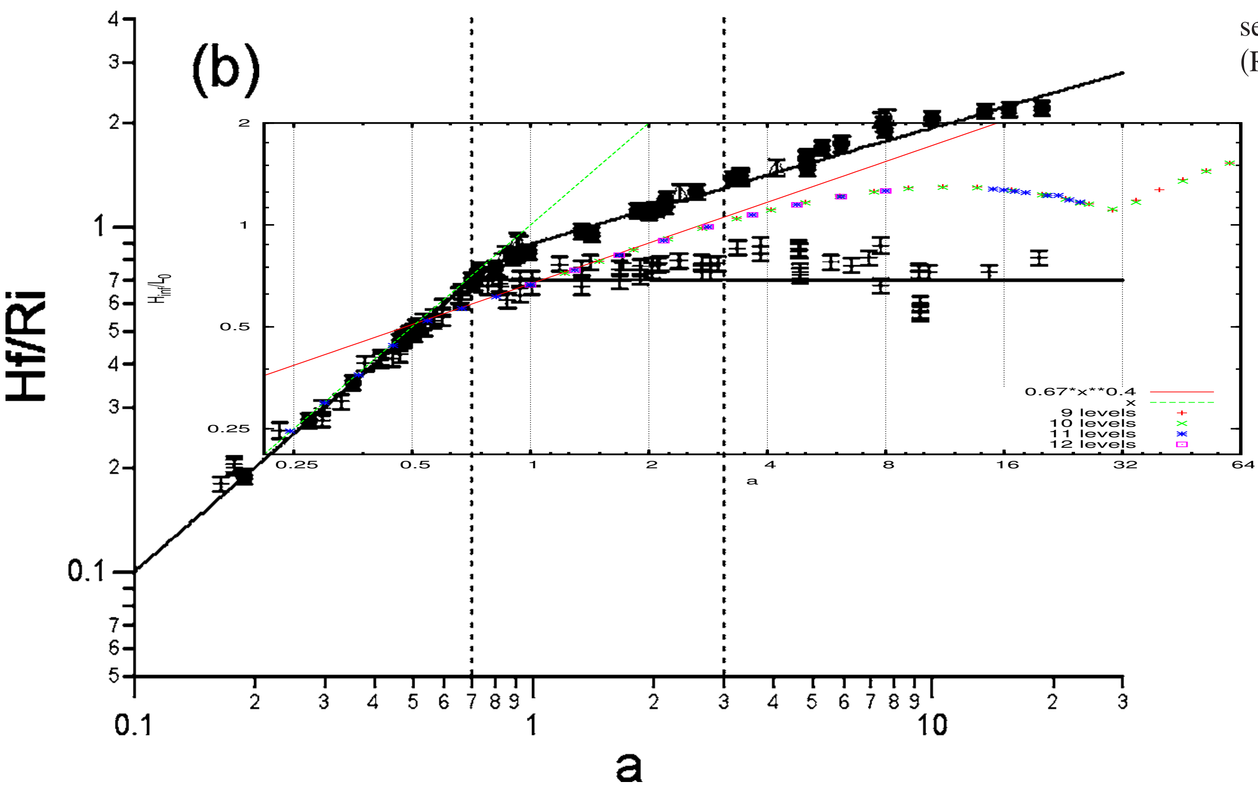


FIG. 6. Scaled runout $\Delta L/L_i$ (a) and scaled deposit height $H_f/L_i$ (b) as functions of $a$. Circles and triangles correspond to experiments performed in the 2D channel working respectively with glass beads of diameter $d$ =1.15 mm or $d$=3 mm. Crosses correspond to the data set of axisymmetric collapses from Lajeunesse *et al.* (Ref. 10).

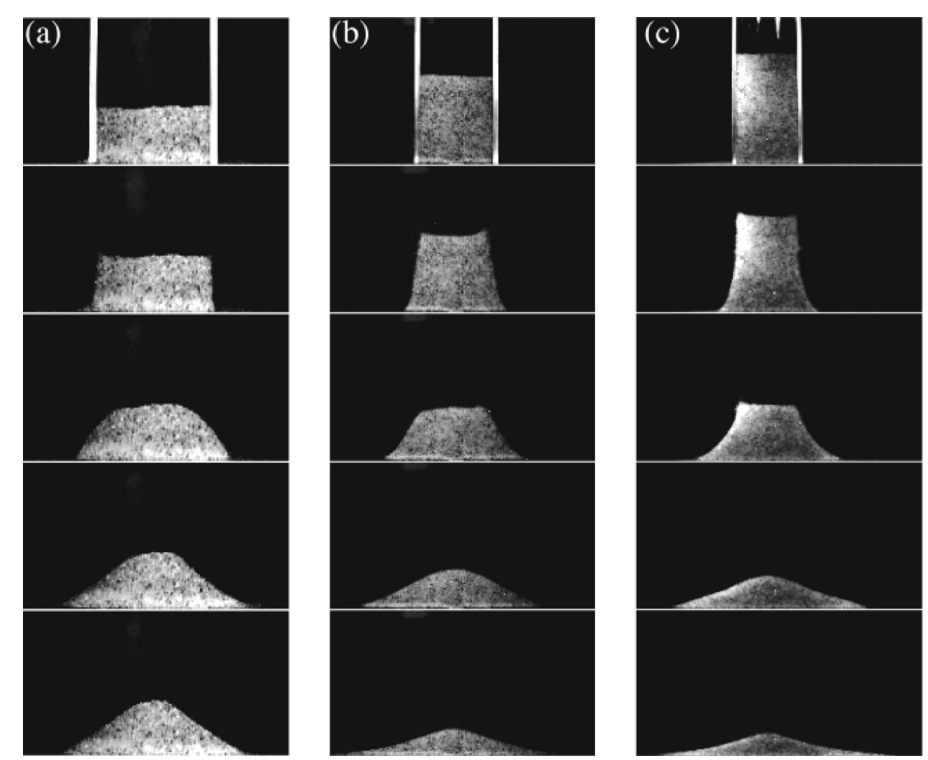

# Collapse of columns simulation *Gerris* $\mu(I)$

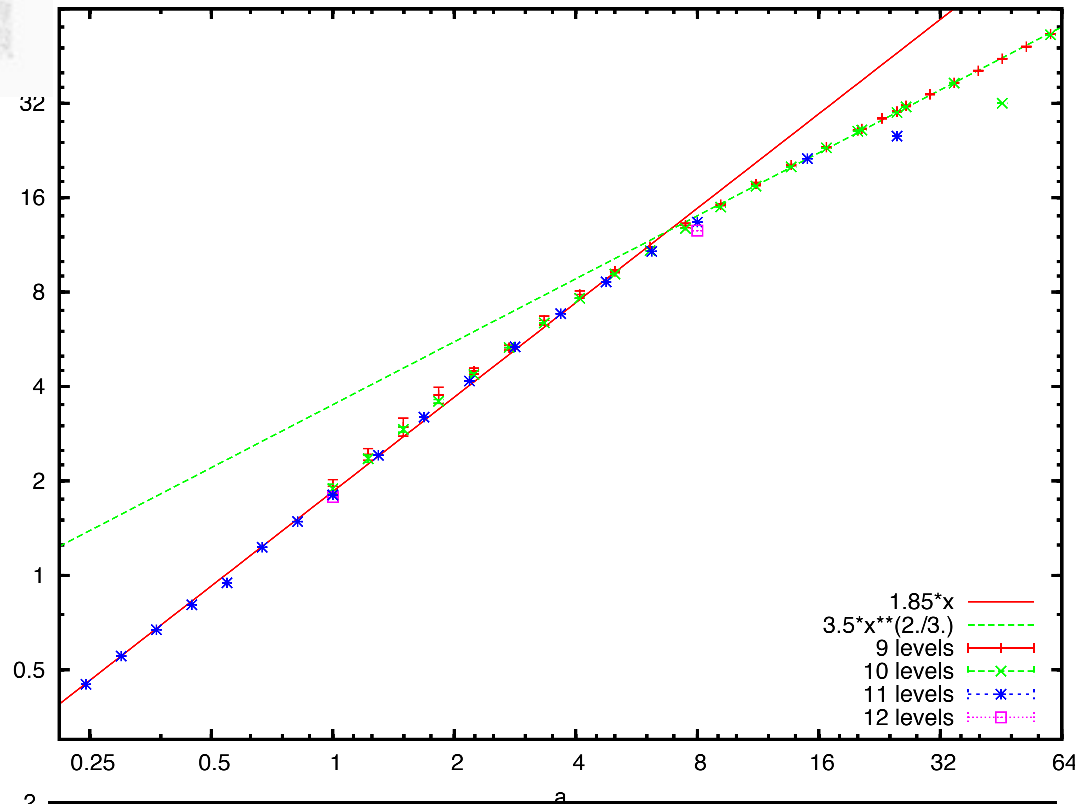


Normalised final deposit extent as a function of aspect ratio *a*.

Well-defined power law dependencies with exponents of 1 and 2/3 respectively.

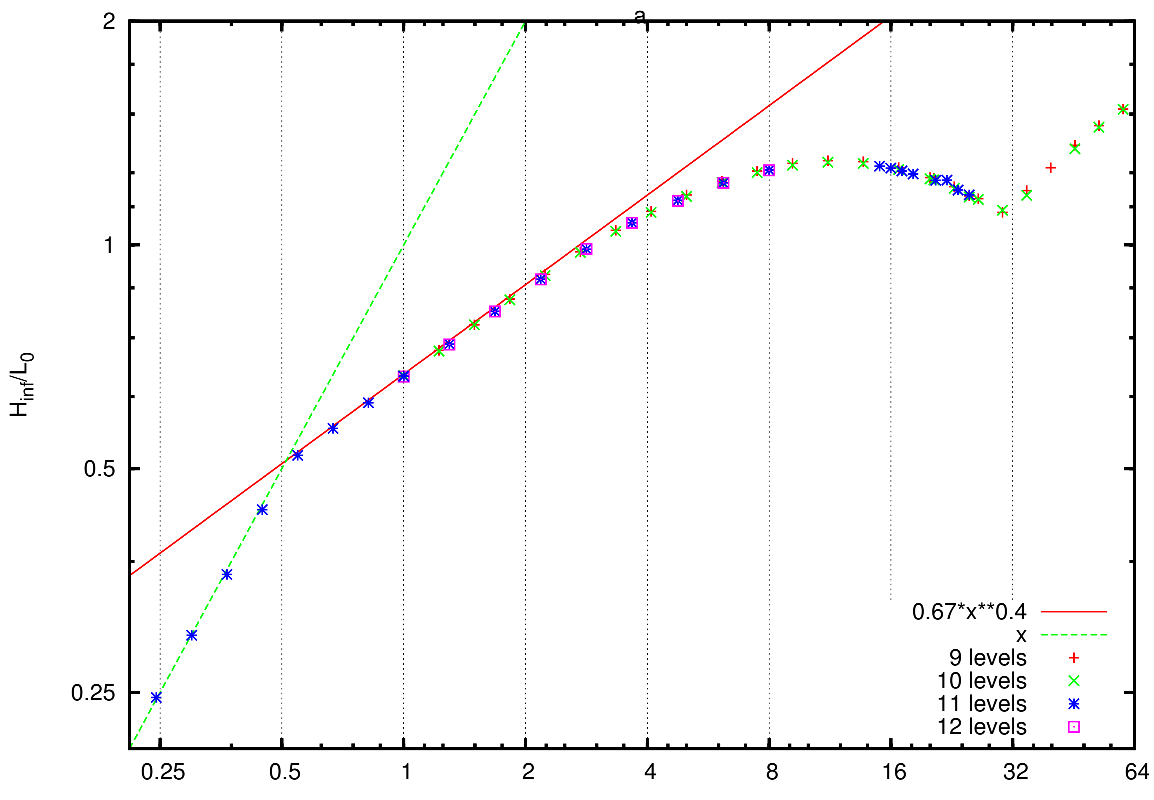


We recover the experimental scaling [Lajeunesse et al. 04] and [Staron et al. 05]. Differences between the values of the prefactors are due to the difficulties to obtain the run out length: friction in the Navier Stokes code tends to underestimate it, whereas direct simulation shows that the tip is very gazeous, it can no longer explained by a continuum mechanic description.

# perspectives

- Other examples under investigation

- Silo, hopper

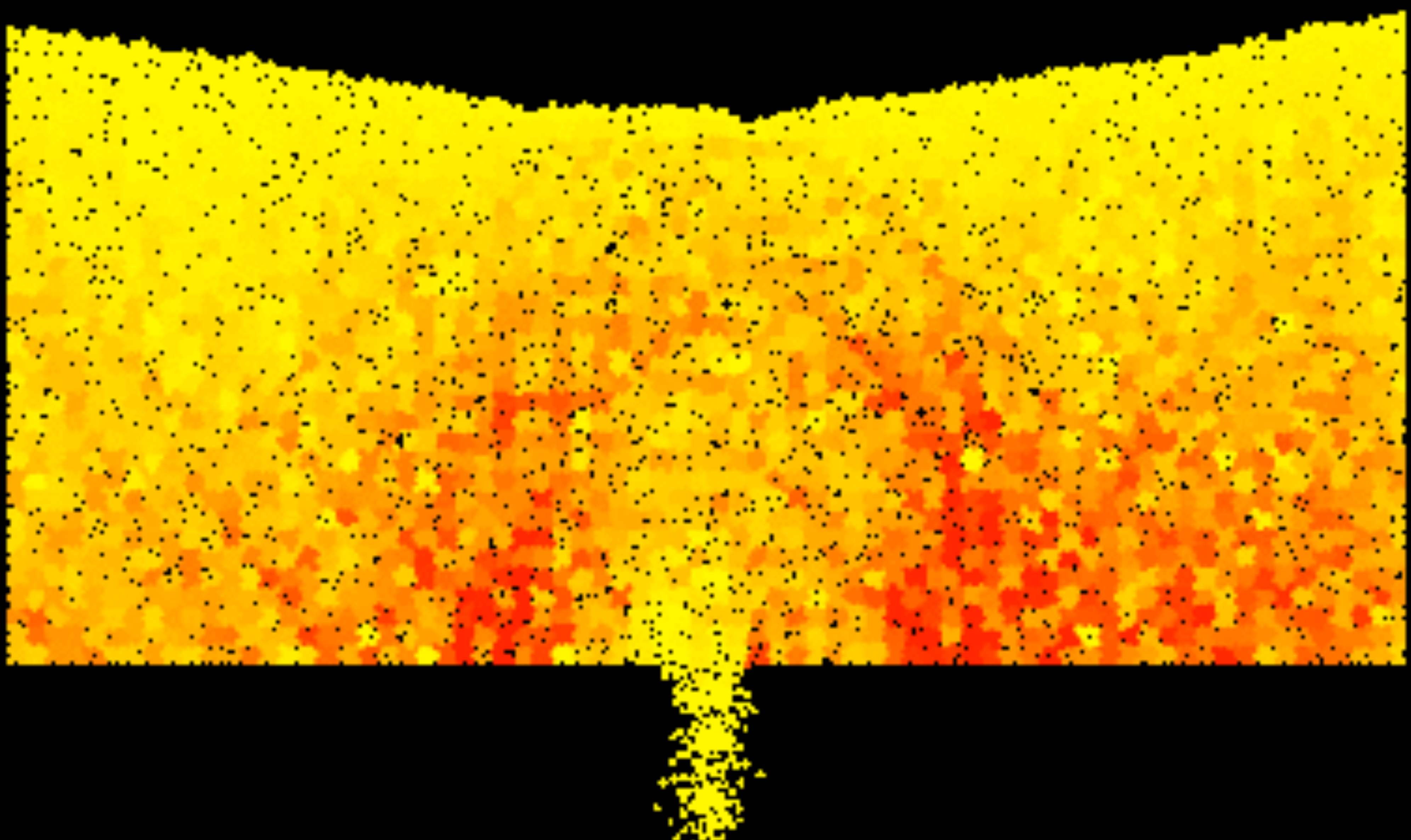

- Vidange de Silo

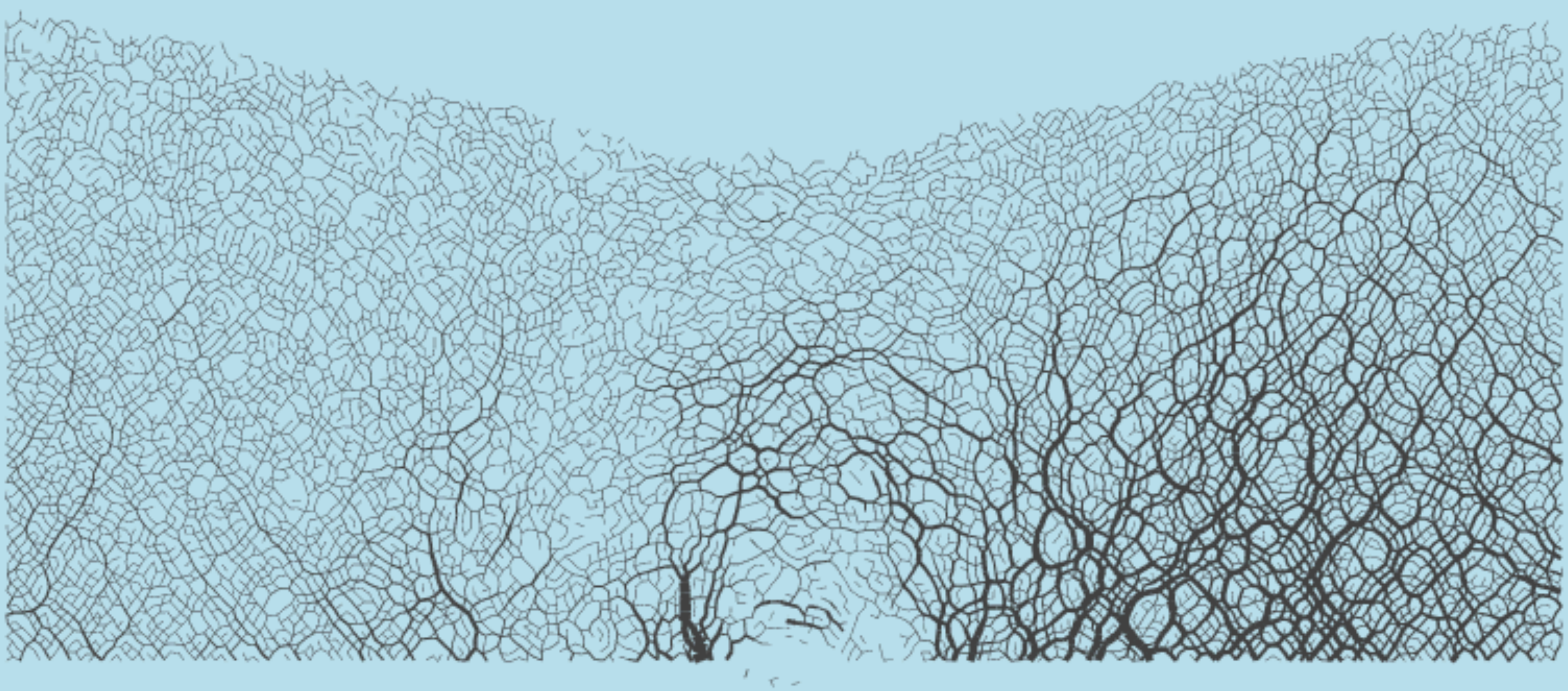

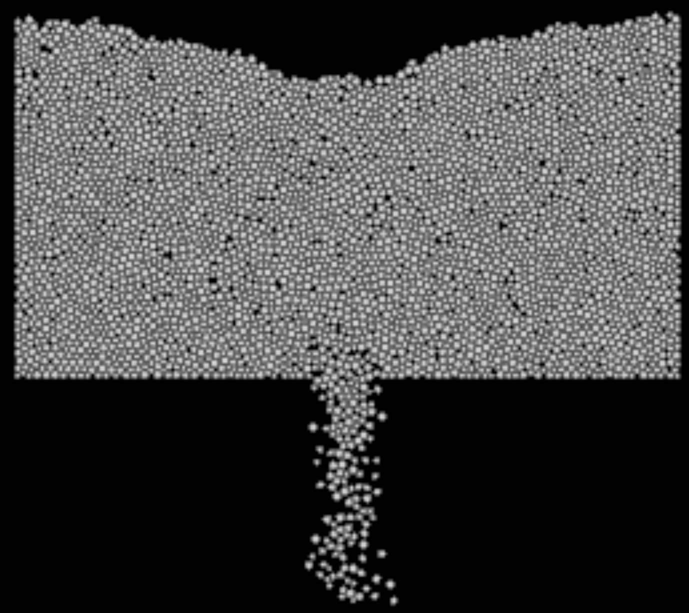

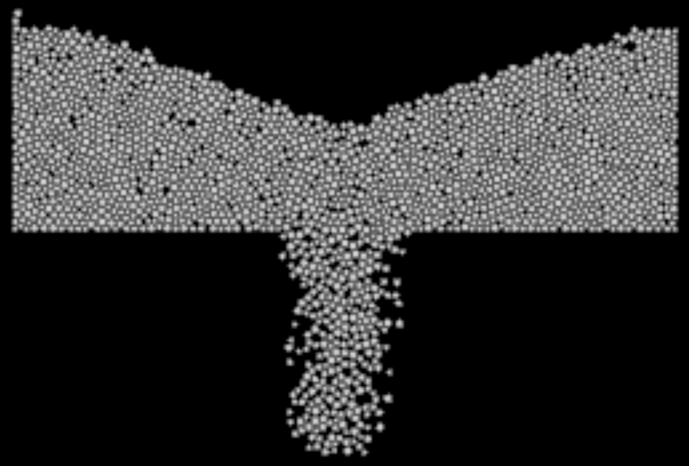

- Vidange de Silo

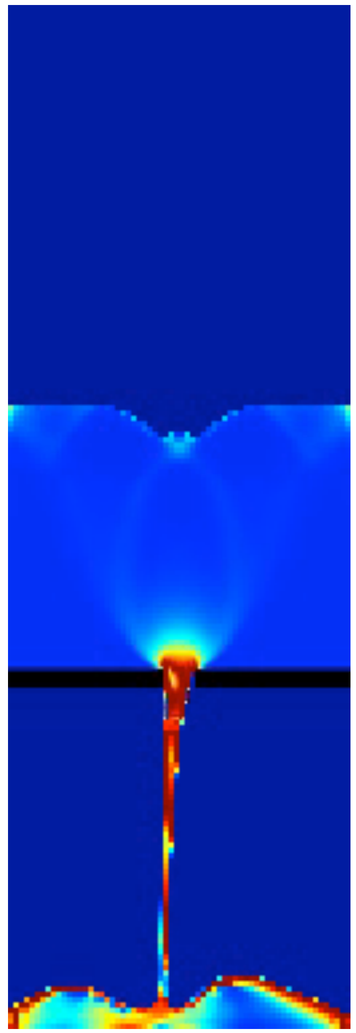

12 grains

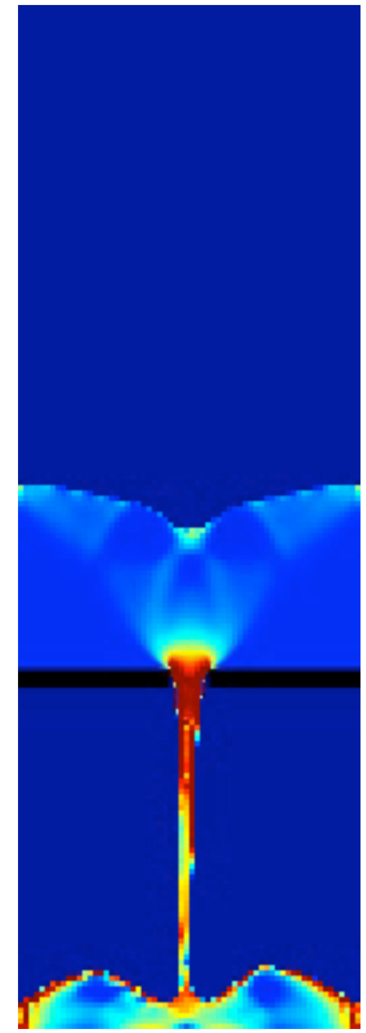

14 grains

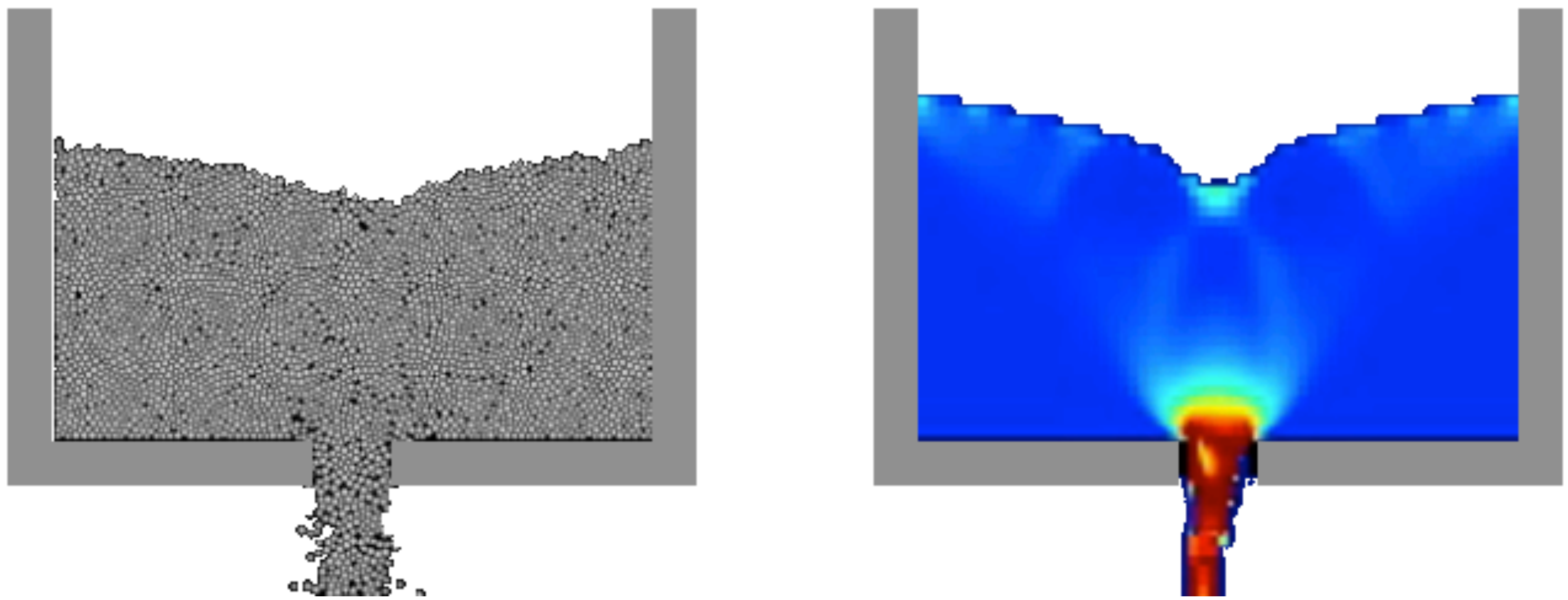

- Vidange de Silo

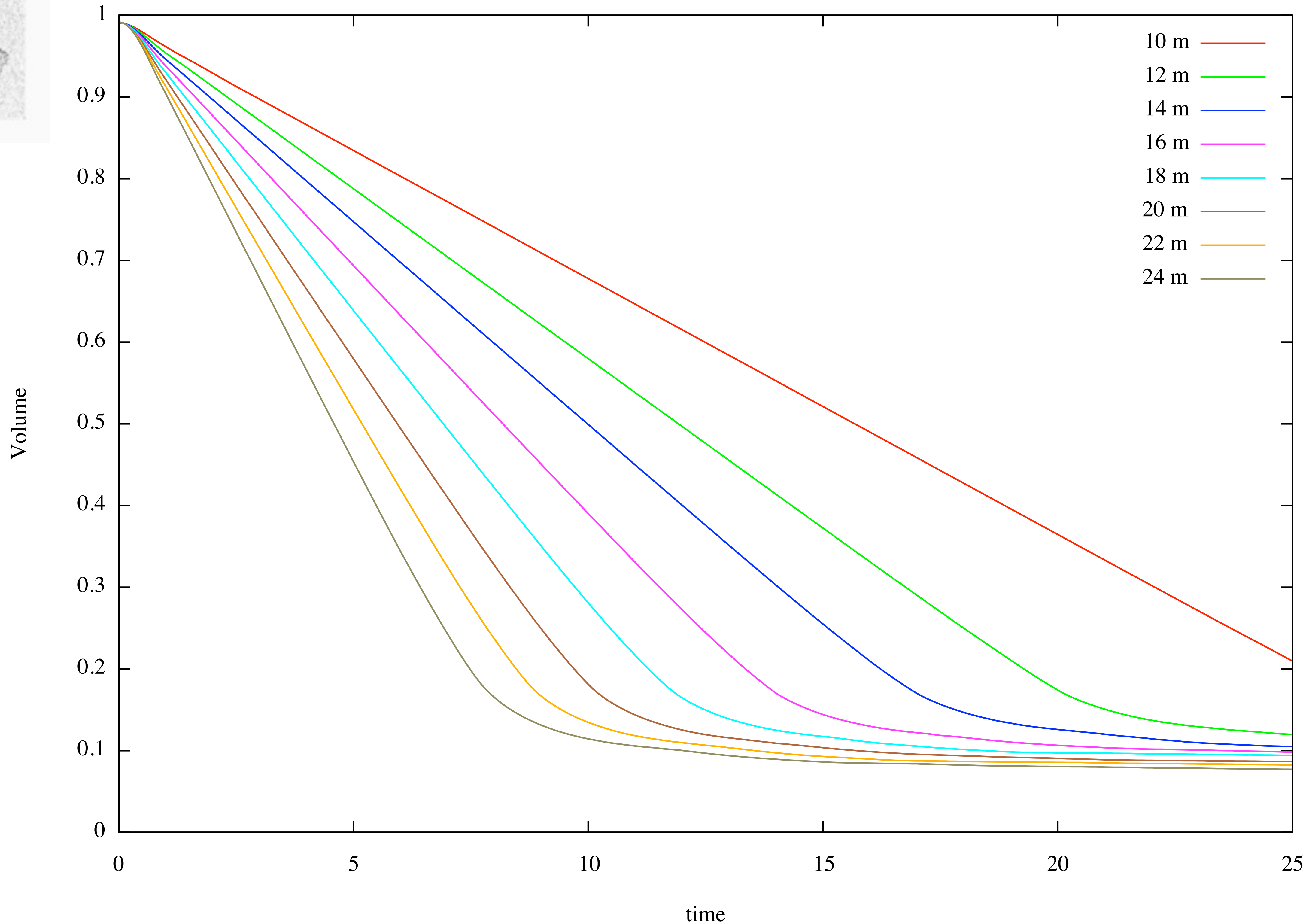

- Vidange de Silo

$$\frac{d\bar{V}}{d\bar{t}} = 1.166(\frac{D}{L} - k\frac{d}{L})^{3/2}$$

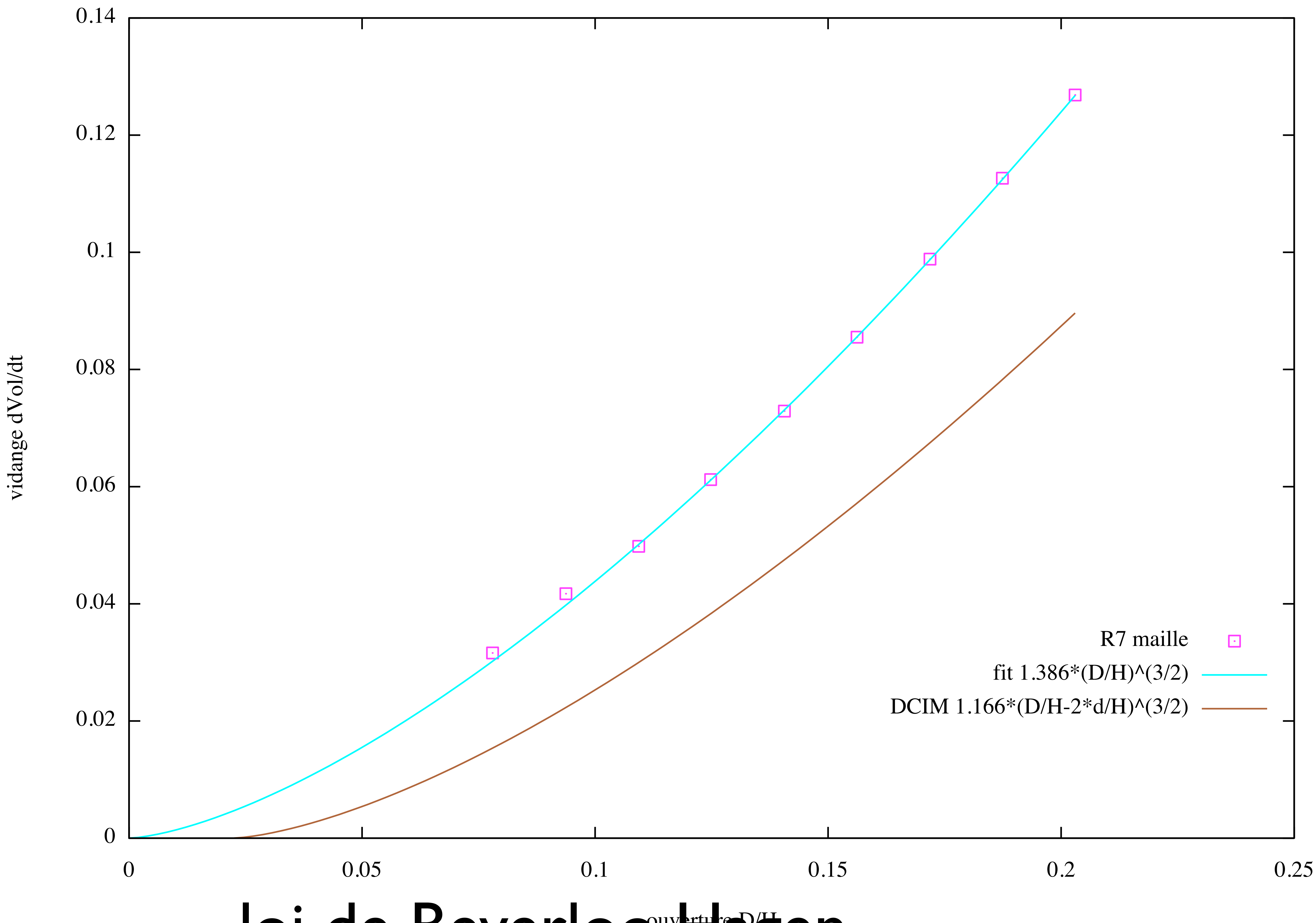


loi de Beverloo Hagen

# conclusion

- μ(I) obtained from experimental flows of dry granular flows [Jop et al. 06], implemented it in *Gerris*
- test case: analytical solution of steady avalanche (Bagnold solution)
- collapse of granular columns (shape as function of time compared to Discrete Simulations).
-The experimental trends of the scaling of the run out are reobtained
- Saint Venant Savage Hutter to be compared with.
- complete spectra: discrete grains/ Saint Venant/ Navier Stokes and plasticity

This opens the door to systematic studies of granular flows using this continuum approach.

## références:


P. Jop, Y. Forterre, O. Pouliquen, (2006) "A rheology for dense granular flows", Nature 441, pp. 727-730 (2006)

P.-Y. Lagrée, L. Staron and S. Popinet (2011) "The granular column collapse as a continuum: validity of a two–dimensional Navier–Stokes model with a μ(I)-rheology", JFM pp1-31 , doi:10.1017/jfm.2011.335

E. Lajeunesse, A. Mangeney-Castelnau, and J.-P. Vilotte, (2004) "Spreading of a granular mass on an horizontal plane», Phys. Fluids, 16(7), 2371-2381.

L. Staron & E. J. Hinch (2005) "Study of the collapse of granular columns using two-dimensional discrete-grain simulation", J. Fluid Mech. (2005), vol. 545, pp. 1–27.